TORSIONAL BRAID ANALYSIS
A SEMIMICRO THERMOMECHANICAL APPROACH TO
POLYMER CHARACTERIZATION

Author: **John K. Gillham**
Polymer Materials Program
Department of Chemical Engineering
Princeton University
Princeton, New Jersey

Referee: C. D. Armeniades
Department of Chemical Engineering
Rice University
Houston, Texas

INTRODUCTION

Dynamic mechanical measurements provide a convenient means for generating the thermo-mechanical spectra of polymeric materials. The spectra are of theoretical interest in revealing the ability of materials to store and to dissipate energy on mechanical deformation, and yet are of practical interest in being readily understood in terms of potential use. In recent years some semimicro mechanical techniques have emerged which permit the characterization of polymers by the synthetic chemist *in mechanical terms*, thereby enlightening him to end use possibilities for his syntheses and lessening the delay between creation and determination of commercial feasibility of new polymers.

One such technique is torsional braid analysis (TBA)[1-49] which uses a torsional pendulum capable of examining small specimens and, for purposes of fabricating a specimen, an inert (braid) substrate and a soluble polymer (or a prepolymer). A composite specimen is prepared simply by impregnating a multifilament inert (glass) braid with a solution of polymer and removing the solvent thermally. The natural period ($\sim$ 1 cps)

and decay of free torsional oscillations, which are induced in the specimen from time to time, are measured. Two curves, one relating to the storage of energy and the other to the dissipation of energy on mechanical deformation, form the thermomechanical spectra. The unique features of TBA are that fabrication of the specimen (the most difficult step in any mechanical analysis and especially with limited quantities of material) is simple, and polymers can be examined throughout the spectrum of mechanical states (glassy, rubbery, and fluid). The technique is therefore particularly suitable for the thermomechanical characterization of nonself-supporting polymers and those which are intractable (e.g. ladder and crosslinked) but which are formed from tractable intermediates.

This review is concerned mainly with the current status of the instrumentation, technique of application, and applications of the torsional braid analysis approach to the characterization of polymers. Prime sources of up-to-date information are the preprints, presentations, and discussions of "The First Symposium on Torsional Braid Analysis," which was held at the Annual Technical Meeting of the Society of Plastics Engineers in Washington, D. C., on May 18, 1971. This was

organized and chaired by the writer upon invitation by the S.P.E.

Since the torsional braid experiments are interpreted as being those from a torsional pendulum and the instrument can be used directly as a classical torsional pendulum, some discussion of the latter is included. This is particularly apt since the American Society for Testing Materials has recently made the torsional pendulum the first standard (ASTM Standard D-2236-70) for measurement of the dynamic mechanical properties of plastic materials.

TORSIONAL PENDULUM

One of the most versatile instruments for low frequency dynamic mechanical studies, especially for coverage of a wide' temperature range, is the torsional pendulum. The instrument is designed to operate generally in the frequency range from 0.1 to 10 cps with the sample enclosed in a chamber which can be cooled and heated in a controlled atmosphere. A number of commercial variants are on the market and ASTM designation D2236-70

describes[50] recommended procedures. The recommended dimensions of the ASTM test specimen for a rectangular strip are: thickness from 0.015 to 0.100 in, width from 0.10 to 0.60 in, and length from 1 to 6 in. For a cylindrical specimen the recommended dimensions are: comparable length and a radius of less than 0.30 in. Schematic diagrams of the elements of the two methods which are used in the design of torsional pendulums for characterizing solid polymers are shown in Figure 1. In both, the specimen is supported vertically between a fixed clamp and a second clamp which is rigidly attached to an inertial member. The tension on the specimen is recommended to be less than 100 psi. When the upper clamp is attached to the inertial member, the tension in the specimen can be controlled by use of counterweights which are attached so as to have a known or negligible torsional effect. The sample is set into free torsional oscillations by an initial torsional displacement of low strain (e.g. no more than 2.5 deg/cm of specimen length for the recommended dimensions). The subsequent displacement-time
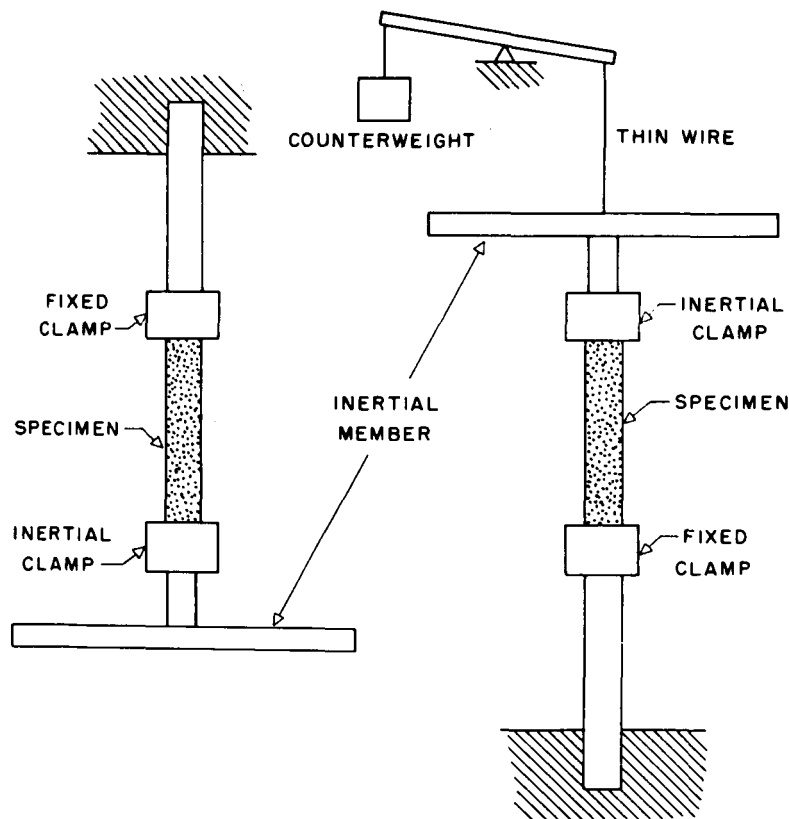

FIGURE 1. Torsional pendulum configurations (schematic).

curve, frequently automatically recorded, provides data which together with numerical, geometrical, and inertial factors are used to obtain the material parameters which are related to the storage and loss of energy on mechanical deformation.

The torsional braid apparatus is used[35] as a torsional pendulum operating around 1 cps, which is ideal for the initial mechanical characterization of materials. Greater resolution (see Figure 21) is achieved in low frequency than in higher frequency dynamic tests (as a consequence of the different activation energies of the thermally active underlying mechanisms in the solid state; the lower activation energies are associated with the lower temperature damping peaks), and the results can be correlated readily with static

nonmechanical (e.g. thermal, dilatometric) and mechanical (e.g. penetrometer, tensile stress-strain, stress relaxation) tests. The apparatus operates over a temperature range of $<-190°C$ to $>+650°C$ with a temperature spread of $\pm1°C$ over an 8 in sample, and can be programmed for increasing, decreasing, and isothermal modes of temperature in tightly controlled atmospheres. It utilizes a no-drag transducer system. Strain in the oscillating system can be low. Decaying oscillations with initial (maximum) displacements of less than one degree per inch of specimen length can be monitored. It can operate with films, rods, or beams with specimen dimensions which satisfy those designated by ASTM standard D2236-70. Smaller specimens can be examined. Figure 2
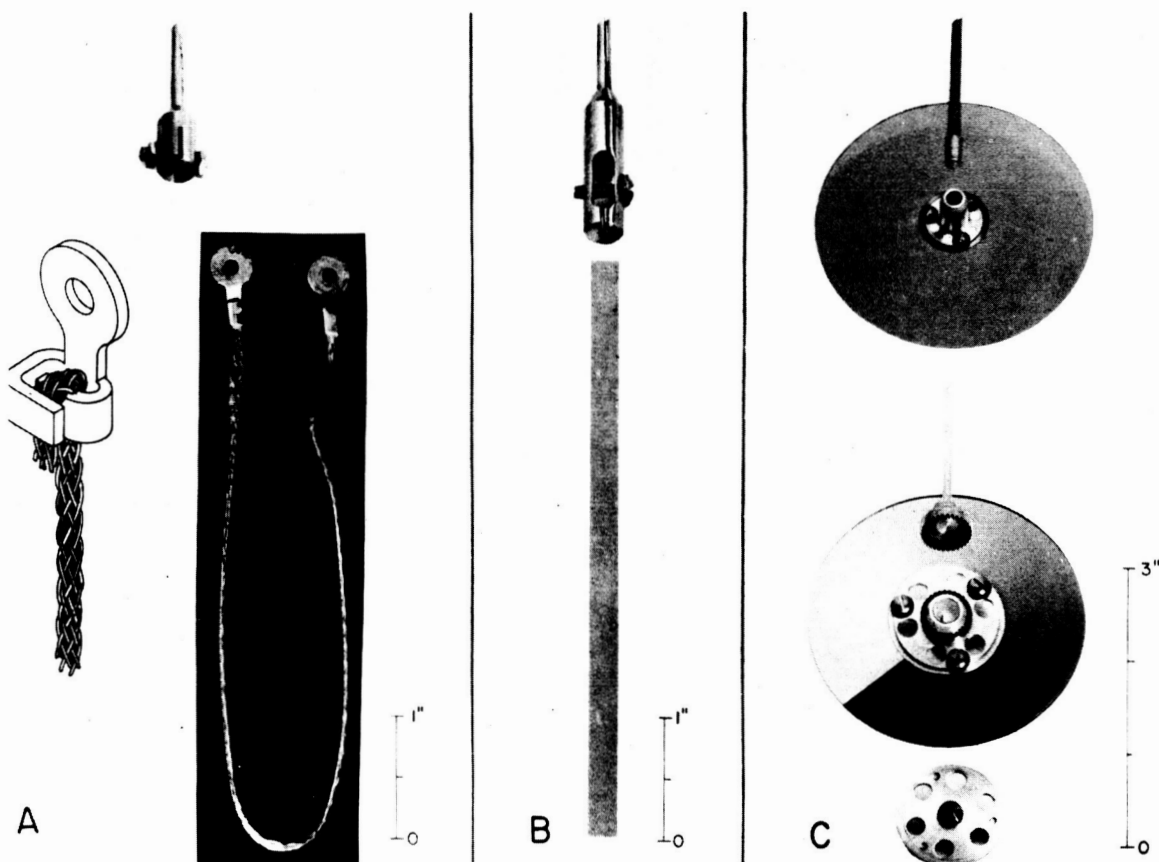

FIGURE 2.   Braid and film specimens, specimen mounting, inertial and transducer discs, supports for discs, and couplings to supporting and extender rods of the pendulum. A) Unimpregnated braid, schematic illustration of the method of placement of the end of the braid into an eyelet so as to prevent slippage, and a braid clamp which clamps an eyelet. B) Free film and film clamp for torsional pendulum experiments. C) At the top is a polarizer disc with a lightweight support for the disc, showing the force-fit coupling for the end of the extender rod which hangs from the specimen. The lower disc is a linear-with-angle transmission (metal-coated) disc. At its center is a support for the disc which incorporates a magnet at its center and serrated teeth at its periphery for coupling with the lower end of the extender rod. The lower end of the extender rod carries a soft iron core and serrated teeth for coupling with the disc support. The lower side of the disc support is shown at the bottom of the figure.

includes a photograph of a film specimen, one of the clamps which is used to mount it, and also shows inertial masses and other couplings.

TORSIONAL BRAID APPARATUS

During the ten years since the introduction of torsional braid analysis, the apparatus has evolved from an all glass instrument[1] using a liquid heat transfer medium, to one (Figure 3) of essentially stainless steel[35] utilizing a fluidized bed[2,4] which operates throughout a wide range of temperatures ($-190°C \leftrightarrow >+650°C$) with minimal temperature spread along the sample. The upper limit of temperature is determined mainly by the inert braid substrate which is used to make the polymer/braid composite specimen. (Figure 39. Cooling curve 625°C $\rightarrow$ $-180°C$ of Se-30
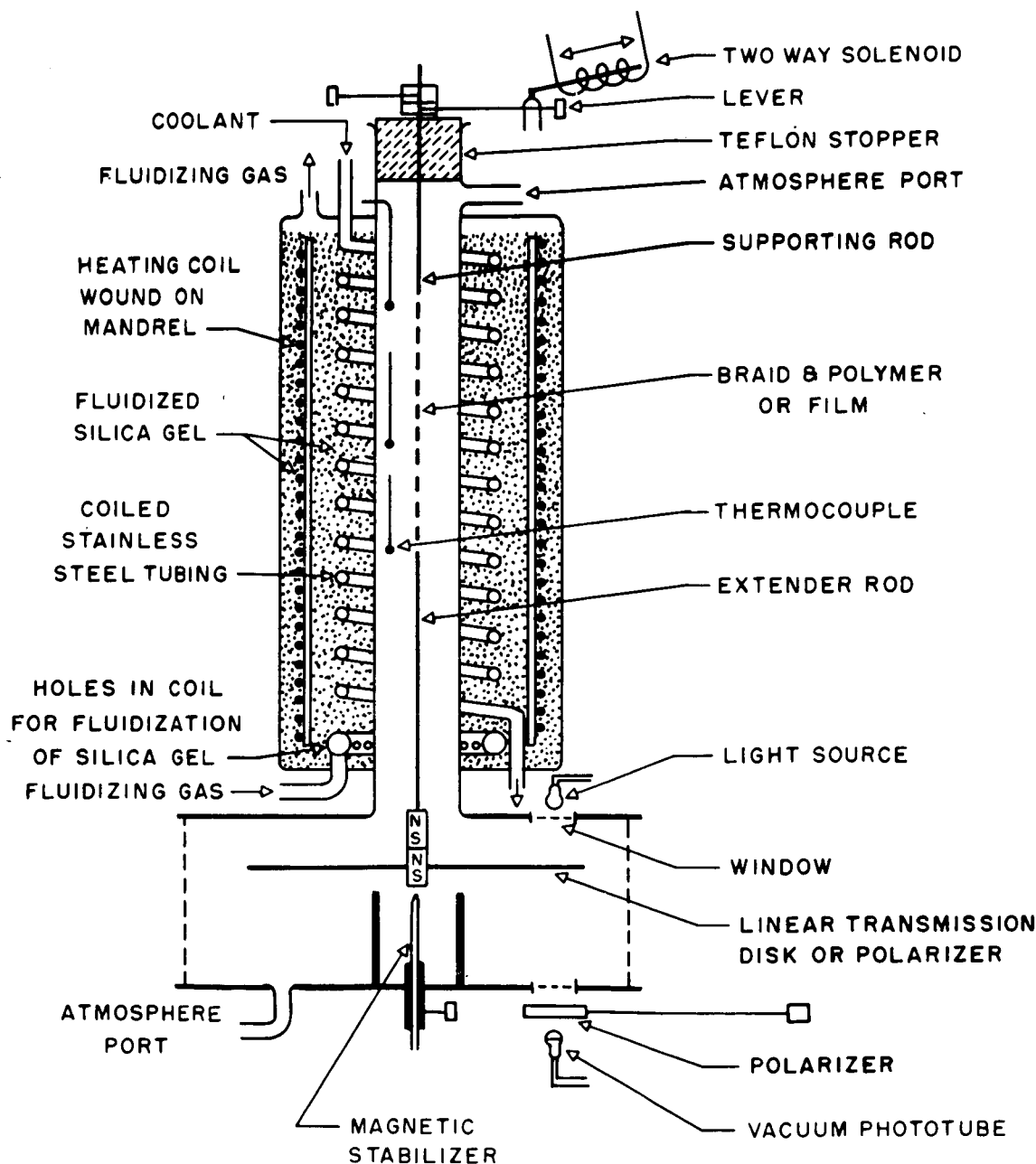

FIGURE 3. Torsional pendulum and torsional braid apparatus of Gillham (schematic).

after complete weight loss.) High-silica glass, high-modulus graphite, amorphous carbon, and quartz braids can be used at temperatures above the limit of the glass braids presently used. Most of the work to date has employed an easy-to-handle loose ($\sim$3 turns/in) braid made from six heat-cleaned glass yarns which form a substrate containing about 3600 single filaments[2,4,35] (Figure 2). The length of the specimen is from 2 to 8 in and is prepared from solutions, with concentrations of from 5 to 100% polymer, by removing solvent in situ. There are several reasons for using a multifilamented support rather than a single filament or rod. A substrate consisting of several thousand filaments can support a relatively large amount of material because of capillary action and the large surface-to-volume ratio. The particular geometry of the two-phase composite minimizes the contribution of the high-modulus component to torsional properties (i.e. anisotropic behavior), and forces the matrix to deform even in the absence of perfect adhesion. The basic premise is related to the behavior of two models, each of which consists of two very different elements of structure: a) in the somewhat analogous situation of drawn organic fibers consisting of crystalline and amorphous elements, the tensile modulus is highly dependent on the draw ratio whereas the torsional modulus is independent of it and b) the response to deformation of a combination of weak and strong springs in series is that of the weak spring. A braid is employed in an attempt to balance any twists in the component yarns. The particular method of mounting (Figure 2) was designed to facilitate the de- and remounting of specimens.

The environment around the specimen is easily controlled: dry nitrogen or vacuum is used for studies of transitions and thermal degradation; oxygen, air, and humidified and ozonized gases, etc., are used in studies of environmental degradation. This control of the environment is facilitated by the absence of electronics within the specimen chamber. A light beam used (see below) to monitor the mechanical oscillations, passes in and out of the chamber through windows.

The pendulum is activated by turning the rod which supports both the specimen and the inertial mass. This is performed by a step-displacement of one of the upper levers (Figure 3) through a small angle using a solenoid, which performs a reverse displacement a predetermined time later. Typical strip chart records of damped waves are illustrated in Figure 4. For a series of alternate waves, a constant neutral position would produce no change in the baseline voltage output of the transducer circuits. However, during changes in the mechanical properties of the polymer, the specimen twists and the positions of the inertial mass and baselines change.

In examining small specimens, it is essential to use a friction-free transducer for converting the mechanical oscillations linearly to a convenient electrical analogue. Since specimens do turn during the experiments, it is also convenient to have a transducer system which need not be centered on a particular reference position. An optical system is used[14,35] in which light from a constant source is attenuated by a linear-with-angle optical transmission wedge, which also serves as the inertial mass of the pendulum. The electrical analogue of the mechanical oscillations is observed by sensing the attenuated light with a linearly-responding photocell circuit. Simple and suitable light and photocell circuits are shown in Figure 5. This optical system gives a differential output which is independent of the neutral position of the oscillations (Figure 6). Suitable transmission discs can be made by vacuum-coating chromium metal onto glass discs.[14] Alternatively,[35] a polarizer disc (Figure 2) can be employed as the inertial member (replacing the metal-coated glass disc of Figure 2) with another polarizer — the analyzer — positioned in the path of the light beam (Figure 3). The ideal neutral position of the mechanical oscillations corresponds to the polarizers' being 45° from the crossed and parallel positions. It can be shown (see Appendix I) that for the range ±15 degrees from the 45° position, the light transmission function ($\cos^2 \theta$) can be approximated by a straight line to within 1.0% error relative to the 45° value (Figure 7). This range (45 ± 15°) for useful light transmission corresponds to one half of the total differential transmission of the pair of polarizers (see Appendix I). Location of the 45° position involves adjustment of the analyzer which is rotated while the inertial disc remains at rest (Figure 8). The minimum or maximum of the analogue voltage signal is initially located, and then the analyzer is moved to the 45° position by means of a step function reorientation within a 45° slot which is machined into its holder. The lower three boxes of Figure 8 show the analogue of the mechanical oscillations with the polarizer
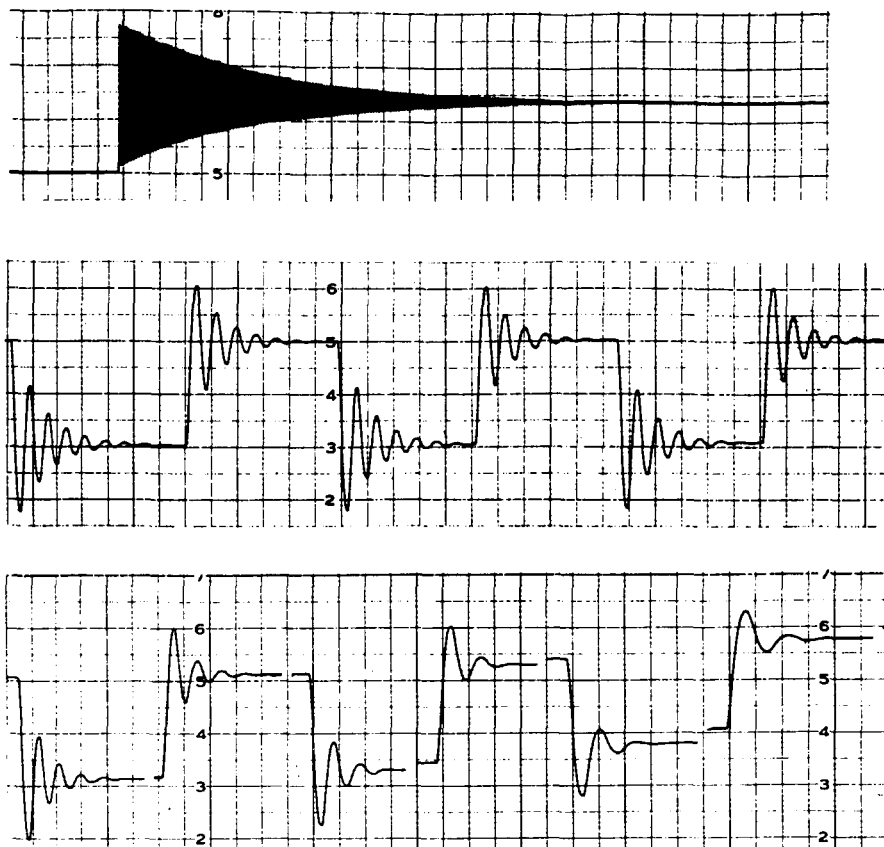
FIGURE 4. Characteristic output of instrument. Response of dried gelatin (a) in the glassy state (b) just below the transition region (c) in the transition region. Note the base-line drift, especially in the vicinity of the transition.

(I)-analyzer (polarizer II) pair in the arbitrary (1), crossed or parallel (2), and 45° (3) relative positions. The polarizer system has the advantages of: 1) the natural basis for the light attenuation (Malus' law) which permits its use at low strain levels (Appendix II); 2) low fabrication and material cost; 3) low mass of the plastic polarizers which is important when dealing with unsupported specimens (Figure 2 shows a polarizer disc with a lightweight support system); 4) ease of handling the plastic discs; 5) the fact that any nonrotational (i.e. translational) motion does not affect the transmission of the light by the pair of polarizers (Appendix III). When the oscillations move outside the linear range, adjustments are made (when the system is not oscillating) in the angular position of the stationary analyzer in order to keep the neutral position and the maximum displacement (used in data reduction) within the linear region (see Appendix I).

There are certain unique features of the

torsional braid analysis technique. The specimen is fabricated simply by drying from solution or forming from prepolymer in situ. Solvent often can be very conveniently removed by heating the specimen above the major transitions of the polymer. Supported samples permit studies in the glassy, rubbery, and fluid states on a single specimen and with one instrument. Small sample size (5 to 100 mg) permits a relatively rapid approach to thermal equilibrium with the chamber and allows dynamic temperature programming with increasing, decreasing, and isothermal temperature modes throughout the range $-190 \rightleftharpoons +650°C$ in a reasonable time. Increasing and decreasing temperature programming reveals features that might be ignored by a unidirectional experiment. TBA produces a mechanical analogue of differential thermal analysis (DTA) and thermogravimetric analysis (TGA).

A main virtue of the technique — its simplicity — may not be apparent from reading the above
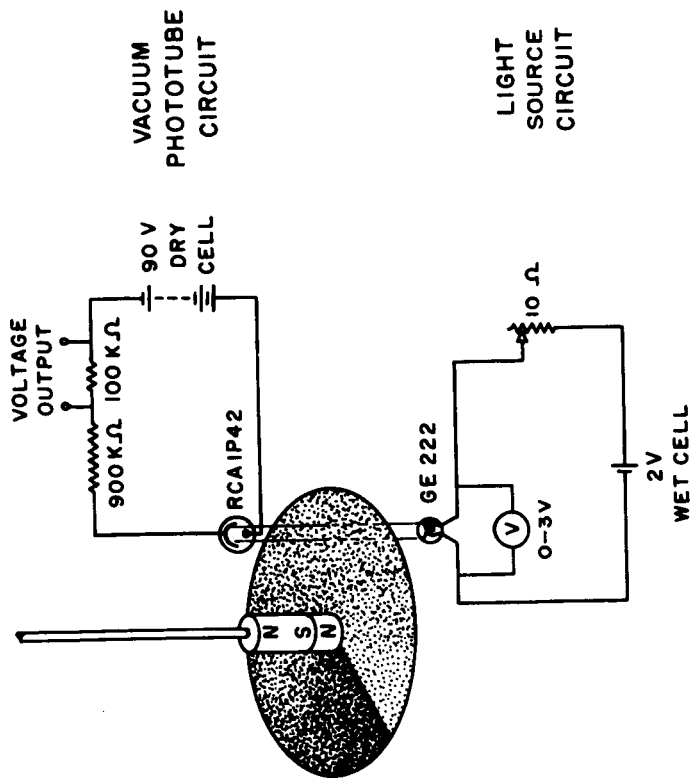
INTENSITY OF
TRANSMITTED LIGHT

PHOTOTUBE CURRENT

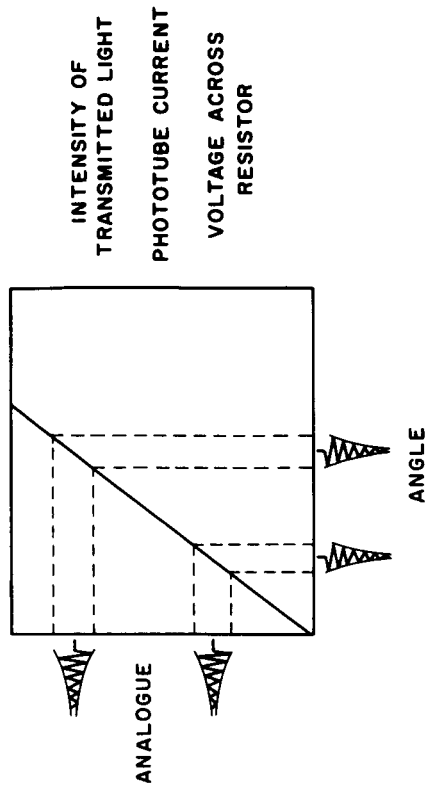VOLTAGE ACROSS
RESISTOR

ANGLE

ANALOGUE

FIGURE 6. Characteristics of a linear transmission system. The figure illustrates that the differential output (intensity of transmitted light) is independent of the neutral position of the mechanical oscillations.
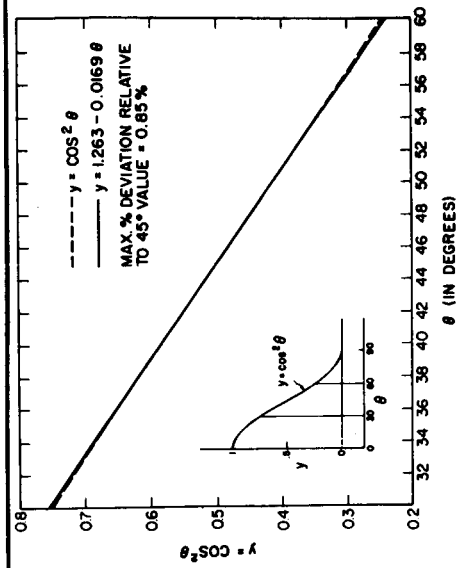
$y = \cos^2\theta$

$y = 1.263 - 0.0169\theta$

MAX. % DEVIATION RELATIVE TO 45° VALUE = 0.85%

θ (IN DEGREES)

$y = \cos^2\theta$

$y \cdot \cos^2\theta$

FIGURE 7. Linearity of $Y = \cos^2\theta$ in 30° to 60° region.

VACUUM
PHOTOTUBE
CIRCUIT

LIGHT
SOURCE
CIRCUIT

90 V
DRY
CELL

VOLTAGE
OUTPUT

900 KΩ 100 KΩ

RCAIP42

GE 222

10 Ω

0-3V

2V
WET CELL

N S N

FIGURE 5. Light source circuit and linearly-responding photocell circuit.

$y = \cos^2 \theta$

| 1 ARBITRARY START | 2 LOCATE MAX. OR MIN. OF LIGHT TRANSMISSION | 3 MOVE ANALYZER 45° |

ANALYZER — POLARIZER II — HOLDER — 45°

RECORDER RESPONSE

TIME → TIME → TIME →

ANALOGUE

TIME → TIME → TIME →

DAMPED UNSYMMETRICAL WAVE
NON-LINEAR RESPONSE

DAMPED RECTIFIED WAVE
NON-LINEAR RESPONSE

DAMPED SINE WAVE
LINEAR RESPONSE

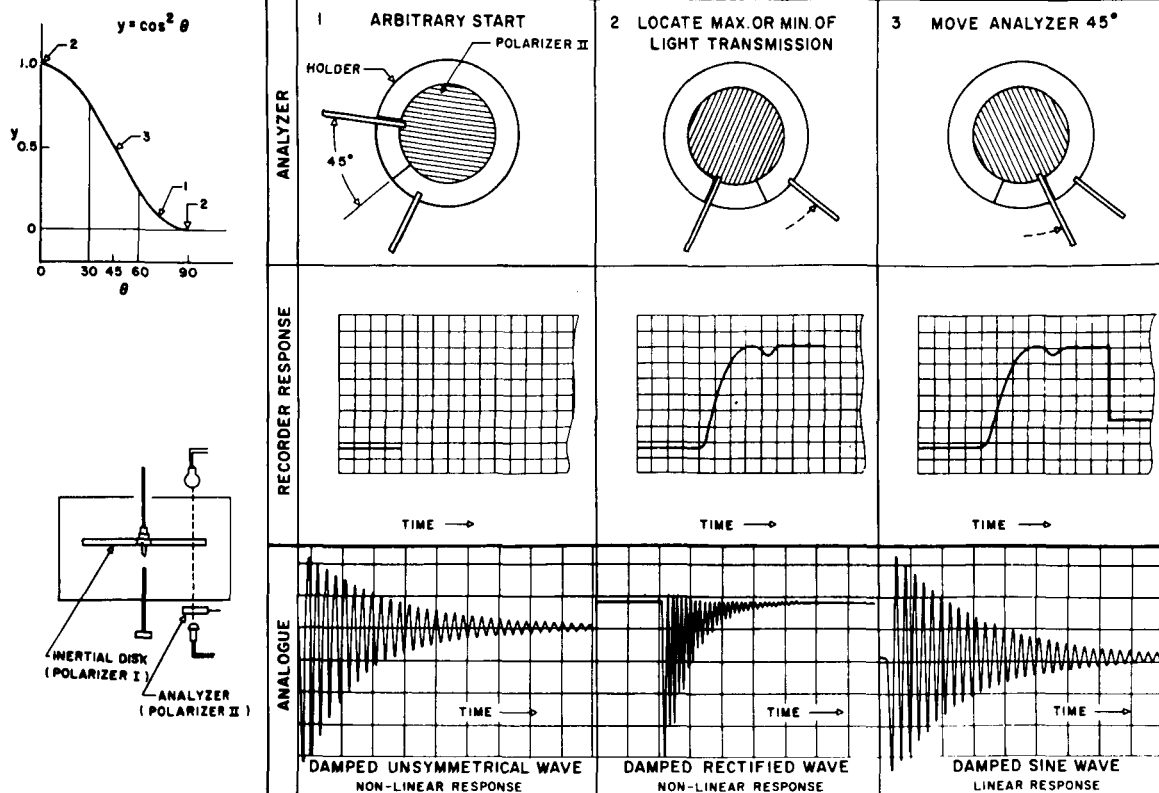INERTIAL DISK (POLARIZER I)
ANALYZER (POLARIZER II)

FIGURE 8. Location of the linear region of a polarizer-analyzer pair by adjustment of the analyzer. On the left are the light transmission function, $Y = \cos^2 \theta$, and a schematic illustration of the optical cell with the inertial disc (polarizer I) and analyzer (polarizer II). The upper horizontal set of figures shows the position of the analyzer (polarizer II) and its slotted holder that correspond to points 1, 2, and 3 on the $Y = \cos^2 \theta$ plot. The middle set of figures shows the response of a strip-chart recorder to the analogue voltage signal in positions 1, 2, and 3. The lower set of figures displays the analogue signal that results from a damped sine wave generated mechanically, with the neutral position centered about positions 1, 2, and 3.

discussion which is concerned with developments in the author's laboratory. Accurate results for the rigidity may be obtained by simply using a stopwatch to monitor the oscillations of a bar which is attached to a polymer-impregnated length of string! Indeed the first publication[1] on the technique was this simple and used a nylon fishline braid as the substrate. A more inert glass braid was used subsequently.[2,4] This original apparatus is shown in Figure 9. It is also valid to obtain an inverse measure of the damping by simply counting the number of oscillations of the bar which can be discerned visually after inducing oscillations.[5,7]

Several commerical-instrumented forms of the torsional braid analyzer are available. An American version (Figure 10) is similar to the author's, differing mainly in that the fluidized bed is not used. A Japanese version is illustrated by a copy of an advertisement (Figure 11). In making a judgment of the performance of any instrument, the linearity of the transducer and the temperature spread along the specimen should be considered as important criteria of performance.

THEORY AND REDUCTION OF DATA (APPENDIX IV)

The ideal torsional pendulum experiment provides a series of damped waves, the envelope of each of which is characterized by a damping constant (α) and the oscillations by a constant frequency (f, in cycles per second) or constant period (P = 1/f, seconds). The equation of the oscillations in a wave is given by
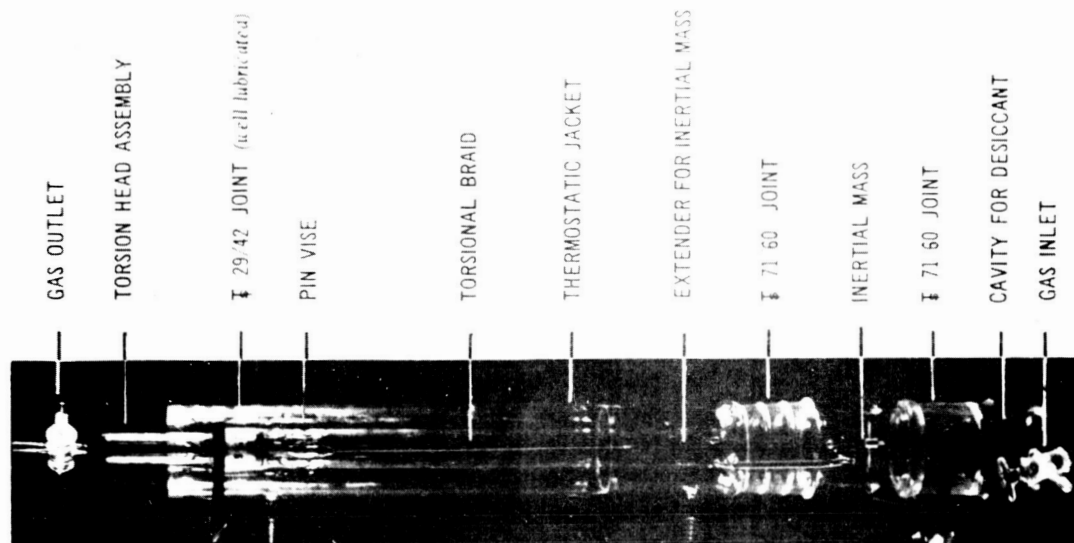
$$A = A_o e^{-\alpha t} \cos 2\pi f t$$

No. 562 Torsional Braid Analysis Tester

Use: For measuring the viscoelastic properties of polymeric materials due to torsional pendulum method.

The specimen is composed of a loosed braided fiberglass substrate impregnated with a solution of the materials to be tested, instead of filmlike, fiberlike and rodlike substrates. (Refer to No. 581 and 504.)

Specifications:

Temperature range: −100°C to 500°C
Cooling medium: Liquid Nitrogen
Gas substitution: possible
Temperature rise: 3°C/min
Temperature accuracy: ±1°C
Specimen length: max. 100 mm
Displacement detection: Rotary differential transformer
Angle of displacement: max. 30°
Frequency range: less than 20 c.p.m.

FIGURE 11. Torsional Braid Analyzer. Commercially available Japanese apparatus. Manufacturer: Toyo Seiki Seisaku-Sho, Ltd., Tokyo, Japan.
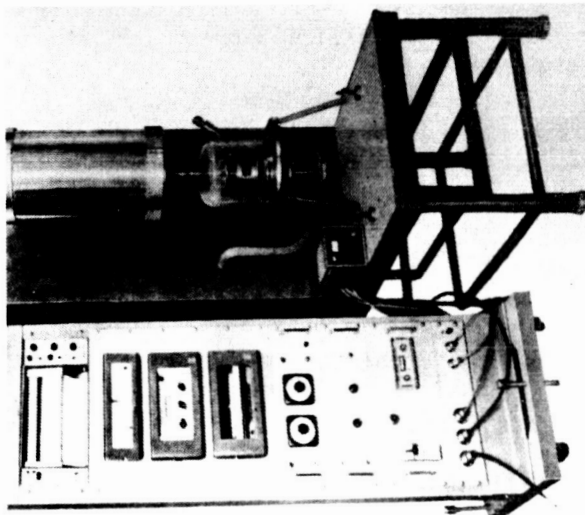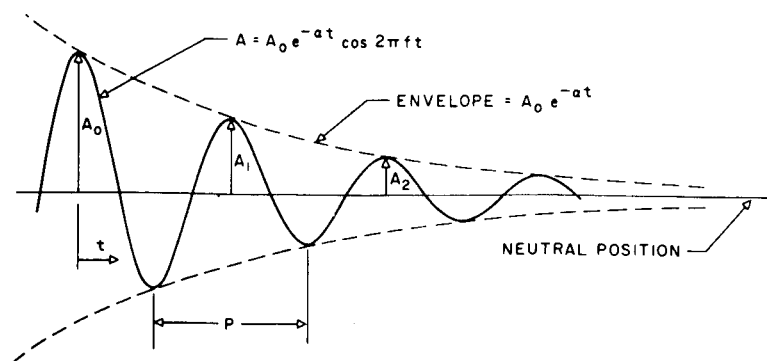
FIGURE 10. Torsional Braid Analyzer. Commercially available American apparatus (after Gillham). Photograph: Courtesy of the Chemical Instruments Corporation, New York.

GAS OUTLET

TORSION HEAD ASSEMBLY

⟂ 29/42 JOINT (well lubricated)

PIN VISE

TORSIONAL BRAID

THERMOSTATIC JACKET

EXTENDER FOR INERTIAL MASS

⟂ 71 60 JOINT

INERTIAL MASS

⟂ 71 60 JOINT

CAVITY FOR DESICCANT

GAS INLET

FIGURE 9. First published (1962) torsional braid apparatus (Lewis and Gillham).

FIGURE 12. Damped cosine ($\equiv$ sine) wave. The equation of the oscillations of the wave is: $A = A_0e^{-\alpha t}\cos 2\pi ft$. The equation of the envelope of the wave is: $A_0e^{-\alpha t}$.

where A is the angular amplitude, t is the time, and A_0 is a constant corresponding to the amplitude at $t = 0$ (see Figure 12). The equation results from solution of the equation of motion of the oscillating system.[51] Experimentally, the period and logarithmic decrement, Δ (= $\alpha \times 1/f$), are measured. The logarithmic decrement is calculated from successive amplitudes of the decaying oscillations:

$$\Delta = \log_e (A_1/A_2) = \log_e (A_2/A_3) = \cdots$$

$$= \log_e (A_i/A_{i+1}) \quad ,$$

where A_i is the amplitude of the ith peak. The results of a torsional pendulum experiment are presented as two separate functions of temperature. G' (often designated by G), the "storage", "elastic", or "in-phase" shear modulus, relates to the storage of energy on mechanical deformation — the maximum (potential) energy per cycle = $\frac{1}{2} \times G' \times$ (peak deformation) squared. The other function relates directly to the ratio of the energy dissipated (ΔW) to the maximum energy stored (W) per cycle and is characterized by the logarithmic decrement, Δ ($\simeq \frac{1}{2} \times \Delta W/W$). Two other parameters, which are used equivalently with dynamic mechanical experiments for characterizing $\Delta W/W$ are the phase angle, δ (usually as $\tan\delta$), and G''/G' (= $\tan\delta$). G'' is the material parameter which determines the dissipation of energy on cyclic mechanical deformation — the energy dissipated per cycle (ΔW) $\simeq \pi G'' \times$ (peak deformation) squared (when the dissipation is small). Relationships between G', G'', δ, ΔW, W, α and Δ are derived in Appendix IV.

For a torsional pendulum, $G' \simeq (8\pi lL/r^4) \times$

$(1/P^2)$ dynes per square centimeter for rod-like specimens, while for specimens of rectangular, cross section, $G' \simeq (64 \pi^2 IL/\mu bt^3) (1/P^2)$ dynes per square centimeter, where I = moment of inertia of the inertial member, $g\text{-}cm^2$; P = period of oscillation, sec; L = length of specimen, cm; b = width of specimen, cm; t = thickness of specimen, cm; r = radius of specimen, cm; and μ = shape factor for rectangular cross sections.[50,51]

In making measurements with small specimens and with specimens of irregular geometry (as in torsional braid analysis), difficulties are encountered in measuring dimensions accurately. Therefore, in work discussed herein, the elastic part of the complex modulus is replaced by the defining expression: Relative Rigidity = $(1/P^2)$. P is obtained by dividing the lapsed time for a conveniently large number of oscillations by that number. This expression implicitly assumes that the contribution of dimensional changes to the value of the relative rigidity parameter is dominated by changes in the modulus of the polymer. It is interesting to note that any uniform weight loss of a homogeneous specimen, with all other parameters remaining constant, would decrease $1/P^2$ by a factor equal to that weight loss. When large percentages of polymer disappear, as in degradation, caution in interpretation is necessary. The first question to be raised is whether or not decreases in the relative rigidity parameter are more than can be accounted for by dimensional changes. A similar problem exists with all other mechanical techniques.

A measure of the logarithmic decrement can be obtained[4,7] rapidly for each member of a series of waves, by simply counting the number (n) of

FIGURE 13. Data compiler for Torsional Braid Analyzer. Photograph: Courtesy of the Chemical Instruments Corporation, New York.

oscillations between two fixed but arbitrary boundary amplitudes (e.g. A_i/A_{i+n} = 20). $1/n$ is directly proportional to Δ and is termed the Mechanical Damping Index ($\Delta = 1/n \log_e [A_i/A_{i+n}]$).

The TBA experiments use a composite specimen with a polymer matrix and a multi-filament loose glass braid as the substrate. The energy dissipated in torsionally deforming the composite specimen of polymer and longitudinal glass filaments is predominantly involved in straining the viscoelastic matrix. Changes in the relative rigidity and damping index parameters are interpreted as far as possible in terms of changes in the polymer.

Several methods are in use for electronically reducing the experimental electrical analogue of the mechanical oscillations. In one[33,37] the generated damped waves are digitalized, recorded on magnetic tape, and subsequently analyzed using a digital computer. In a second method,[36,52] a bench-top system measures the peak amplitudes and their times and presents the required parameters (G' and Δ) immediately to the experimentor on a digital counter or printed paper tape. A commercially available data compiler is shown in Figure 13. An inexpensive laboratory-built instrument[52] is used by the author.

The data which have been reported to date (and in this review) have been calculated by hand-reduction methods, or by machine-reduction programs which have simulated hand-reduction. For example, the damping has been machine-reduced by measuring n, which in effect is a digital scale incapable of resolving Δ to better than 1 part in 1000 parts. The current methods of using most of the wave to determine $1/n$ seriously limits the resolution of the data (vs. temperature and time) further, since a single wave is assigned one temperature and in the glassy state the time of decay of the oscillations through the two boundary conditions can be as long as 20 min. Complications also arise from the amplitude-dependence of the period, especially when the period is obtained by averaging a different number of cycles for different waves. Application of the torsional braid apparatus as a torsional pendulum for examining thin free-films quantitatively has been limited because the oscillations of thin films (e.g. 0.001 in. thick) take even longer to decay than the composite specimens of TBA. The immediate future will see a drastic improvement in the accuracy and resolution of the mechanical spectra produced both by torsional braid analyses (TBA), and by torsional pendulum experiments on thin unsupported films. Analyses will be made by

programs which determine the desired parameters (e.g. ω, Δ,T) using only a few cycles and a rapid sampling of many digits of the digitalized analogue signals. This will be an important development for the reason that thermomechanical spectra can be complex (e.g. see Polyimide spectra) and it is these complexities which confer the subtle and important differences in behavior between polymeric materials. This will be facilitated for the author by the "on-line" connection of the analogue signals (of the experiment) to a response-type digital computer (IBM/1800) which in turn is connected to another very powerful digital computer (IBM/91).

As an example of reduced data and their correlation with other techniques, the thermomechanical spectra of a specimen of highly acetylated cellulose triacetate, together with the corresponding results for thermogravimetric (TGA) and differential thermal analyses (DTA), are presented[14,15] in Figure 14. The glass transition (T_g) in the vicinity of 190°C is accompanied by a drastic decrease in rigidity, a prominent maximum in damping, and an endothermic shift in DTA. The subsequent increase in rigidity at temperatures above 200°C is attributed to crystallization and/or chain stiffening processes and is accompanied by an exothermic maximum (DTA). The melting transition (T_m) at 290°C is accompanied by an abrupt decrease in rigidity, a maximum in damping, and an endothermic maximum (DTA). The subsequent increase in rigidity, decrease in damping, exotherm (DTA), and weight loss (TGA) are attributed to crosslinking and/or chain stiffening processes.

The bottom diagram of Figure 14 shows the drift of the neutral position of the inertial mass vs. temperature for a composite specimen of the cellulose triacetate and glass braid. The specimen was not oscillated. The motion is a consequence of the stresses which develop in the composite sample. The sense of the drift correlates with the expansion or the contraction of the matrix. It is seen that drifts which correspond to the glass and melting transitions (which are accompanied by volume expansion of the matrix) are in the opposite sense to the processes corresponding to crystallization and crosslinking (which are accompanied by volume-contraction of the matrix).

APPLICATIONS

I. Torsional Pendulum and Torsional Braid Analyses of a Polyimide Film and Polyimide-Forming Varnish[29,35]

Thermomechanical spectra of polymers are often sufficiently complex to serve as "fingerprints" of the combined effects of composition and thermal prehistory. Illustrative of this is a comparative study of torsional pendulum results on an intractable (infusible and insoluble) polyimide film and TBA results on a polyimide-forming varnish. The two materials are commercially available from the Du Pont Company, which provides little information on differences between them.

1. Kapton® ("H"-film) was examined as a free film with dimensions: 0.0045 in. x 0.17 in. x 5 in. in a torsional pendulum experiment with tensile stress <70 psi.

2. Pyre-M.L.®. A TBA braid was impregnated with a 7.5% solution in dimethylacetamide (b.p. = 166°C) and N-methyl 2-pyrrolidone (b.p. = 202°C).

Both specimens were preheated from 25°C to 300°C at 3°C/min in dried nitrogen. In the case of the Pyre-M. L.® varnish, this involved removal of solvent and curing (ring-closure reaction of the polyamic acid). In the case of the "H"-film this was done in order to duplicate the prehistory of the Pyre-M. L.® (and tacitly assumed that previous thermal treatment of the "H"-film was to less than 300°C) and to remove any moisture and residual solvent.

From the data (Figure 15), generated at 3°C/min in dried nitrogen, both polyimides appeared to be mechanically very similar, with damping maxima peaking at about -90°C, +30°C +200°C, and +400°C. In terms of the rigidity modulus, both materials displayed a steady decline from -180°C to about 300°C, with subtle inflections at temperatures corresponding approximately to those of the damping peaks. Above 300°C both rigidity curves decreased at an increasing rate to a minimum at about 450°C and then displayed a small rise at 500°C. The large decrease in rigidity, coupled with the magnitude of the 400°C damping (relative to the peaks at lower temperatures) would lead one to suspect that this was the glass transition region. In both materials
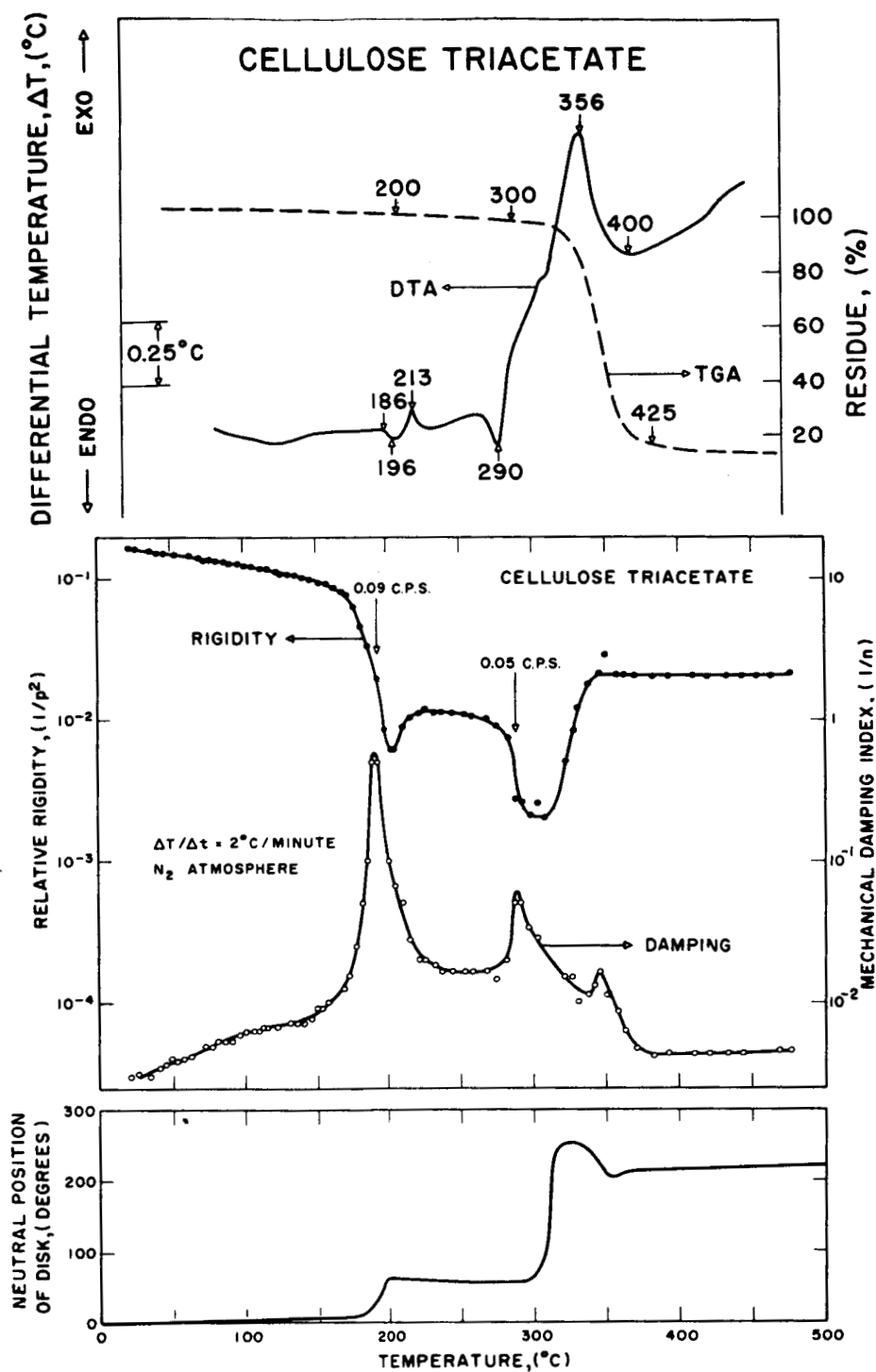
FIGURE 14. Cellulose triacetate: Comparison of thermomechanical (TBA), differential thermal analysis (DTA) and thermogravimetric analysis (TGA) data. The bottom figure shows the twisting which the composite specimen undergoes with changing temperature (even in the absence of oscillations). The senses of twisting correspond to expansion (e.g., at T_g and T_m) and to contraction (e.g., with crystallization and crosslinking) of the polymer matrix.
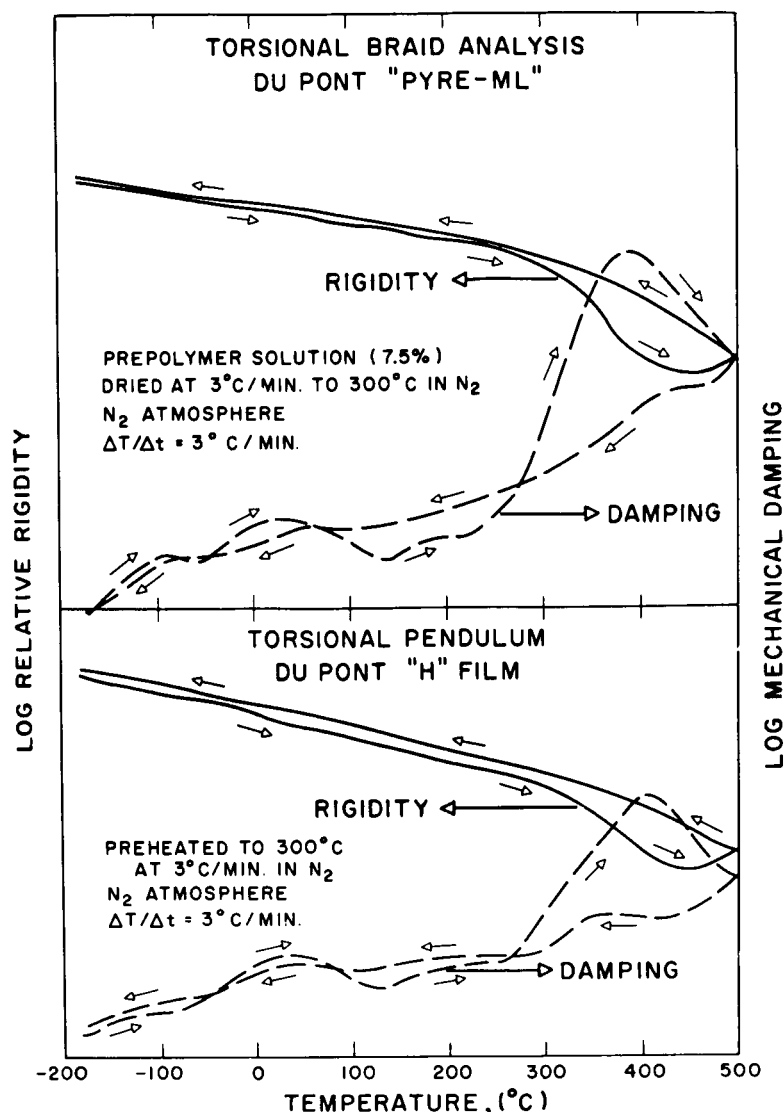
FIGURE 15. Torsional pendulum and Torsional Braid Analyses as "finger-prints" of thermomechanical behavior. The upper figure shows the thermomechanical behavior of a cured polyimide-forming varnish while the lower figure shows the thermomechanical behavior of a polyimide film.

the peak was broad and skewed. The shape of the damping peak and the corresponding upturn in the relative rigidity parameter indicated that a degree of chain stiffening and/or crosslinking occurred in the region of the glass transition, where molecular motion and diffusive processes increase by orders of magnitude. For both polymers the thermal cure raised and broadened the glass transition region in a manner consistent with contemporary theories on the subject. On the other hand, although the 200°C shoulder- had disappeared, the 50°C and -90°C peaks remained after the pyrolysis to

500°C. The implication was that whatever the mechanism of the stiffening process, it was of long enough range so as not to interfere with the short-range motions associated with the low temperature damping peaks. Figure 16 is a plot of TGA data in argon for "H"-film and Pyre-M. L.®; both were preheated to 300°C at 3°C/min in argon. In an inert atmosphere, both polymers retained 98% of their postdrying sample weight to 500°C. Both thermograms were basically the same until beyond 600°C where the Pyre-M. L.® lost more weight, which provided evidence for there

DU PONT POLYIMIDES

A— "H" FILM
B— PYRE - ML

ΔT/Δt = 3°C/ MIN.
ARGON ATMOSPHERE
(PREHEATED TO 300°C)

WEIGHT FRACTION VOLATILIZED

0
0.2
0.4
0.6
0.8
1.0

TEMPERATURE ,(°C)

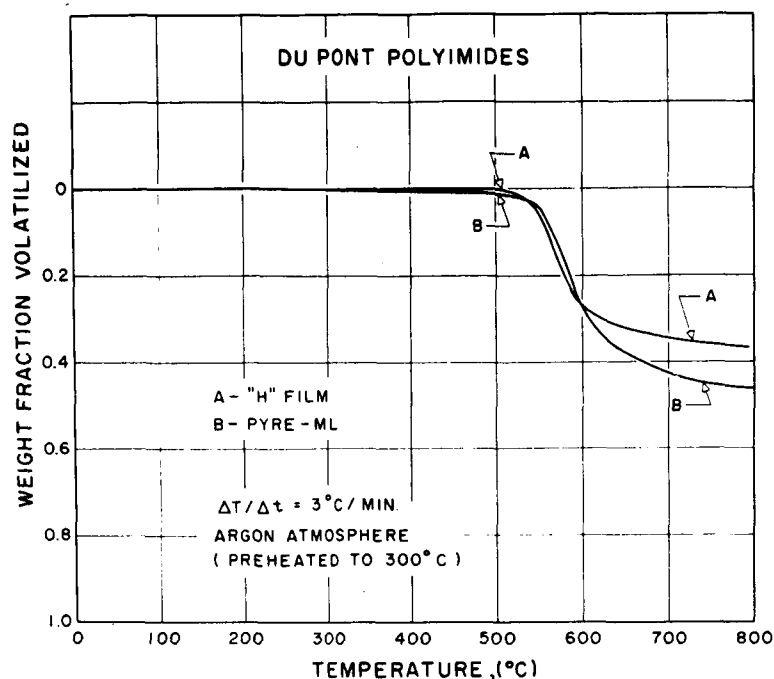0   100   200   300   400   500   600   700   800

FIGURE 16. Thermogravimetric analyses (TGA) of "H"-film and cured Pyre-M.L.® varnish in argon.
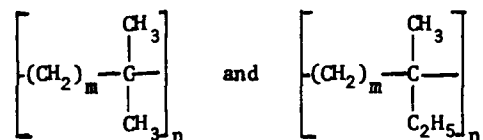
being some differences between the "H"-film and cured Pyre-M. L. ® polyimides.

It is of interest that the thermomechanical spectra of these commercially available polymers are very similar to the spectra of polyimides made from the reaction of pyromellitic dianhydride and certain "flexible" diamines (Figure 27: p,p'-methylene dianiline and p,p'-diamino benzophenone, and p,p'-diamino diphenyl ether[48]).

II. Amorphous Polyolefins[41,58]

In order to elucidate the molecular mechanisms of the transition and relaxation processes in solid polymers, many investigations have been undertaken[51,53-55] using three techniques for the most part: mechanical spectroscopy, dielectric loss, and nuclear magnetic resonance. These studies have shown that amorphous polymers display at least two types of dispersion processes, the high temperature process being attributed to longer range segmental motions of the main chain, while the low temperature ones are attributed either to the motion of side groups or to local relaxation modes of the main chain. In crystalline polymers, in addition to the relaxation processes associated with the amorphous regions, additional processes associated with the crystalline transitions occur.

The availability of a semimicro technique expands the applicability of dynamic mechanical methods to a host of materials made by the organic chemist. Series of structually similar polymers are being collected, studies of which will provide insights into the molecular basis of mechanical behavior in terms of the relaxations which are so easily identified by low frequency dynamic mechanical methods. Application of TBA to two series of polyolefins represented by the formulae

$$\left[(CH_2)_m - \underset{\underset{CH_3}{|}}{\overset{\overset{CH_3}{|}}{C}} - \right]_n \quad and \quad \left[(CH_2)_m - \underset{\underset{C_2H_5}{|}}{\overset{\overset{CH_3}{|}}{C}} - \right]_n$$

where   m = 1,2,3 . . .

follows. These polymers are of fundamental importance to polymer science and yet have been neglected. A reason for their importance lies in the systematic in-chain variation of one -CH₂- between consecutive members of each homologous series, since it is the structure and influence of the main chain per se which is central to polymeric behavior. A reason for the neglect is that synthetic problems remain. The absence of polar forces and

crystallinity eliminates variables which would complicate the discussion. The polymers were synthesized by cationic polymerization of alpha olefins.[56] They were provided by Professor J. P. Kennedy of The Institute of Polymer Science, Akron, Ohio. The first ^{member} of each series (m = 1) results from 1-2 polymerization of the parent monomer. The resulting polymeric structures for the second and third members of the series do not represent simple 1-2 addition, but display structures resulting from isomerization of each terminal monomer residue unit before the propagation step. For these polymerizations, the isomerization is a hydride shift favored by the thermodynamic stability of the tertiary carbenium ion. The solution polymerizations are carried out at low temperatures (-78 to -130°C) so that the hydride shift can occur before the propagation step and also so that other competing reactions (e.g. transfer by proton elimination which leads to low molecular weight species) are rendered less competitive. By way of illustration, the steps which determine the polymeric repeat unit which arises from the monomer 3-methyl-1-butene are summarized in Figure 17.

The third member of each series does not display a completely isomerized structure. Because two consecutive hydride shifts are required to form the stable tertiary carbenium ion, some propagation occurs before complete isomerization, and results in "1-2" and "1-3" repeat units being

ISOMERIZATION POLYMERIZATION

FIGURE 17. Initiation, hydride shift, and propagation steps in the cationic isomerization polymerization of 3-methyl-1-butene.

incorporated into the chain.[57] Studies are currently being directed toward obtaining pure forms of the third member of each series by determining the effect of polymerization variables, especially temperature, solvent, and counterion, upon the hydride shift reaction and ultimately upon the resulting polymer microstructure.[58] For the sake of discussion, the third member of each series is assumed pure in the interpretation of the mechanical results; as discussed below, this assumption does not alter the general pattern of the conclusions.

The high resolution solution NMR spectra of each of the polymers are shown in Figure 18. The spectra for the first two members of each series are consistent with the pure structures, whereas the spectra for the third members show the presence of undesired complexities.

The dynamic thermomechanical spectra (~1 cps) of the polymers are shown in Figures 19 and 20; the curves are displaced vertically for purposes of clarity without altering their shapes. Torsional braid analysis provides a convenient method for obtaining the dynamic mechanical spectra because of the physical difficulties which would be encountered in preparing other types of specimens (e.g. films and molded bars) from materials which are rubbery and gummy at room temperature. The specimens used were prepared by solvent-casting onto a glass braid from a 5 to 10% solution of polymer in n-heptane (b.p. 98.4°C); solvent was removed by heating to 200°C ($\Delta T/\Delta t = 2$°C/min) in a flowing nitrogen atmosphere. Since identical spectra were obtained in both heating and cooling modes of operation, and, in addition, no changes in the spectra were observed in recycling the specimens over the temperature range of the experiments, crystallinity was considered to be absent. The essential features of the spectra, using the loss peaks for assignment of transition temperatures, are summarized in Table 1. Molecular weights were estimated from intrinsic viscosity data using an equation for polyisobutylene.

The frequency dependence of the transitions of polyolefins of the first series is presented in Figure 21. These dielectric measurements[59] confirmed (by extrapolation) the assignments of the mechanically-determined transitions, and in addition revealed a secondary transition in the second member which was not observed mechanically above -180°C. The dielectrically determined
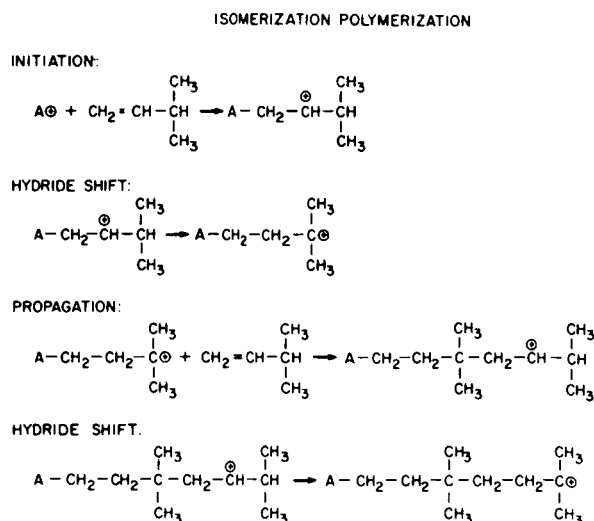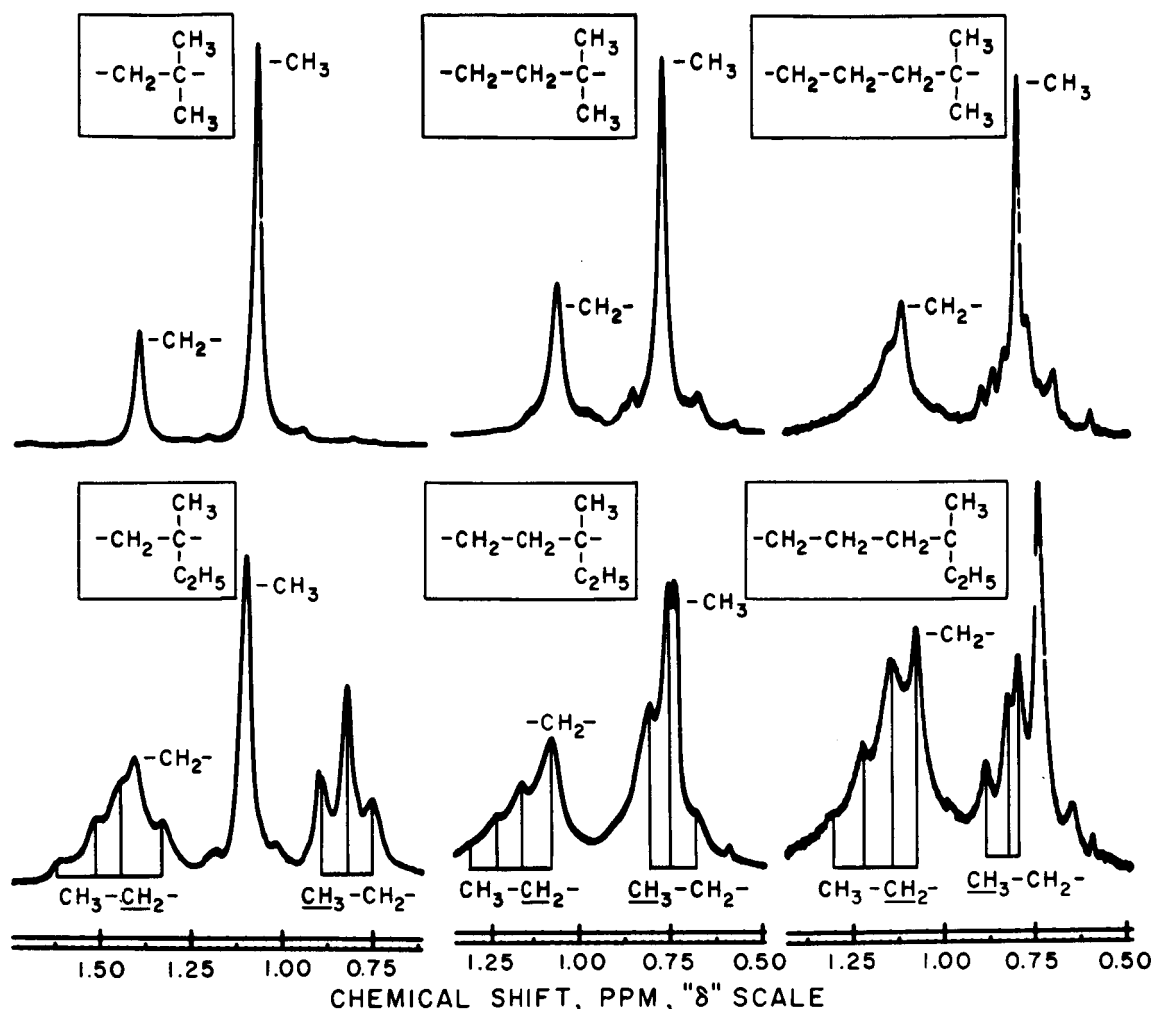
FIGURE 18. High resolution 100 MHz NMR spectra obtained at 90°C using 20% solutions of polymer in hexachloro-1,3-butadiene.

activation energies for the loss processes of the relaxations are included in Table 1.

Table 1 also includes a value for a secondary transition (-229°C at 0.8 cps) for polyisobutylene. This was obtained on a TBA specimen with measurements made above 4°K in a suitable apparatus.[43]

The glass transition is identifiable by a sharp damping peak with a concommitant abrupt drop in modulus as the material passes from the glassy to the rubbery state. From a molecular viewpoint the glass transition represents the onset of large scale rotations and oscillations of submolecular segments which through thermal expansion have acquired the necessary free volume for the process to occur.

In both series studied, the glass transition

temperature rises going from the first to the second member of the series and then decreases going from the second to the third member of the series. The effect is less pronounced in the second series, $[-(CH_2)_m-C(CH_3)\,(C_2H_5)-]$, Figure 20, than in the first, $[-(CH_2)_m-C(CH_3)_2-]$, Figure 19. Although the molecular weights within a series are not strictly comparable, higher molecular weight for the second member of the first series would, if anything, raise the glass transition temperature and not affect the general pattern of results. Similarly, a lower molecular weight for the third member of the second series would, if anything, lower the glass transition temperature with the maximum in the second member of the series still being retained. Mechanically obtained glass transition temperatures ($\sim$1 cps) have been reported[60] for
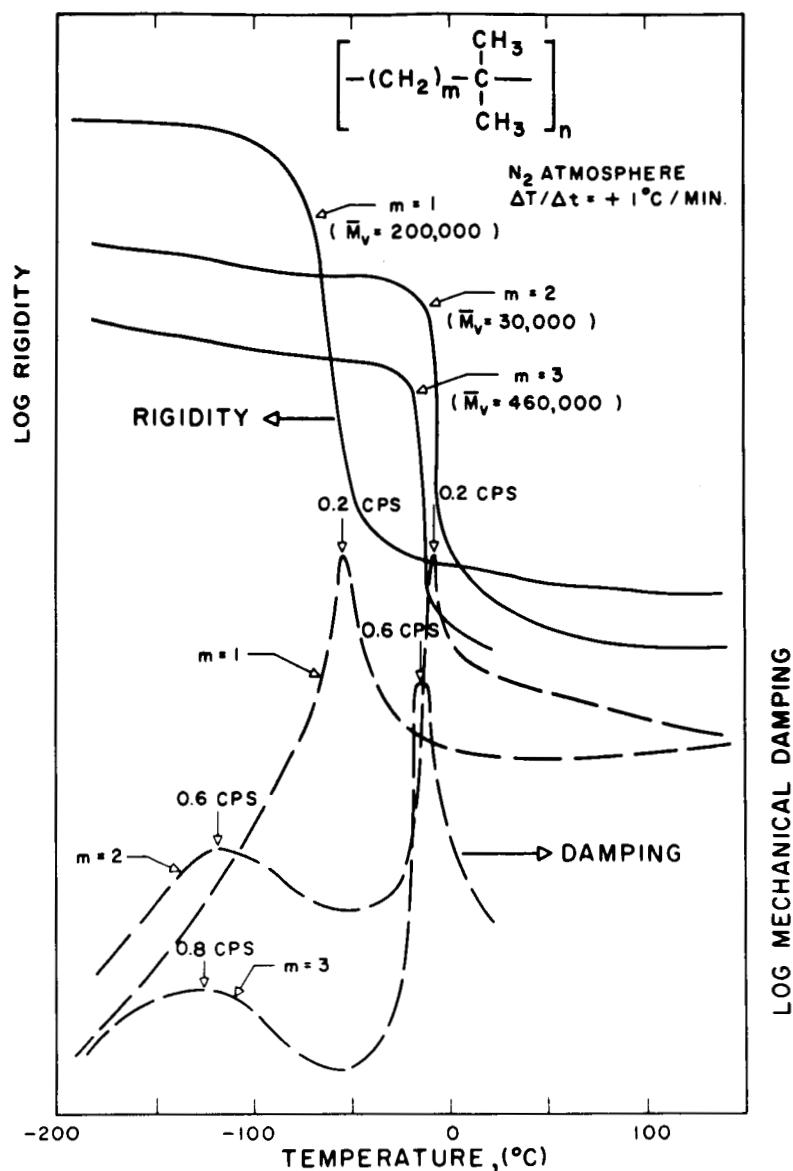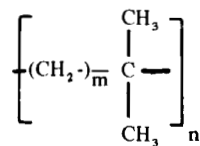
FIGURE 19. Thermomechanical spectra of a series of amorphous polyolefins
with repeat structure:

$$\left[(CH_2\text{-})_{\overline{m}}\; \underset{\underset{CH_3}{|}}{\overset{\overset{CH_3}{|}}{C}} \text{---} \right]_n$$

members of the first series; within the limits of
experimental error, these results are in agreement
with the results presented here.

The molecular structure of the first member of
each series exhibits a high degree of *intra*molecular
steric hindrance which could be expected to
decrease along each series with increasing number
of in-chain contiguous methylene groups. Other
things being equal, the effect of this *intra*molecu-
lar steric hindrance should be to raise the glass
transition temperature so that the glass transition
temperature would decrease along each series.
Such an effect is observed in the glass transition
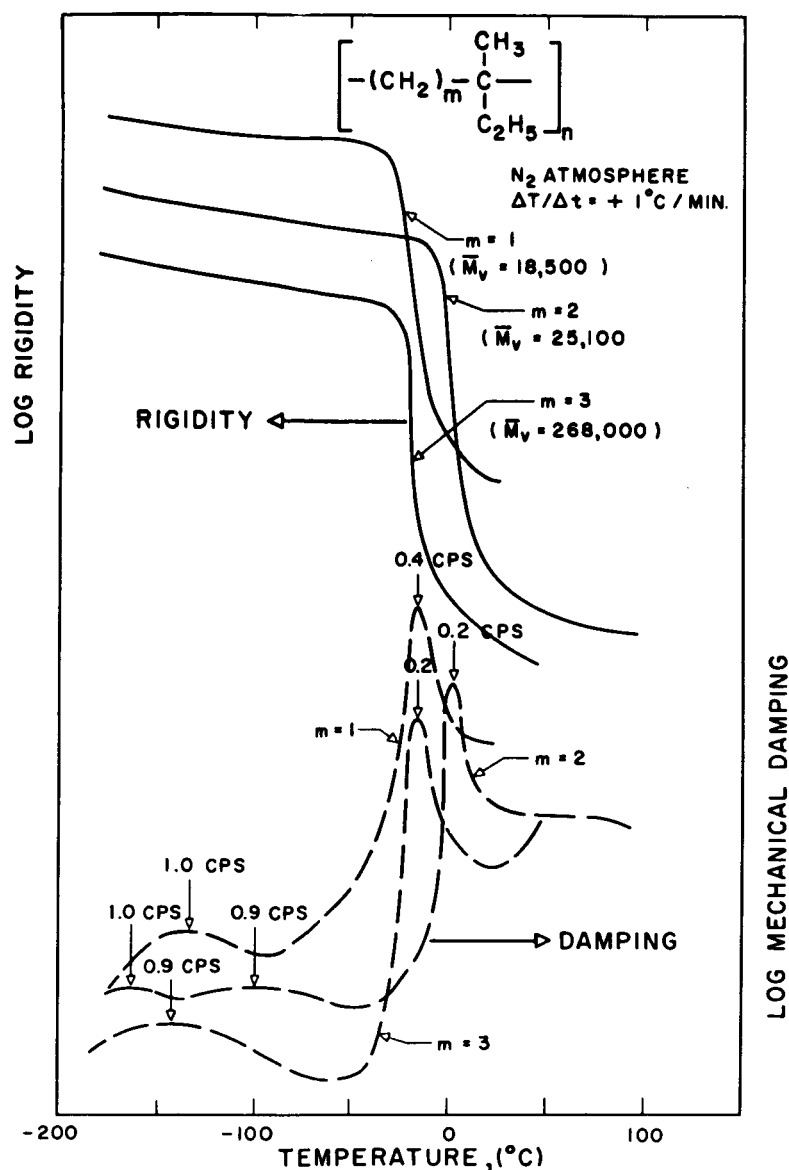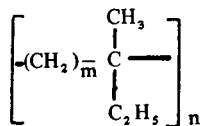temperatures of a series of polymethylene

$$\left[-(CH_2)_m-\overset{\overset{\textstyle CH_3}{|}}{\underset{\underset{\textstyle C_2H_5}{|}}{C}}-\right]_n$$

N$_2$ ATMOSPHERE
$\Delta T/\Delta t = + 1°C / MIN.$

m = 1
($\bar{M}_v$ = 18,500)

m = 2
($\bar{M}_v$ = 25,100

m = 3
($\bar{M}_v$ = 268,000)

LOG RIGIDITY

RIGIDITY ◁

0.4 CPS

0.2 CPS

0.2

m = 1

m = 2

1.0 CPS

1.0 CPS   0.9 CPS

0.9 CPS

DAMPING

m = 3

LOG MECHANICAL DAMPING

-200   -100   0   100
TEMPERATURE, (°C)

FIGURE 20. Thermomechanical spectra of a series of amorphous polyolefins with repeat structure:

$$\left[-(CH_2)_{\overline{m}}-\overset{\overset{\textstyle CH_3}{|}}{\underset{\underset{\textstyle C_2H_5}{|}}{C}}-\right]_n$$

terephthalates[61] and polymethylene oxides[62] where the dominance of *intra*molecular effects causes the glass transition temperature to decrease with increasing number of in-chain contiguous methylene groups. Since, in the polymer series investigated here, this regular decrease in glass transition temperature along each series is not observed (i.e., the glass transition temperature is at a maximum for the second member of each series), it would seem that in these polymers the dominant factors determining the glass transition temperature are *inter*molecular rather than *intra*molecular. Since the polymers are nonpolar, the observed *inter*molecular effects must arise from geometrical rather than polar effects.

These conclusions rest upon the supposition of

	$\bar{M}_v$	GLASS TRANSITION	SECONDARY TRANSITION	NMR CHEMICAL SHIFTS* PPM, "δ" SCALE	
				$-CH_2-$	$-CH_3$
$-CH_2-\overset{\overset{\displaystyle CH_3}{\mid}}{\underset{\underset{\displaystyle CH_3}{\mid}}{C}}-$	200,000	-65°C (0.2 CPS) (22 KCAL/MOLE)	-229°C (0.8 CPS)	1.40	1.07
$-CH_2-CH_2-\overset{\overset{\displaystyle CH_3}{\mid}}{\underset{\underset{\displaystyle CH_3}{\mid}}{C}}-$	30,000	-7°C (0.2 CPS) (48 KCAL/MOLE)	-115°C (0.6 CPS) (12 KCAL/MOLE); -148°C (100 Hz) (4 KCAL/MOLE)	1.055	0.76
$-CH_2-CH_2-CH_2-\overset{\overset{\displaystyle CH_3}{\mid}}{\underset{\underset{\displaystyle CH_3}{\mid}}{C}}-$	460,000	-15°C (0.4 CPS) (44 KCAL/MOLE)	-130°C (0.8 CPS) (9 KCAL/MOLE)	1.105	0.785
$-CH_2-\overset{\overset{\displaystyle CH_3}{\mid}}{\underset{\underset{\displaystyle C_2H_5}{\mid}}{C}}-$	18,500	-20°C (0.4 CPS)	-140°C (1 CPS)	1.40	1.10
$-CH_2-CH_2-\overset{\overset{\displaystyle CH_3}{\mid}}{\underset{\underset{\displaystyle C_2H_5}{\mid}}{C}}-$	25,100	+5°C (0.2 CPS) (44 KCAL/MOLE)	-100°C (0.9 CPS) (9 KCAL/MOLE); -165°C (1 CPS) (6 KCAL/MOLE)	1.075	0.75
$-CH_2-CH_2-CH_2-\overset{\overset{\displaystyle CH_3}{\mid}}{\underset{\underset{\displaystyle C_2H_5}{\mid}}{C}}-$	268,000	-15°C (0.2 CPS)	-145°C (0.9 CPS)	1.055	0.73

* 20% SOLUTION IN HEXACHLORO-1,3-BUTADIENE; 100 MHz; 90°C

TABLE 1. Amorphous Polyolefins: Summary of Formulae, Molecular Weights, Transitions and Activation Energies, and NMR Chemical Shifts.

increased *intra*molecular flexibility with increasing number of in-chain contiguous methylene groups. Considering the flexibility as a *kinetic* phenomenon, as in the case of dynamic mechanical spectra, the decrease in glass transition temperature with increasing number of in-chain contiguous methylene groups for the poly-methylene terephthalate, and polymethylene oxide series, provides evidence for the assumption of increased *intra*molecular flexibility along such a polymer series. *Equilibrium* flexibility of the isolated polymer molecule could be estimated through solution measurement of polymer coil dimensions by light scattering and intrinsic viscosity measurements.[63] Similarly, with light crosslinking of these elastomers, force-temperature measurements above the glass transition temperature, where the molecular segments act in-dependently of one another, could yield information regarding chain conformation in free space through application of the equation of state for rubber networks.[64] Theoretical calculations can also quantitatively describe the energy barrier to segmental rotation within a polymer molecule from an equilibrium point of view.[65] The application of these calculations to sterically hindered molecules, such as polyisobutylene, is quite complex and currently an active area of investigation.[66] The behavior of the high resolution solution NMR spectra of the polymers provides evidence for the high *intra*molecular steric hindrance (considered as a time averaged equilibrium phenomenon) in the first member of the series. As illustrated in Table 1, both the methyl and methylene peaks are shifted significantly downfield for the first member of each series. This
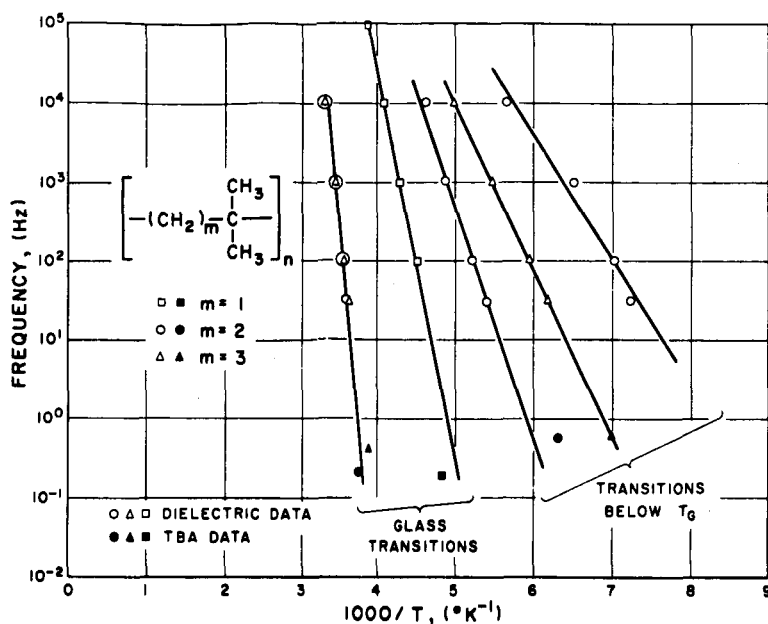
FIGURE 21. Frequency-dependence of transitions in a series of amorphous polyolefins.

$$-\!\!\!\left(\, CH_2-CH_2-\underset{\underset{CH_3}{|}}{\overset{\overset{CH_3}{|}}{C}}\,\right)_{\!\!n}$$
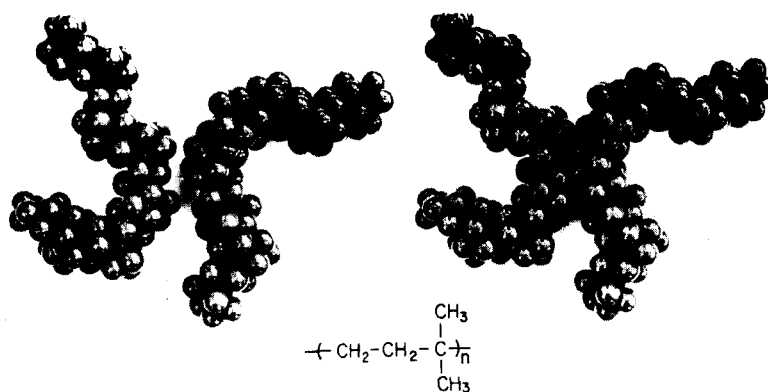
FIGURE 22. Fisher-Taylor-Hirschfelder molecular models showing segments of separated and interlocked macromolecules.

behavior has previously been reported[67] for members of the first series. Similar behavior is also displayed by the NMR spectra of a series of low molecular weight paraffins with structure analogous to the polymer series.[68] The downfield shift results from *intra*molecular interference of the neighboring pairs of geminal methyl groups which appears as a maximum when these groups are separated by a single methylene linkage.

The *inter*molecular geometrical factors, which result in a maximum in glass transition temperature with the second member of each series, are interpreted in terms of *inter*molecular interlocking. Through molecular models, this can be

shown to result in maximum restriction to segmental motion in the second member of each series. The internally hindered polyisobutylene molecule can be conceived of as a backbone chain sheathed by methyl groups with no available sites between pendant methyl groups to allow interlocking with neighboring molecules. Such sites would allow intermolecular interlocking which would serve to inhibit the segmental motions and raise the glass transition to higher temperatures. As the number of in-chain contiguous methylene groups is increased from one to two (moving from the first to the second member of each series), space for segmental interlocking between pendant

methyl groups is made available, and the glass transition temperature is raised as a result of this restriction to segmental motion. With the addition of a third in-chain contiguous methylene group (moving from the second to the third member of each series) the opportunity for motion between interlocked molecules is increased and the glass transition temperature decreases. This segmental interlocking is illustrated in Figure 22 which shows molecular models for two molecules, both separated and interlocked, for the second member of the first series. The interlocking occurs by a snug fitting of the pendant methyl groups into the spaces between the pendant methyl groups on the adjacent molecule. The interlocking at the point of juncture, which may be considered a form of molecular entanglement, is such that motion of one interlocked molecular segment with respect to the other is restricted. The interlocking in the third member of the series (not shown) is not as restrictive and allows slight relative motion at the point of juncture. Because of the steric hindrance and bond angle strain involved in the molecules of the first member of each series, standard molecular models of these molecules cannot be constructed.[63] However, it is precisely this heavy substitution which appears to prevent intermolecular interlocking and leads to a glass transition temperature lower than the other members of the series. Based on these considerations, one can predict that if the series were extended, the glass transition temperature would continue to decrease with increasing number of in-chain contiguous methylene groups. As a limiting case, the glass transition would approach the low temperature amorphous glass transition temperature of polyethylene[69] which, in the absence of crystallinity, could be expected to exhibit minimal *inter*- and *intra*molecular effects.

Similar arguments would contribute to the explanation of the high glass transition temperature of amorphous polypropylene (-10°C) relative to the values for amorphous polyisobutylene and amorphous polyethylene, and similarly to the explanation of the high glass transition temperature of polyvinyl chloride (80°C) relative to the values for polyvinylidene chloride (-20°C) and polyethylene.

Additional evidence for this proposed *inter*molecular interlocking lies in consideration of the structure of the third member of the first series as an alternating copolymer of ethylene and iso-

butylene. A plot of copolymer composition vs. glass transition temperature for such a hypothetical system in which the minor component is *evenly* distributed along the chain would clearly pass through a maximum at the equimolar composition, as represented by the structure of the third member of the first series. This maximum is indicative of some sort of *inter*molecular interaction of the type discussed above. Although the relationship between glass transition temperature and copolymer composition is, in most cases, closely approximated by a linear relationship, some copolymer systems have been shown to display a pronounced maximum of glass transition temperature with composition. Transition-composition plots for two such systems, acrylonitrile-styrene[70] and vinylidene chloride-methylacrylate[71] show such maxima near the point of equimolar concentration of the two comonomers. Although these copolymers contain polar groups which can be expected to contribute to *inter*molecular interactions, the interlocking phenomena can still be considered contributory, particularly in the case of the copolymer involving vinylidene chloride units. Like isobutylene units, vinylidene chloride units are by themselves sterically hindered and heavily substituted enough to render interlocking prohibitive. It is particularly significant to note that for the vinylidene chloride-methyl acrylate system, the free volume at the glass transition temperature, calculated from expansion coefficients presented with the glass transition temperatures,[71] is lower than the generally accepted iso-free volume values[72] on either side of the maximum, but approaches the generally accepted "average" value at the maximum in glass transition temperature. These results bear significantly upon the free volume theory which sets a specific free volume as the criterion determining the glass transition temperature.[73] Although the free volume theory as a corresponding-states approach to the glass transition is a generally accepted theory, the premise of an iso-free volume applicable to all polymers at the glass transition is not so widely accepted.[72] There are notable exceptions to the iso-free volume theory where the free volume at the glass transition temperature is both larger [e.g. polyethylene terephthalate and poly(bisphenol A carbonate)] and smaller (e.g. polyisobutylene, hevea, and polymethylacrylate) than the generally accepted average value. In considering the importance of

geometrical intermolecular effects, it seems apparent that the *shape of the free volume* must be accounted for when relating free volume to the glass transition temperature. These geometrical considerations seem particularly important in view of the fact that many of the polymers deviating from the iso-free volume state are those which are highly substituted enough to prevent intermolecular interlocking (e.g. polyisobutylene and vinylidene chloride-methylacrylate copolymers rich in vinylidene chloride) or those systems containing bulky groups within the main chain [e.g. polyethylene terephthalate and poly(bisphenol A carbonate)].

It follows from the above discussion that geometrical interlocking can increase the free volume and decrease the density by constraining interlocked segments to fixed conformations. Such reasoning could contribute to an explanation of the observation that amorphous syndiotactic polymethylmethacrylate has a higher glass transition (Tg $\simeq$ 127°C at 0.25 cps) than amorphous isotactic polymethylmethacrylate (Tg $\simeq$ 55°C at 0.31 cps), and yet the former has lower density at 30°C.[74] TBA thermomechanical spectra for the three types of polymethylmethacrylate are presented in Figure 23.[39,45,46]

*Inter*molecular interactions between polymer molecules have usually been attributed to polar groups within the molecule. These polar groups serve to form *inter*molecular bonds which inhibit segmental motion and, at the same time, decrease the free volume; both these effects result in an increase in the glass transition temperature. These *inter*molecular effects are quantitatively dealt with through use of the cohesive energy density related, for simple liquids, to the energy of vaporization, and, for polymers, to the solubility parameter.[73] Attempts to correlate the glass transition temperature with the cohesive energy density, CED, show a linear relationship between Tg and $\sqrt{CED}$. Generalized correlations for many polymers[72] show two such linear relationships, one for symmetrically substituted molecules (e.g. polyvinylidene chloride, polyisobutylene, polytetrafluoroethylene, polydimethylsiloxane) and another for unsymmetrically substituted molecules (e.g. polystyrene, polymethylmethacrylate, polyvinylchloride). The existence of these two correlations may well be attributable in part to bulk

phase *inter*molecular interlocking occurring in the unsymmetrically substituted molecules which would not be observed in the polymer-solvent studies generally used to determine the cohesive energy density. (*Intra*molecular effects undoubtedly do play an important role in symmetrically substituted molecules for which the *intra*molecular barrier to rotation is less than that for unsymmetrically substituted molecules.)

The secondary transitions observed in these polymer series display behavior similar to that of the glass transition temperatures. Based on the similarity of location of temperature, and activation energies, these secondary transitions, observed in all the polymers except polyisobutylene, appear to arise from the same source as the main secondary transition observed in polyethylene and other polyolefins.[55,75] The molecular interpretation of this glassy state, amorphous transition, is generally considered to involve a small number of monomer residue units within the main chain. The presence of three to five contiguous in-chain methylene groups has been suggested to be a necessary criterion for this transition to occur.[75,76] The precise molecular motion related to these secondary transitions is uncertain, although several discrete mechanisms have been proposed. Among these mechanisms are: the "crankshaft mechanism" involving crankshaft motion[76] of four to eight consecutive methylene units about two colinear carbon atoms; localized vibrational modes[77] involving the vibration of a small number of consecutive monomer residue units; and loosening of some sort of *inter*molecular packing or seating.[78] The results presented here seem to provide additional evidence for the concept of dissociation of molecular packing and, from the heavy substitution in these polymers displaying the secondary transition, evidence that the crankshaft motion is invalid.

The temperatures of these secondary transitions follow a pattern similar to that of the glass transition temperature in that in going from the first to the second member of the second series, the transition temperature increases and then decreases in going to the third member of the series. The occurrence of this effect in the secondary transition, where the transition results from localized, short-range motion, indicates that the interlocking is rather extensive in the glassy state.

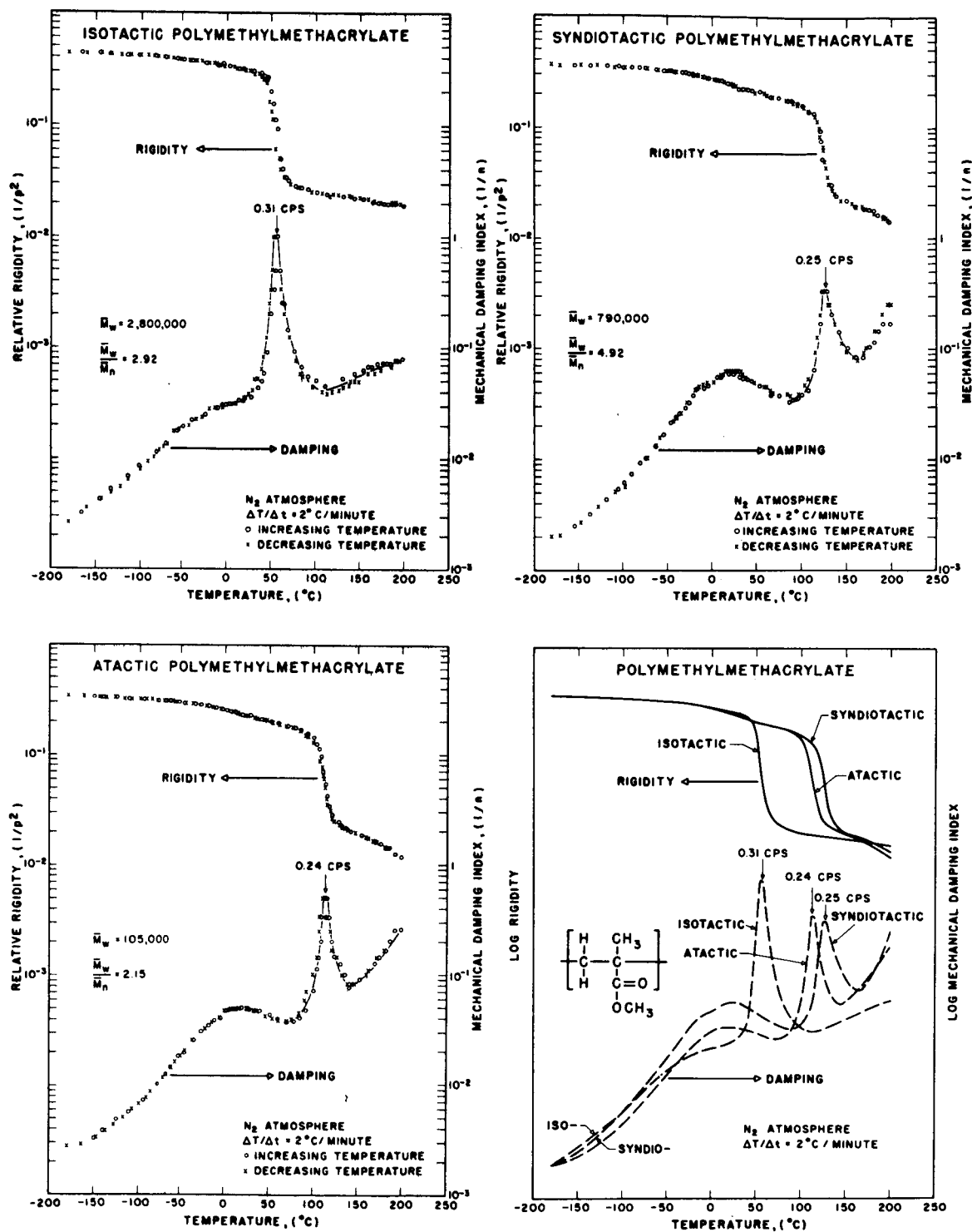One of the polymers shown above, poly(isomer

FIGURE 23. Thermomechanical spectra of amorphous isotactic, syndiotactic and atactic polymethylmethacrylates. The polymer/braid composite specimens were prepared using 10% solutions in tetrahydrofuran which was removed by the thermal prehistory of heating ($\Delta T/\Delta t$ = 2°C/min) to 200°C. Data were collected while cooling to −180°C and during the subsequent heating to 200°C.

of 3-methyl-1-pentene), displays two secondary transition peaks below the glass transition observed both mechanically and dielectrically. The corresponding member of the first series, poly(isomer of 3-methyl-1-butene), displays two dielectrically observed relaxations below the glass transition temperature.[59] The location of the lower secondary peak correlates with studies of alpha methyl group rotation in a-alkyl acrylate ester polymers.[79] Based on the latter results, the lower transition could be assigned to rotation of the pendant methyl group on the main chain. It might be presumed that the other polymers investigated also display such additional secondary transitions below the temperature limits of the experimental technique.

The proposed theory of intermolecular interlocking is based on the premise that molecular *flexibility* increases along each series. The relationship of transitions to flexibility depends on the fundamental definition of chain flexibility. The actual submolecular motions responsible for transition are speculative, and it may well be that different submolecular motions may be responsible for the "same" transition in different polymers. For example, in polyisobutylene complete rotation of the carbon-carbon bond in the main chain is energetically difficult and cooperative rotation is even more difficult; therefore the glass transition in polyisobutylene is likely to arise from motions more restrictive than complete rotation. Similarly, the glass transition phenomena in the semi-ladder polymers which are used at high temperatures (see polyimides, polybenzimidazoles, and "BBB" polymers) must involve torsional oscillations, rather than complete segmental rotation.

Different mechanisms for processes would be expected to result in different activation energies. The activation energy reported in Table I for the glass transition of polyisobutylene (22 kcal/mole) is different from those of the next members of the series (48 and 44 kcal/mole, respectively).

These results and the discussion point to different molecular mechanisms for the glass transition of polyisobutylene (and probably for the first member of the second series for which an activation energy is not yet available) and the other immediate members of the series. Not until the nature of the dispersion phenomena in these most basic series of polymers is understood, can we expect to have confidence in explanations of relaxation behavior in the wider field of polymers.

III. Polyimides[29,35,39,48]

A discussion on polyimides illustrates the application of torsional braid analysis in obtaining relationships between chemical structure, processibility, thermal history, and thermomechanical behavior. Sensitivity of the thermomechanical spectra of the polar polymers to trace amounts of water is also illustrated. The soluble precursors to the polyimides were synthesized and provided by Dr. Vernon L. Bell and Dr. Norman Johnston of the National Aeronautical and Space Administration at Langley Research Center, Hampton, Va.

Effect of cure — A variable of major importance when studying bulk polymer systems is the prehistory of the specimen. This is particularly important with many new polymer systems where the final intractable polymer is prepared in situ from a tractable prepolymer. The provided prepolymer solutions of polyamic acid (10% in dimethylacetamide weight/volume) were prepared by reacting equal moles of dianhydride and diamine in dimethylacetamide at room temperature. Polyimides were prepared from the prepolymer solutions of polyamic acid in dimethylacetamide (b.p. = 166°C) by removing solvent and effecting a ring-closure reaction in situ (e.g. see Figure 24).

The thermomechanical spectra of two specimens prepared from the same prepolymer sample are shown in Figure 25. The top set of data (-180°C → 500°C → -180°C) was generated after
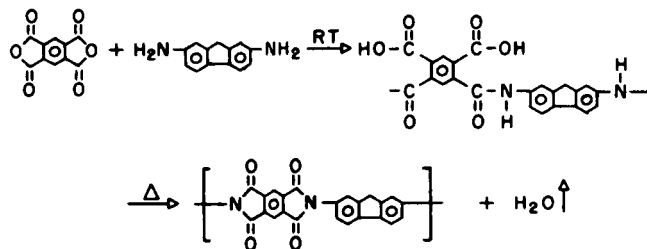

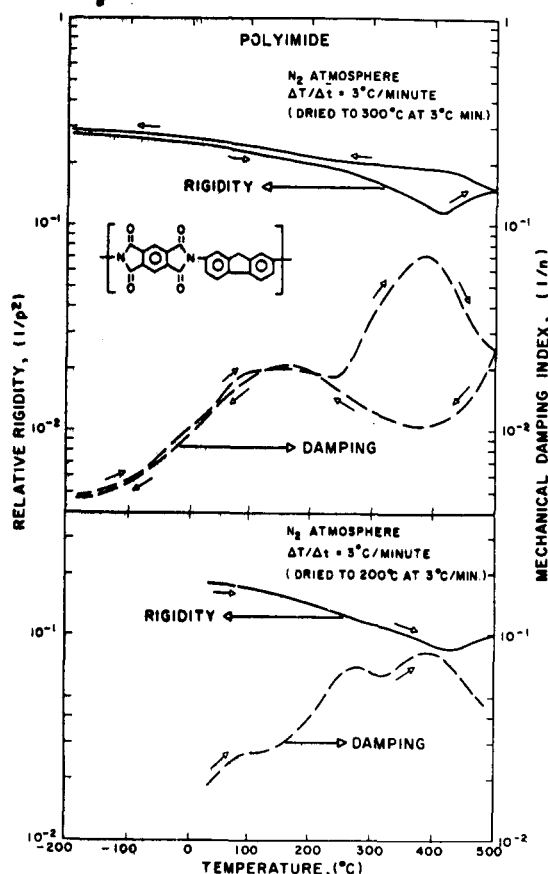FIGURE 24.   Reaction: Dianhydride + diamine → polyamic acid → polyimide.

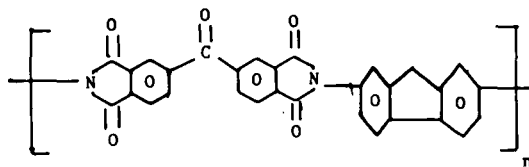FIGURE 25. Polyimide: effect of thermal prehistory.

a drying/curing cycle of 25°C to *300*°C at 3°C/min. The lower set of data (25 °C → 500°C) was generated after a prior history of heating from 25°C to *200*°C at 3°C/min. The specimen which was dried to 200°C displayed an additional damping peak and an inflection in the rigidity curve in the 200 to 300°C region of the experiment. This difference can be attributed to either the removal of associated solvent that remained absorbed to the polymer more than 30°C above its boiling point and/or to the continuation of the ring-closure reaction which is not completed during the 25° to 200°C cure cycle.

Effect of high temperature — The upper set of data in Figure 25 displays the thermomechanical behavior of the material which resulted from heating the prepolymer to 500°C at 3°C/min in nitrogen. The glass transition region was shifted from about 350°C to 500°C, whereas the glassy state relaxation (with a damping peak at about 150°C) was virtually unaffected by the thermal treatment to 500°C. These results are explained by suggesting

crosslinking and/or chain-stiffening reactions, which increase the modulus above 400°C, are of sufficient density to affect the longer range motions which are associated with the glass transition, and yet are of insufficient density to affect the more localized motions which are associated with the glassy state relaxation. Since the damping peak in the glassy state (150°C) was observed after cure to 300°C and also after pyrolysis to 500°C, it represents a relaxation of the polyimide material per se (cf. effect of solvent and/or curing reaction as above). From these results it appears that the polyimide structure can be formed by heating the prepolymer to ∿300°C at 3°C/min. In other words, it may be stated that a logical cure cycle for obtaining the polyimide structure from polyamic acid has been determined. On the other hand, the controlled pyrolysis to 500°C resulted in a new material which differed in having a higher load-limiting glass transition region, but had much the same thermomechanical properties as its precursor polyimide in the glassy state. That is, thermally-induced chemical reactions can be regulated so as to freeze out preferentially longer range relaxations thereby extending the glassy state behavior and the utility of the material to higher temperatures.

Effect of Trace Moisture — A well-known characteristic of many polymers is the ability of polar groups to attract and associate with water. For example, with nylons, the amount of water absorbed can be as much as 16% and can function as a plasticizer. Although the plasticization effect may be commercially desirable, when investigating structure-property relationships in new research polymers (e.g. especially those of the type represented by polyimides, polysulfones, polyquinoxalines, and pyrrones), it is important that the mechanical spectra represent the properties of the polymers per se.

Figure 26 illustrates the problem with a polyimide of the following structure:

The data are thermomechanical spectra of the same polymer, obtained after heating a prepolymer solution to 300°C at 3°C/min. to effect solvent removal and chemical ring-closure. The top
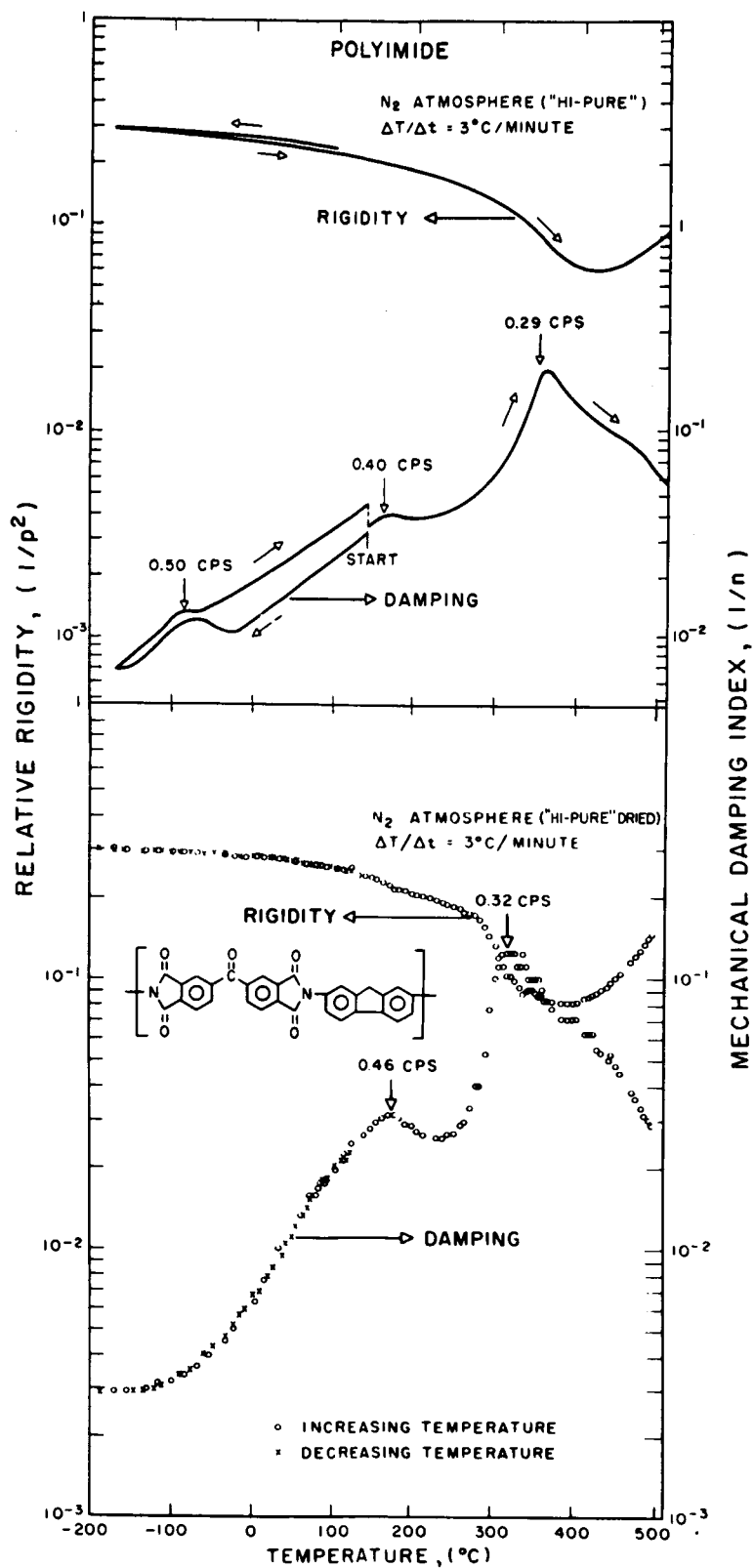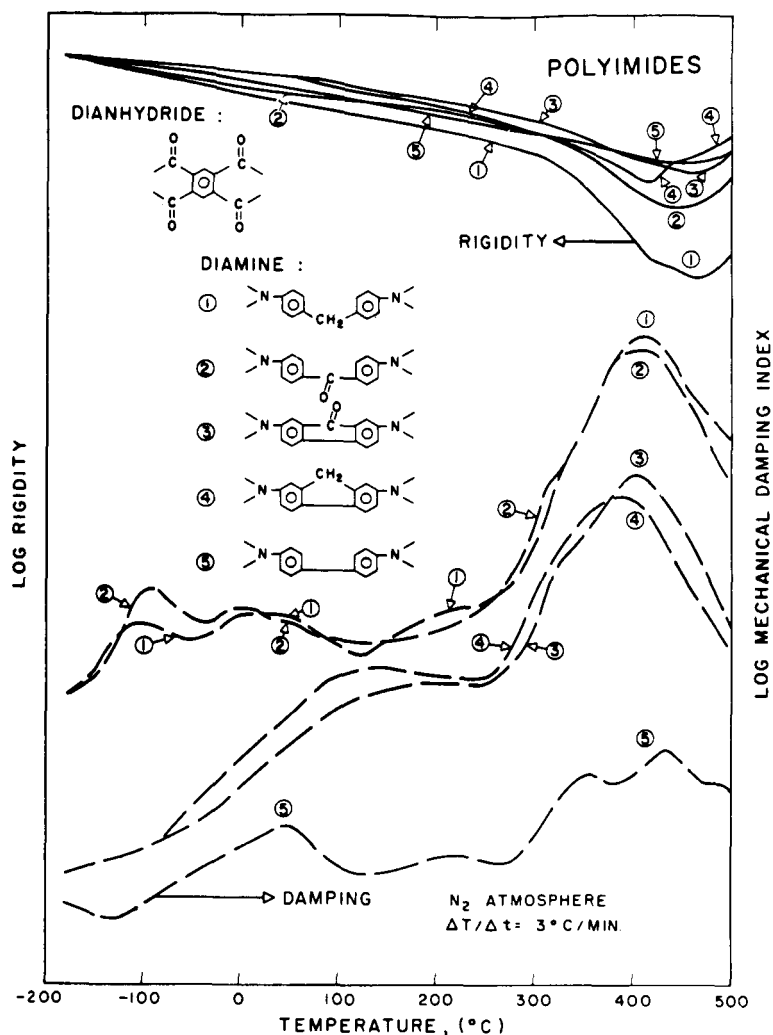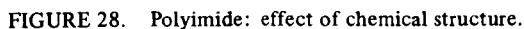
FIGURE 26. Polyimide: effect of trace moisture.

FIGURE 27. Polyimide: effect of chemical structure.

set of data was obtained using an atmosphere of "Hi-Pure" nitrogen which is specified as 99.996% pure with 5 ppm water and 10 ppm oxygen. It is apparent that the cooling and subsequent heating data below 130°C are not reproducible and that there is a damping peak at about -80°C. After these low temperature experiments the specimen was taken to 130°C and held overnight. It is apparent that the damping returned overnight to the level of the pre-low temperature experiment, which implies that the associated water was driven off by heating overnight at 130°C. The lower set of data (130°C → -180°C → 500°C) was obtained using "Hi-Pure" nitrogen that was passed through liquid nitrogen cold traps and drying columns. The up and down reproducibility of the low temperature region and the

absence of the -80°C peak are noteworthy. All subsequent experiments employed purposely dried nitrogen. After being held overnight at 130°C, the specimen was taken from 100°C to 500°C. The high temperature (130 to 500°C) behavior of the two sets of data are basically similar in that both sets display a damping peak in the glassy state at 170°C and a peak associated with the glass transition region at about 350°C, both of which are accompanied by decreases in rigidity.

Effect of chemical structure – The chemical formulae and data showing the thermomechanical behavior of two series of polyimides are shown in Figures 27 and 28. The specimens were prepared from solutions of the precursor polyamic acids by heating to 300°C ($\Delta T/\Delta t = \pm 2°C/min$). The curves for the relative rigidity parameter have been

FIGURE 28. Polyimide: effect of chemical structure.

shifted vertically so that the rigidity is the same for each series of the polymers at -190°C. This normalization facilitates comparison of materials and is made possible by having the specimens, which are to be compared, have the same polymer content. (Solutions of the same concentration and approximately the same viscosity were used in the preparation.) The damping curves have been displaced vertically by arbitrary amounts.

The data support the à priori prediction which could be made on the basis of the relative flexibilities of the molecules that there would be several distinct types of behavior. Polymers formed using benzophenone tetracarboxylic acid dianhydride (Figure 28) would be expected to be more flexible than those formed by using pyromellitic dianhydride (Figure 27), since the former is less double-stranded with rigid linkages than the latter. Polyimides which are derived from benzophenone oianhydride do have lower glass transitions and soften more through them than do the polyimides made from pyromellitic dianhydride.

On the other hand, the presence of methylene vs. carbonyl linkages in the backbone would have less influence on the molecular flexibility and inter-molecular forces, and hence on the thermo-mechanical behavior. Indeed, very similar thermomechanical behavior is displayed by polyimides synthesized from fluorene diamine④ and fluorenone diamine.③ In the same manner similar thermomechanical spectra are displayed by polyimides synthesized from p,p'-methylene dianiline① and p,p'-diamino benzophenone,② and also from p,p'-diamino diphenyl ether.[48]

Interpretation of the data on the two series of polyimides bears further on the molecular inter-pretation of the thermomechanical behavior. The polyimides with incorporated benzophenone dianhydride residues have thermomechanical spectra which are not unlike those of simpler amorphous polymers such as amorphous isotactic, syndiotactic, and atactic polymethylmethacrylates (see Figure 23) which display a glassy state damping region ("β"-peak) and a glass transition region as main features. (The ratio T_g/T_β was ∿ 1.3 to 1.5 for these polyimides and depends on the thermal prehistory used to obtain the polyi-mides, whereas this ratio is ∿ 1.2 to 1.34 for the polymethylmethacrylates.) On the other hand, the thermomechanical spectra of polyimides containing pyromellitic dianhydride residues can be more complex in displaying multiple damping peaks. This suggests that highly discrete modes of submolecular motion are activated in raising the temperature in some of these polymers. In contrast, a more continuous mode of activation of submolecular motions is suggested for the polyimides made from benzophenone dianhydride. Since insertion of pyromellitic dianhydride (versus benzophenone dianhydride) residues results in more change in thermomechanical spectra than is produced by the other changes in molecular architecture, it may well be that this special influence is due to the high density of polar carbonyl groups in a very rigid anhydride residue which drastically affects intermolecular inter-actions and controls the thermomechanical behavior. In contrast, intramolecular flexibility appears to control the thermomechanical behavior of the polyimides synthesized from benzophenone dianhydride.

The glass transitions of the polyimides containing pyromellitic dianhydride residues are ill-defined. This is probably a consequence of

thermally-induced chemical reactions which compete with the softening process of the glass transition. In all the polymers, these reactions cause an increase in rigidity. The region of low rigidity ($T > T_g$) has a wider temperature range for the benzophenone anhydride-derived vs. the pyro-mellitic anhydride-derived polyimides. Should advantage be taken of the high temperature (400 to 500°C) reactions to form engineering polymeric materials which would have significant strength and modulus in the temperature range 400 to 500°C, then there may well be advantages in processing (e.g. forming) with the more fusible polymer and then pyrolyzing in situ. However, variations in the formation of volatiles formed on degradation as a function of molecular structure would have to be taken into account.

The results of thermogravimetric analysis (TGA) for the two series of polyimides are shown in Figures 29 and 30. The prehistory for all of the polymers was the same as for the thermo-mechanical experiments. Comparative thermal stability in the decomposition range was estimated in three ways: 1) using the temperature of onset of increasing rate of weight loss; 2) using the relative weight loss incurred by a particular temperature (e.g. 550°C); and 3) using the relative temperatures by which a particular fraction (e.g. 10%) had volatilized. Regardless of the technique employed, the order of stability (and inflexibility) for both series was benzidine⑤ > fluorenone③ > fluorene④ > benzophenone② > methylene dianiline.① Similarly, incorporation of the flexible benzophenone dianhydride lowered the stability so that polyimides synthesized from any given amine were less stable than those synthesized from pyromellitic dianhydride. Ease of processibility would appear to be in the opposite order to molecular stability and inflexibility.

It might be noted that systematic studies of structure-property relationships in (high-temper-ature ring-containing) polymers are meaningful only when the structures are well-defined. The synthetic routes which lead to polymers containing fused rings in their backbone generally lead to a complex mixture of isomers of the *cis/trans* type. On the other hand, polyimides are unique in that the symmetry of the imide rings precludes this type of imperfection. However, other types of imperfection may well be present, such as incomplete ring-closure and intermolecular chemical links. Since the results of this study do
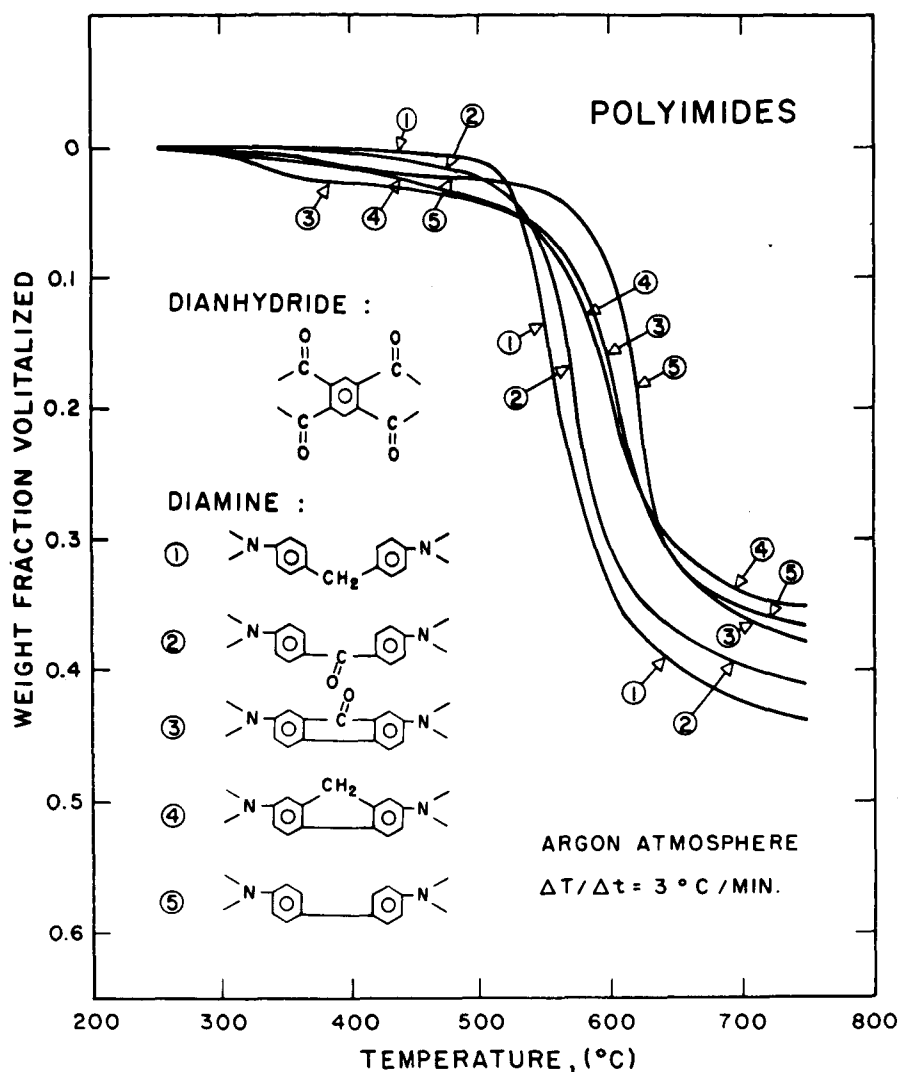
FIGURE 29. Thermogravimetric analyses of polyimides.

show very definite structure-dependent similarities and differences, they appear to substantiate both the validity of the syntheses and the thermomechanical spectra.

IV. Polybenzimidazole System[17]

So complex are the requisites of materials which are being synthesized for application in hostile environments, that to date no organic polymer with satisfactory mechanical properties exists which is capable of withstanding continuous service in air above 260°C. The lack of success in the field of heat resistance is largely a consequence of the expensive and time-consuming sequential processes of synthesis, scale-up, fabrication, and evaluation of new polymers. Polymers are usually evaluated in mechanical terms after their fabrica-

tion; there is a need for a semimicro method which would permit assessment of the thermomechanical properties of polymers before fabrication (i.e., immediately after synthesis). This is particularly desirable since, until the techniques of fabrication have been perfected for a new reactive system, the evaluation often reflects the defects of the fabrication process rather than the properties which the polymer is capable of conferring. A discussion of a polybenzimidazole system illustrates the use of Torsional Braid Analysis in optimizing the properties which can be obtained with a new reactive system using small amounts of material.

Materials (Figure 31) — Polybenzimidazole prepolymer, formed by partial reaction of 3,3'-diaminobenzidine (Formula A, Figure 31) and
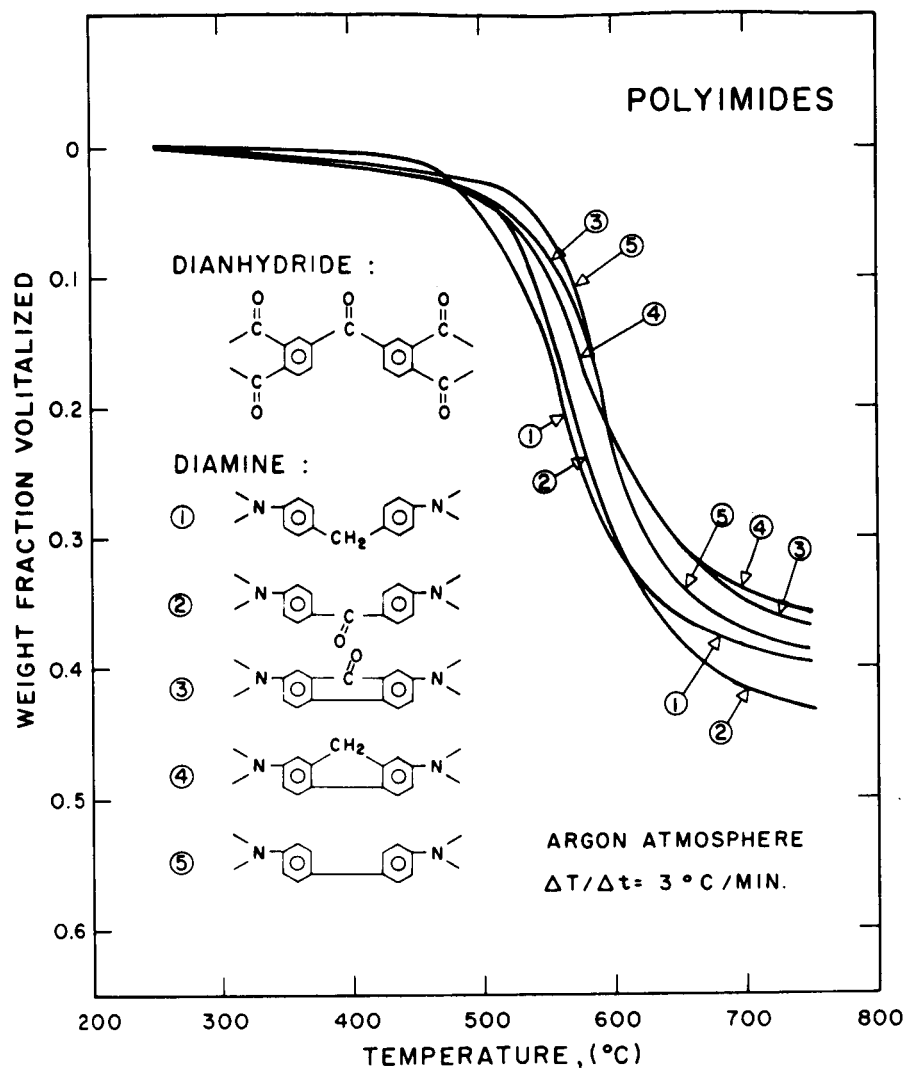
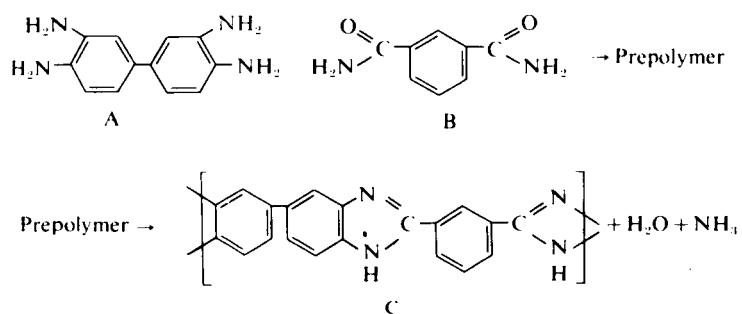FIGURE 30. Thermogravimetric analyses of polyimides.

FIGURE 31. Reactions: monomers to prepolymer to polybenzimidazole.

isophthalamide (Formula B, Figure 31), was provided by the Air Force Materials Laboratory, Dayton, Ohio, and was designated AF-R-151. The polymer (Formula C, Figure 31) was the culmination in 1965 of an extensive program to provide composite structural materials with significant retention of room temperature mechanical properties at temperatures above 400°C in nitrogen. According to the technical report[80] on the development, it would appear that the prepolymer (polymer melt temperature, PMT = 180°C) was prepared by heating equal moles of the monomers in melt form for 40 min at 270°C. A pyridine solution (5 to 7% prepolymer) was used for preparation of the TBA specimens. Experiments, except for oxidation, were performed in an atmosphere of undried "Hi-Pure" nitrogen.

Results and Discussion

A. Thermomechanical Behavior (25°C to 500°C) of the Polybenzimidazole Prepolymer (Figure 32)

The prepolymer was advanced in order to minimize loss of unreacted monomer in subse-

quent thermal treatments. This was performed by heating the PBI-prepolymer (PMT = 180°C)/glass substrate preparation to 270°C (solvent being removed during this process) and then heating isothermally at 270°C for 1 hour. According to the data on the prepolymer, a PMT of about 240°C would be expected. The cooled specimen formed the specimen which was used to obtain the thermomechanical spectra (Figure 32). Five distinct regions of behavior are revealed:

1. At low temperatures and below 200°C, the prepolymer is a glassy material with low mechanical loss and a modulus which changes little with temperature.

2. The transition region shows a drastic drop in modulus above 220°C to a minimum at 280°C and a prominent damping maximum at 260°C. Using the latter as an index, the glass transition temperature of the prepolymer may be designated as $T_g = 260°C$.
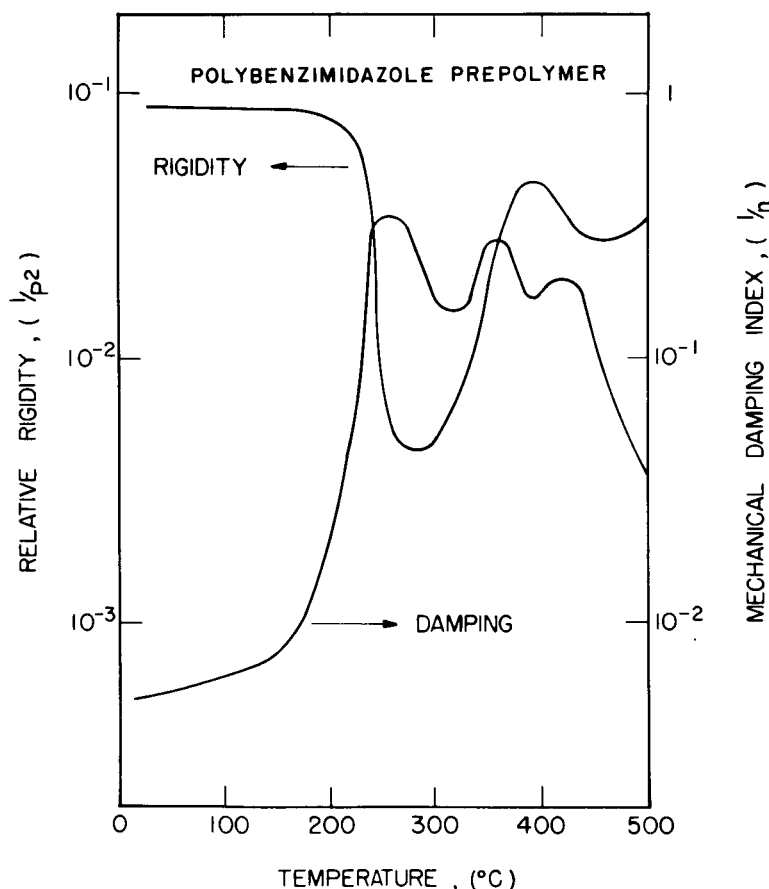

FIGURE 32. Thermomechanical behavior of the polybenzimidazole prepolymer in nitrogen.

3. Above 290°C the modulus increases while the damping passes through a maximum during the polymerization process which presumably leads to the polybenzimidazole. A concurrent total loss of 5% by weight of the sample occurred approximately linearly between 290°C and 390°C.

4. The modulus drops above 390°C (through a damping maximum at 420°C) as the result of either a further transition (the glass transition, T_g, of the newly formed polymer) or of degradation. The polymer lost, concurrently and approximately linearly, less than 2% of its weight from 390°C to 500°C.

5. Above 460°C the modulus increases in consequence of further chemical reaction while damping decreases to values characteristic of the glassy state. The product of this last reaction at 500°C could be structurally useful to this temperature.

B. Isothermal (380°C) Behavior of the Polybenzimidazole (Figure 33)

The nature of the process which occurs between 390°C and 450°C in the thermomechanical spectra of Figure 32 is of importance since it might be either degradative or physical (transition). If it is degradative, then the development of an optimum cure cycle would have to take this into account. Furthermore, the chemical reaction occurring above 450 might be expected to give an essentially different product from that formed by heating the prepolymer to 380°C. This, of course, need not be undesirable. If it is nondegradative, then the processes occurring
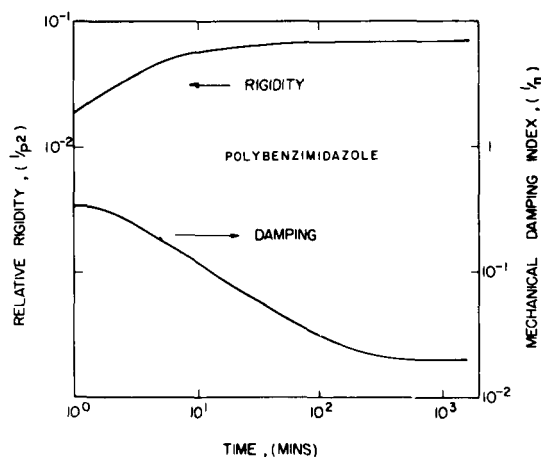
above 450°C may be essentially the same as those occurring below 380°C, in which case the transition (with a damping maximum at 420°C) would presumably be shifted to higher temperatures by heating above 450°C.

The physical or chemical nature of the process might be inferred from the isothermal behavior, monitored at a temperature just below the onset of the decrease in modulus which is due to the process in question. Degradation could lead eventually to a drop in modulus; a transition would not. Figure 33 shows that over a relatively long period of 24 hr at 380°C the modulus fails to decrease (the sample had been prepared by heating the prepolymer, T_g = 260° from 25° to 380°C). It is inferred then that the drop in modulus which occurs immediately above 390°C in Figure 32 is associated with a glass transition, T_g, which may be characterized by the maximum in damping at 420°C.

C. Thermomechanical Behavior (-170°C to 500°C) of the Polybenzimidazole (Figure 34)

The same polybenzimidazole/glass braid sample, used to provide Figure 33, was cooled to -190°C and the thermomechanical spectrum of Figure 34 obtained. (The experimental modulus curve is normalized relative to the value at 25°C.)

Three distinct transition regions are apparent in the thermomechanical behavior which may be designated by the temperatures of the damping maxima: -70°, 310°, and 430°C. Distinct changes

FIGURE 33. Isothermal (380°C) behavior of the polybenzimidazole in nitrogen.
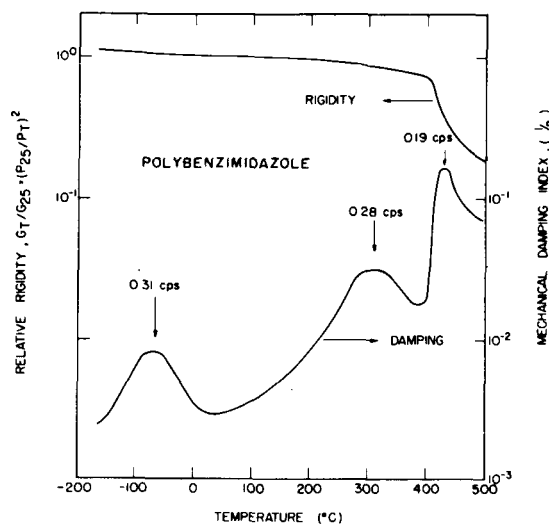

FIGURE 34. Thermomechanical behavior (-170°C to 500°C) of the polybenzimidazole in nitrogen.
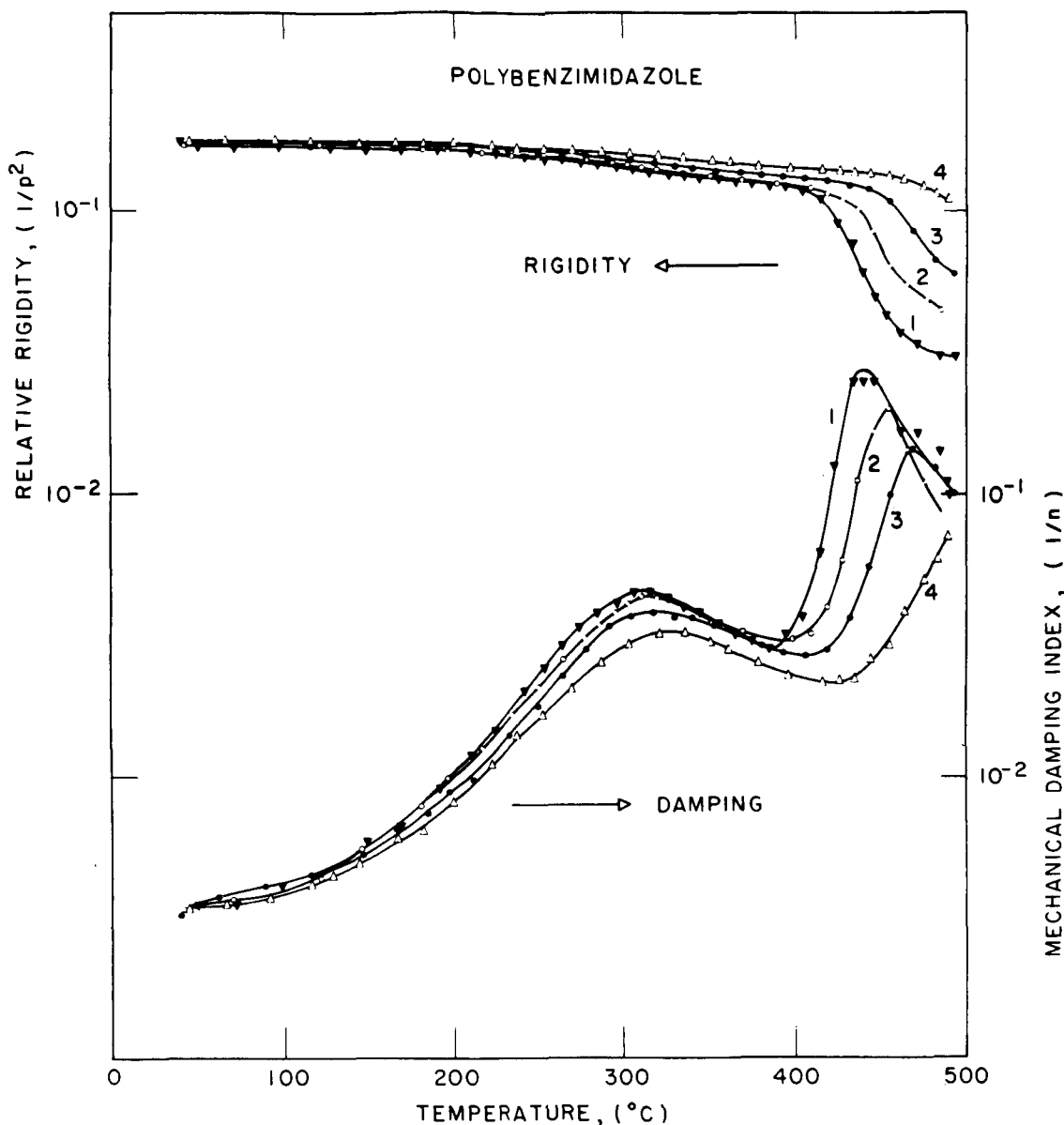
FIGURE 35. Polybenzimidazole: effect of thermal treatment in nitrogen.

in the modulus are associated with each of these loss maxima.

From the results one would predict not only that the polymer would be structurally useful to above 380°C, but that resistance to impact above -100°C would be good. The low temperature damping maximum is indicative of the presence of a relaxation mechanism which could contribute to mechanical behavior in the same way that the low temperature dispersion region of polycarbonate resins confers impact properties.

D. Effect of High Temperature on the Thermomechanical Behavior of the Polybenzimidazole (Figure 35)

A polybenzimidazole/glass braid specimen was prepared by heating the given prepolymer (PMT = 180°C) isothermally at 400°C for 5 hr before cooling to 25°C. The thermomechanical behavior to 500°C, shown in curve 1 of Figure 35, demonstrates (by comparison with the results of Figure 34) that the differences in prepolymer preparation and cure resulted in only minor

differences in thermomechanical behavior. After the heating cycle the sample was cooled and then recycled successively to give curves 2, 3, and 4 of Figures 35. (The specimens from curves 2 and 3 were held at 500°C for 30 min and 200 min, respectively, before being cooled.) Such thermal treatments result in a shift of the main glass transition to successively higher temperatures (from 430°C to 500°C) as monitored by the drop in modulus and by the damping maxima. The intensity of the damping maxima decreases as the transition temperature rises.

These results demonstrate that by suitable thermal treatment a polymer can be formed which would be structurally useful to 500°C in nitrogen. Other results which are not presented herein show that the modulus of the composite polymer/glass specimen is reversible for cycles in which chemical reaction does not occur, demonstrating the excellent adhesion and ductility (sufficient to accomodate stresses arising from the composite nature) in the system.

Several interpretations for the influence of thermal history on the glass-transition temperature of the polybenzimidazole are plausible. Among these are: completion of the ring-closing reactions, increase of molecular weight, crosslinking, and removal of plasticizing agents by volatilization.

The fact that the primary (430°C) transition is affected by the thermal treatment at 500°C to a much greater extent than the relaxations which occur in the glassy state is evidence that the only significant structural changes introduced are those which affect the longer range motions associated with the primary transition. Shorter range motions, for example those associated with the relaxation at 310°C, are scarcely affected by the thermal treatment.

The thermomechanical spectra of the polybenzimidazole are typical of those of amorphous polymers (cf. polymethylmethacrylate in Figure 23 and "flexible" polyimides in Figure 28) in displaying a main glassy-state relaxation in addition to the glass transition dispersion region.

E. Air Oxidation (Figure 36)

Polymer with a glass-transition temperature of about 500°C was subjected to oxidative attack by air at 400°C. [The specimen was that used to obtain the results of Figure 35. After reaching 500°C (Figure 35, curve 4), the specimen was

cooled·from 500° to 400°C, and the atmosphere was changed from nitrogen to air.] The results of Figure 36 show that samples (prepared by pyrolysis to 500°C in nitrogen) with large surface-to-volume ratios are oxidatively unstable in air at 400°C.

The results of these TBA experiments on an experimental prepolymer demonstrate that investigation on less than 0.5 g of a polymer precursor permits a prediction of the mechanical behavior of the polymer which agrees with and extends the results of much more extensive evaluation of glass cloth-reinforced laminates made from the same system.[80] The predictions apply to the conditions necessary for preparing the polymer (i.e., the cure cycle), to the thermomechanical behavior of the polymer, to the effect of thermal history on the thermomechanical behavior, and to its oxidative stability. A thermomechanical spectrum (from -180°C to +500°C) demonstrates the presence of three distinct relaxations at -70°, 310°, and 430°C. The main glass transition temperature of 430°C can be increased to 500°C by thermal treatment. The relaxation process which begins below –70°C would predictably confer good impact qualities to the polymer above about -100°C. The results also demonstrate that the adhesive qualities of the polymer to glass from -170° to 500°C are outstanding and that the polymer has a degree of ductility throughout the same temperature range. Oxidative stability of the thermally treated polybenzimidazole is not good at 400°C in air.

Excellent thermomechanical properties are reported for glass cloth-reinforced laminates made from the prepolymer. For example, the data of
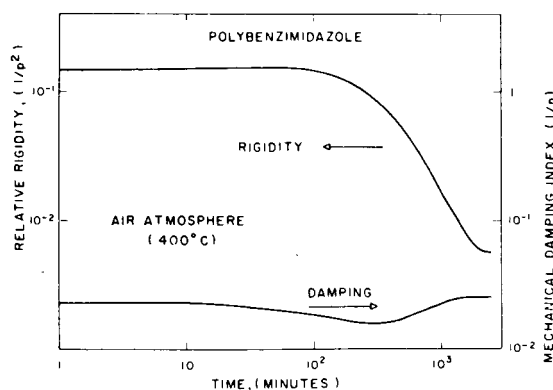

FIGURE 36. Polybenzimidazole: air oxidation (400°C).

Table 2 appear on page 147 of reference 80. The particular laminate had been heated in nitrogen at 950°F (510°C) for 6 hr. Its thermomechanical properties were better than those of laminates prepared by curing schedules at 750°F (400°C) for 6 hr. This is readily understood in terms of the work of this present discussion.

It is evident that the type of development represented by the polybenzimidazole system under discussion could be facilitated greatly by the TBA approach. Thermal transitions and transformations of the solid-state reactions can be monitored in terms of mechanical parameters which have both a theoretical basis (mechanical spectroscopy) and a practical relevance. Since the composite specimen of polymer and glass fibers itself may be considered as being an element of desired gross structures (e.g., glass cloth-reinforced laminates), predictions are direct. It might be emphasized that little material is required in the experiments since the testing is nondestructive. This should be very useful in the early examination of preparations of new polymeric materials.

V. Poly(Metal Phosphinate)[31,39]

The problem of how to determine the thermal and chemical procedures which optimize material behavior is particularly difficult with new and reactive two-component systems. Conversion of a brittle poly(metal bisphosphinate) into a tough poly(metal trisphosphinate) represents such an example.[81] The method of solving the problem for a particular ratio of the two reactive components, which is presented herein, is based on an examination of thermohysteresis by torsional braid analysis.

A poly(chromium III bisphosphinate), $[Cr(H_2O) (OH) [OP(CH_3) (C_6H_5) O]_2]_n$ with number-average molecular weight $M_n = 60000$, formed brittle films when cast from solution

$(CH_3Cl$ or o-dichlorobenzene); however, flexible and tough films could be formed by heating at 120°C a solution-cast mixture of the linear polymer and equal moles of dioctyl phosphinic acid (per polymer repeat unit). Compositions approximating the trisphosphinate were formed upon heating at 150 to 175°C for 2 to 3 hours.[82]

The reaction mechanism between the polymer and acid has been postulated[82] to involve two steps (Figure 37), each freeing one mole of water. Intra- and inter-molecular reactions between the reactive groups would lead to a linear and a network structure, respectively (Figure 37). A distinction between a truly linear and a network trisphosphinate structure may possibly be made on the basis of solubility studies.

The two-component system was examined in dried nitrogen by torsional braid analysis, the data for which are presented in Figure 38. For purposes of clarification the three sets of data (Curves I, II, and III) are displaced vertically on the logarithmic scales. The experimental procedures for each follow:

Thermal History for Curve I: A 20% solution in chloroform was advanced by heating at 45°C for 1½ hr. Subsequent storage was in a refrigerator. Chloroform was removed from the solution-impregnated braid in situ by heating to 200°C in dry nitrogen at 3°C/min.

Curve I: 200°C → -180°C → 300°C in dry nitrogen, $\Delta T/\Delta t = 2$°C/min. (T < 25°C), 3°C/min (T > 25°C).

Thermal History for Curve II: A 20% solution in o-dichlorobenzene (b.p. 180°C) was formed and advanced to a thick solution before being used (and stored in a refrigerator). Solvent was removed from the solution-impregnated braid in situ by heating to 300°C in nitrogen at 3°C/min.

Curve II: 300°C → -180°C → 400°C in dry nitrogen, $\Delta T/\Delta t = 2$°C/min (T < 25°C); 3°C/min (T > 25°C).

Thermal History for Curve III: As for Curve II (same specimen) including 300°C → -180°C → 400°C.

Curve III: 400°C → -180°C → 500°C in dry nitrogen, $\Delta T/\Delta t = 2$°C/min (T < 25°C); 3°C/min (T > 25°C).

The polymer system displays extensive hysteresis in mechanical modulus between cooling to -180°C and subsequent heating to temperatures below 400°C (Curves I and II). The lower the maximum temperature in an hysteresis cycle, the

TABLE 2

Thermomechanical Behavior of a Glass Cloth-Reinforced Laminate of the Polybenzimidazole[80]

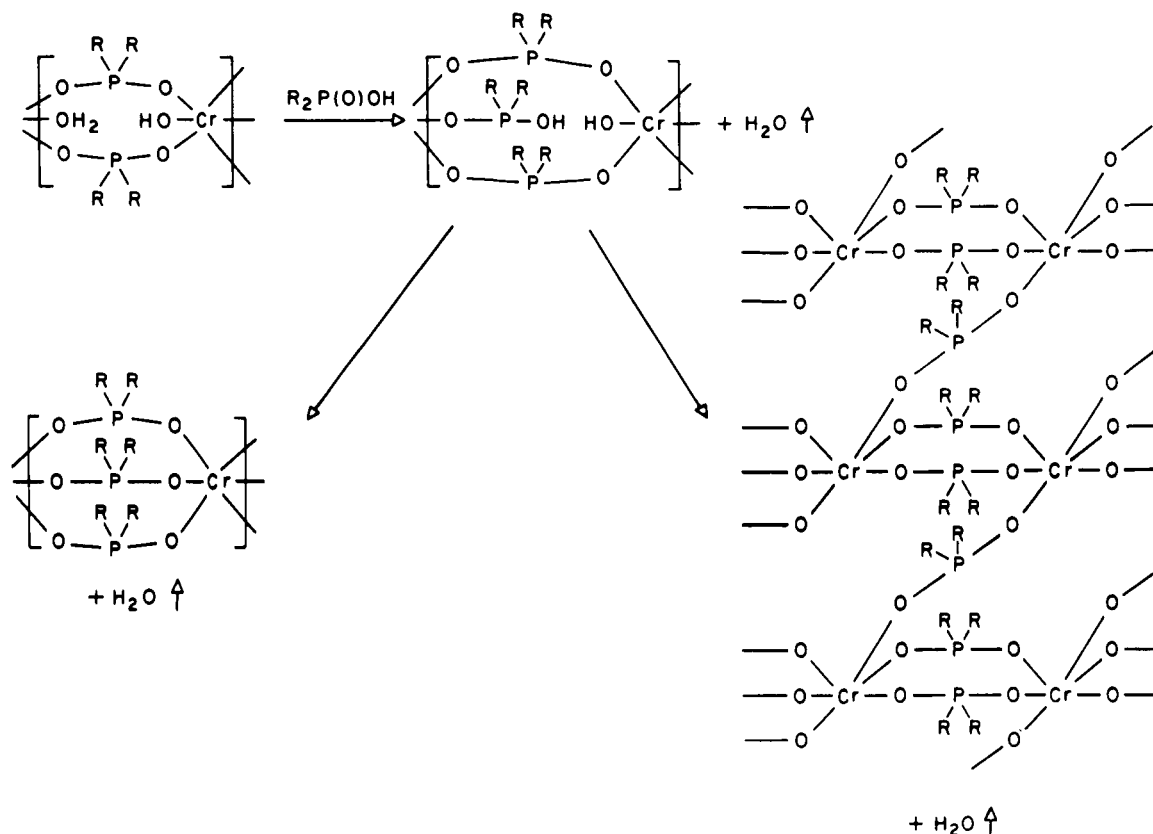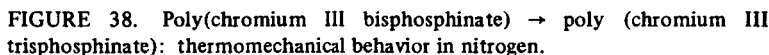| Test temperature	Flexural strength	Flexural modulus
70°F	117,000 psi	5.0×10^6 psi
700°F (after one hour at 700°F)	91,000 psi	4.5×10^6 psi

FIGURE 37.   Poly(chromium III bisphosphinate) → poly(chromium III trisphosphinate):   competitive reaction paths.

greater the difference between the results for cooling and heating. It appears that the mechanical properties are stabilized by preheating the system to close to 400°C (Curve III). In contrast to the behavior of the modulus, the mechanical damping changes but little with pretreatment in the temperature range 200 to 400°C.

The trisphosphinate and the precursor polymers display major transitions centered at about 0°C and 250°C. The form of the modulus curves suggests that the former is a very broad glass transition with glasslike properties displayed only below -100°C and leathery behavior displayed at room temperature. A glassy state transition is rendered apparent by the high damping at -190°C; relaxations which precede degradation are made apparent by the rising damping above 350°C. The trisphosphinate is stable to above 400°C in nitrogen: the system loses less than 3% of its solvent-free weight in being heated to 400°C and films remain intact and green to above 400°C.

The thermohysteresis in mechanical behavior can be explained by considering increases in modulus (to 400°C) (which counteract thermal softening and close the hysteresis loops) as the consequence of chemical reaction — presumably that changing the bisphosphinate to trisphosphinate. Since the damping curves are not sensitive to these reactions, the latter do not severely restrict the mobility of the submolecular motions. Therefore extensive crosslinking is not of prime importance since this would significantly alter the temperature of the transitions and the loss curves. The reaction scheme proposed above involving change of double-stranded flexible (-O-P-O-) linkages to triple-stranded flexible linkages or to a network would appear to produce an increase in elastic modulus and yet not necessarily produce a change in submolecular mobility and in the dissipative modulus (damping).

The decrease in rigidity, which is the other factor producing the hysteresis in the modulus

POLY (METAL PHOSPHINATE)

N$_2$ ATMOSPHERE

LOG RIGIDITY

I

START

END

II

RIGIDITY

START

III

END

END

END

START

START

END

START

START

START

END

I

II

III

DAMPING

LOG MECHANICAL DAMPING

$\{ Cr(H_2O)(OH)[OP(CH_3)(C_6H_5)O]_2 \}_x + X (C_8H_{17})_2 P(O)OH$

-200   -100   0   100   200   300   400   500

TEMPERATURE ,(°C)

FIGURE 38. Poly(chromium III bisphosphinate) → poly (chromium III trisphosphinate): thermomechanical behavior in nitrogen.

curves, presumably arises from microcracking of the composite specimens. In contrast to the bisphosphinate, the trisphosphinate can withstand the thermal stresses induced in the composite specimen by changes (decreases) in temperature.

Determination of thermal procedures which give optimal material behavior in the polyphosphinate was aided by the ability to determine mechanical behavior with both increasing and decreasing temperature modes. In contrast with most mechanical apparatus, the author's torsional pendulum is suited to this type of experiment.

VI. Poly(Carborane-Siloxane) s[44]

-CB$_{10}$H$_{10}$C- nuclei — This section summarizes an extensive investigation of structure-property relations in dried nitrogen for a series of well-defined polymers which form the backbone components of recently developed high temperature elastomers. The linear poly(carborane-siloxane)s whose structures and transition data are presented in Table 3 were synthesized and molecularly characterized at the Olin Research Center, New Haven, Connecticut.[83-85] The basic structure of these polymers is designated 10-SiB-X,

|	DESIGNATION	STRUCTURE	T_m	T_{crys}	T_g	T_{sec}	T_m/T_g
I	10-SiB-1		260°C	n a	25°C	-90°C	1.78
II	10-SiB-3	$[\eta]_{XYLENE} = 0.15-0.20$ dl/g GPC PEAK MAX ~10-12,000	40	10	-68	-140	1.54
III	10-SiB-3 END-CAPPED	$[\eta]_{XYLENE} = 0.15-0.20$ dl/g MADE FROM II	40	10	-68	-140 → -145	1.54
IV	10-SiB-3 HIGH MW	$[\eta]_{XYLENE} = 0.65$ dl/g MW ~ 50-100,000	A	A	-70	-140	
V	10-SiB-3 PARA	GPC PEAK MAX ~15,000	110	90	-35	-115	1.61
VI	10-SiB-3 FLUORINATED	GPC PEAK MAX ~8,500	A	A	-15	<-180 -90?	
VII	10-SiB-4	GPC PEAK MAX ~24,000	A	A	-75	-135	
VIII	10-SiB-4 φ RANDOM	$\bar{M}_n = 12,000$ GPC PEAK MAX ~15-20,000 RANDOM COPOLYMER	A	A	-58	-130 → -140	
IX	10-SiB-4 φ	GPC PEAK MAX ~12-18,000	A	A	-57	-140	
X	10-SiB-4 φ END-CAPPED	GPC PEAK MAX ~12-18,000 MADE FROM IX	A	A	-57	-140	
XI	10-SiB-5	GPC PEAK MAX ~20,000	A	A	-88	-140	
XII	10-SiB-∞ SE-30	MW > 10⁶	-40	-55	-125	A	1.58

A = ABSENT
n a = NOT AVAILABLE

TABLE 3. Chemical Formulae and Transitions of 10-SiB-X Polymers.

where 10 refers to the ten-boron cage and X to the number of oxygen atoms separating the cages in the polymer backbone.

$$\left\lvert \begin{array}{c} CH_3 \\ | \\ -Si \\ | \\ CH_3 \end{array} - CB_{10}H_{10}C - \left[\begin{array}{c} CH_3 \\ | \\ Si \\ | \\ CH_3 \end{array} - O \right]_X \right\rvert_n$$
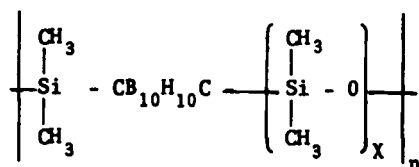
Although most of the polymers contain meta-carborane nuclei, one incorporates the para-carborane isomer.

—CB$_{10}$H$_{10}$C—
META

—C$\overbrace{O}$C—
B$_{10}$H$_{10}$
PARA
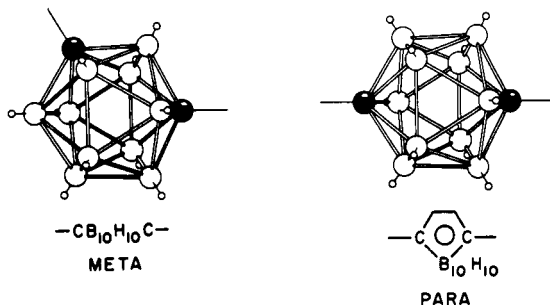
10-SiB-X series (I, IV, VII, XI, and XII) — The thermomechanical spectra for the series of polymers, in which the backbone structure varies systematically in the number of dimethyl-siloxane linkages which separate the regularly spaced meta-carborane cages, are shown in Figure 39 and in Figure 45 (for VII). Glass transition temperatures (T_g), melting temperatures (T_m), crystallization temperatures (T_c), and transitions of the glassy state (T_{sec}) are apparent.

The glass transition temperatures of each polymer fit the copolymer equation[86] when each is considered as a copolymer of $[Si(CH_3)_2\text{-}O]$ and $[Si(CH_3)_2\text{-}CB_{10}H_{10}C]$ (See Figure 40). The data for 10-SiB-2 is from the literature[87] for a cross-linked and semicrystalline mixture of uncertain structure[88] which approximated the 10-SiB-2 polymer in overall composition. The poor fit of the 10-SiB-1 data suggests that at some decreasing siloxane chain length, association of the carborane cages rather than intramolecular considerations, dominates the physical properties of the polymer. Another straight line can fit the glass transition data of these carborane-containing polymers. That presented was chosen because there are more uncertainties for X=1, due to the broad glass transition region, than for X=∞(polydimethyl-siloxane).

The high temperature regions of the thermo-mechanical spectra show that the carborane-containing polymers (I, IV, VII, XI) stiffen in nitrogen to form either a highly crosslinked resin or a very highly crosslinked elastomer. The decrease in rigidity with decreasing temperature, after pyrolysis to 625°C, of IV is indicative of a crosslinked rubber (theory of rubber elasticity), whereas the flat and high modulus curves of I, VII, and XI are indicative of highly crosslinked resins. The polydimethylsiloxane depolymerizes without stiffening. The order of thermomechanical stability (for the given thermal history) is IV > VII, XI > I > XII. Three siloxane linkages per repeat unit appear to be optimal for thermal stability, as indicated by the higher temperature for the onset of crosslinking and by the less highly crosslinked material after pyrolysis to 625°C.

The thermogravimetric data (TGA) in argon (Figure 41) display maximum rates of weight loss near 550°C for the poly(carborane-siloxane)s and near 475°C for the pure silicone (XII). The loss of weight which had occurred by 800°C increased linearly with the number of siloxane groups per repeat unit (Figure 42) and extrapolated to total loss of weight for 10-SiB-9.5 (and presumably higher). This indicated that the high temperature degradation process was a rupture of the siloxane bond, leading to a weight loss which increased with the fraction of those bonds. This scission may not lead to volatile cyclic products for the carborane polymers. On the other hand, the thermal degradation of pure poly(dimethyl-siloxane)s does lead to cyclic species and need not involve the formation of new end groups. Cyclization can proceed without the formation of active species which could initiate crosslinking.

10-SiB-3 series (II-VI) — Differences in the structures of this series are shown in Table 3. Thermomechanical spectra are presented in Figure 43 and in Figure 39 (for IV). Thermogravimetric data are shown in Figure 44.

The hydroxyl end group is reactive with respect to chain extension and interchange reactions, whereas the trimethylsilyl group [-Si(CH_3)_3] is inert. The type of end group and molecular weight (50,000 to 100,000 vs. 10,000 to 12,000) appeared to have no effect on the glassy state transition, glass transition temperature, and thermomechanical stability. In contrast to the lower molecular weight samples (II and III), which were semicrystalline, the polymer sample with
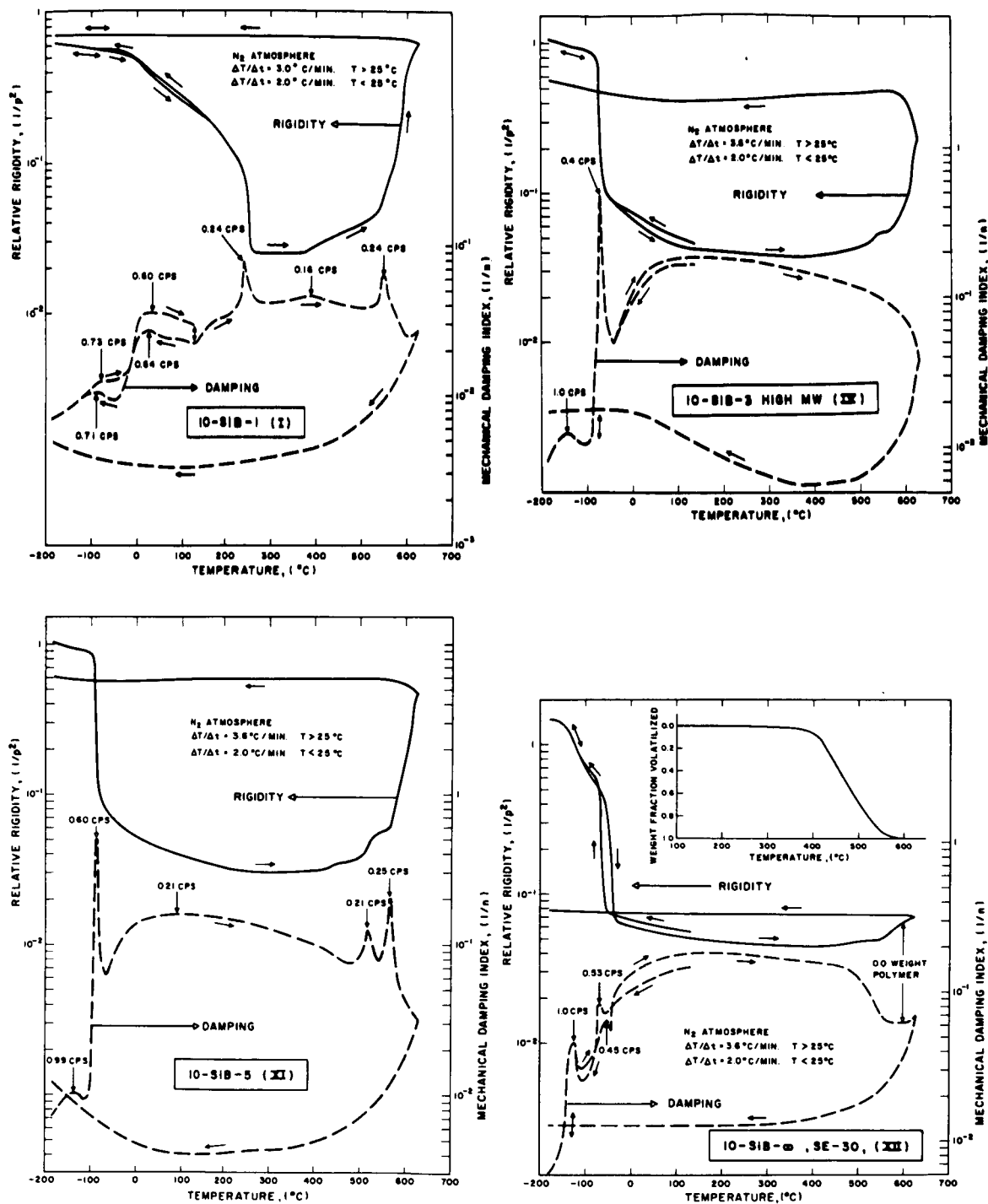
FIGURE 39. 10-SiB-X Polymers: thermomechanical behavior (–190°C ⇄ 625°C) in nitrogen for X = 1,3,5, and ∞. (See Figure 45 for X = 4).

COPOLYMER EQUATION FOR CARBORANESILOXANE POLYMERS

$$\left[\left(\begin{array}{c}CH_3\\ |\\ Si-\\ |\\ CH_3\end{array}\ \bigoplus\right)\left(\begin{array}{c}CH_3\\ |\\ Si-O\\ |\\ CH_3\end{array}\right)_x\right]_n$$

$$\frac{1}{T_g} = \frac{W_1}{T_{g_1}} + \frac{W_2}{T_{g_2}} = W_1\left(\frac{1}{T_{g_1}} - \frac{1}{T_{g_2}}\right) + \frac{1}{T_{g_2}}$$

x	T_g (°K) 10-SiB-x	T_g (°K) 5-SiB-x	W_1 10-SiB-x	W_1 5-SiB-x
1	298	213	0.730	0.655
2		185		0.488
2'	243 *		0.575	
2"	239 †		0.575	
3	205	177	0.475	0.400
4	198	171	0.404	0.346
5	185	165	0.351	0.281
∞	148	148	0.0	0.0

✽ 10-SEC. MODULUS ⎱ LITERATURE
† VOLUME-TEMP. ⎰

⊕ = –CB₅H₅C–
5-SiB-x OVERALL COMPOSITION RANDOM COPOLYMER. AT LEAST ONE -Si(CH₃)₂O- BETWEEN –CB₅H₅C– 'S

⊕ = –CB₁₀H₁₀C–
REGULARLY SPACED BY x ⊣Si(CH₃)₂O⊢ GROUPS

-65°C   -7°C   -13°C   103°C

W_1 = WEIGHT FRACTION –Si(CH₃)₂– ⊕ –

FIGURE 40. 10-SiB-X polymers as copolymers of 10-SiB-0; and 10-SiB-∞. Also, 5-SiB-X polymers as copolymers of 5-SiB-0 and 5-SiB-∞. Glass transition temperatures fit the copolymer equation.
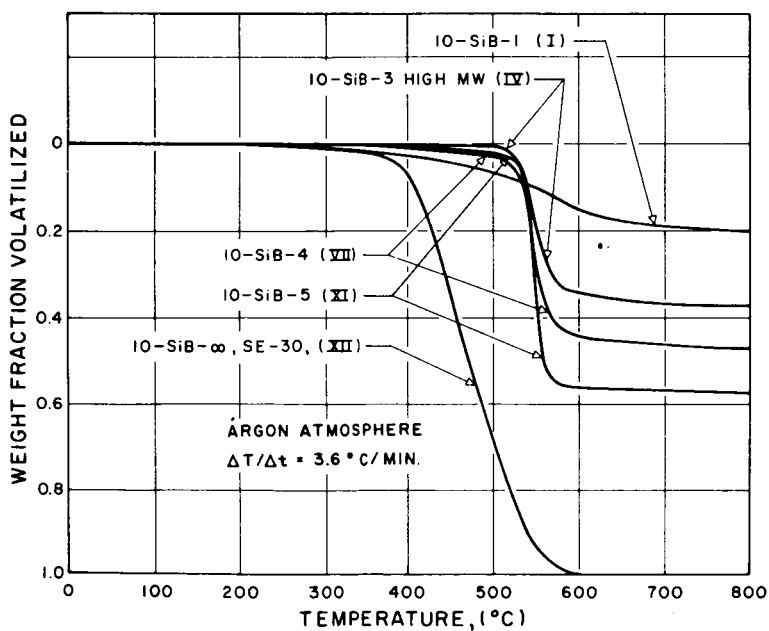
FIGURE 41. 10-SiB-X polymers. Thermogravimetric analyses in argon.
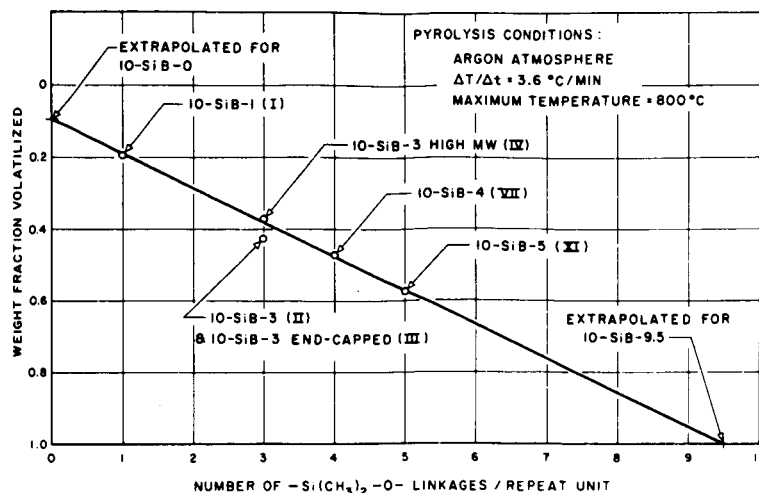
FIGURE 42. 10-SiB-X polymers. Correlation between molecular structure and pyrolysis in argon. The weight fraction volatilized by heating to 800°C is plotted vs. the number of -Si(CH$_3$)$_2$-O- linkages per repeat unit.

higher molecular weight (IV) was amorphous and appeared to be much more viscous as evidenced by the high damping (T_g < T < 500°C). The higher weight loss, displayed by the lower molecular weight species, could have arisen from volatilization of the small molecules of their distributions. Replacement of the meta-carborane linkage by the para-carborane linkage raised the glassy state secondary transition by 25°C, the glass transition temperature by 35°C, and the melting transition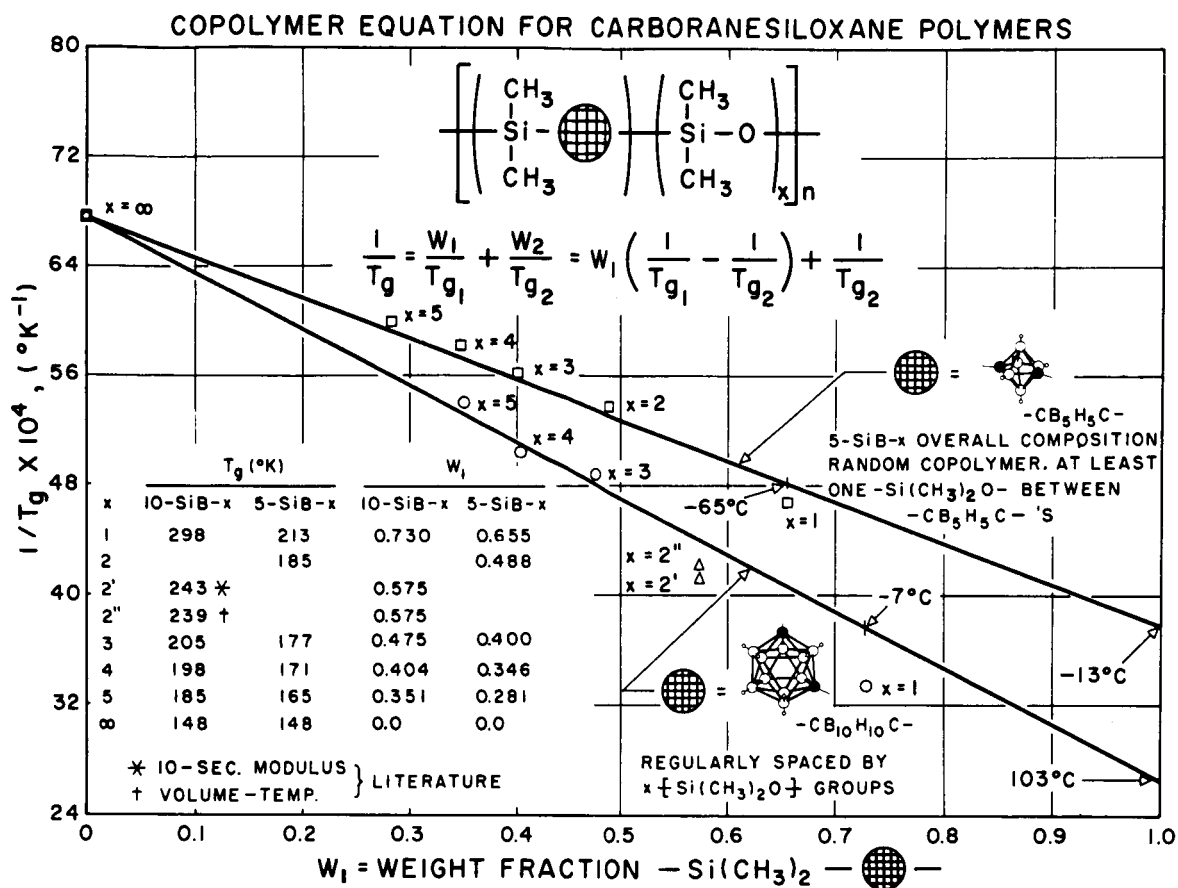 by 70°C. The direction of these changes would have been expected for a less-kinked molecular architecture. Since the thermomechanical stability was virtually unaffected, it appears that incorporation of para- versus meta-carborane cages is detrimental to the temperature range of elastomeric behavior, especially in the critical region around 25°C. The para-substituted polymer experienced a maximum rate of loss of weight about 50°C higher than the meta-carborane polymer, but the residual weight (700 to 800°C) was unaffected by the differences in the two structures. If loss of weight in the carborane polymers was due to cyclization reactions, as in the pure silicone, the colinearity of the linkages of the para-carborane would have been expected to inhibit these reactions, thereby decreasing the weight loss.

The fluorinated polymer (VI) displays a glassy state transition at about -180°C, which is probably related to motions of the trifluoropropyl groups, and a glass transition (-15°C) about 55°C

higher than the parent 10-SiB-3 polymer (despite its low molecular weight). It appeared to be less thermally stable than the latter which has half the organic content of the fluorinated polymer. The fluorinated polymer lost twice as much weight by about 540°C as did the totally methylated 10-SiB-3 (by about 620°C). Embrittlement occurred (480°C) some 80°C lower than for the parent 10-SiB-3 (560°C). After pyrolysis, it (VI) was a highly crosslinked resin, whereas the other 10-SiB-3 polymers (II to V) appeared to be highly crosslinked elastomers.

10-SiB-4 series (VII, VIII, IX, and X) — The structural formulae of these polymers, as presented in Table 3, need clarification only for that designated "10-SiB-4ϕ Random" (i.e. VIII) where the repeat unit contains an average of one -Si(C$_6$H$_5$)(CH$_3$)-O- unit per carborane nucleus. The other polymers (VII, IX, and X) have well-defined repeat units. Three of the polymers (VII, IX, X) have 10% of the methyl groups of the basic 10-SiB-4 structure replaced by phenyl groups and one (X) is end-capped with trimethylsilyl groups.

The thermomechanical spectra and thermogravimetric analysis data are presented in Figure 45 and Figure 46, respectively. The phenylated polymers display virtually identical behavior at low and high temperatures in having a glassy state transition at about -140°C, a glass transition temperature at about -57°C, and stiffening beginning at 430°C. The parent 10-SiB-4 polymer has a glassy state secondary transition at about

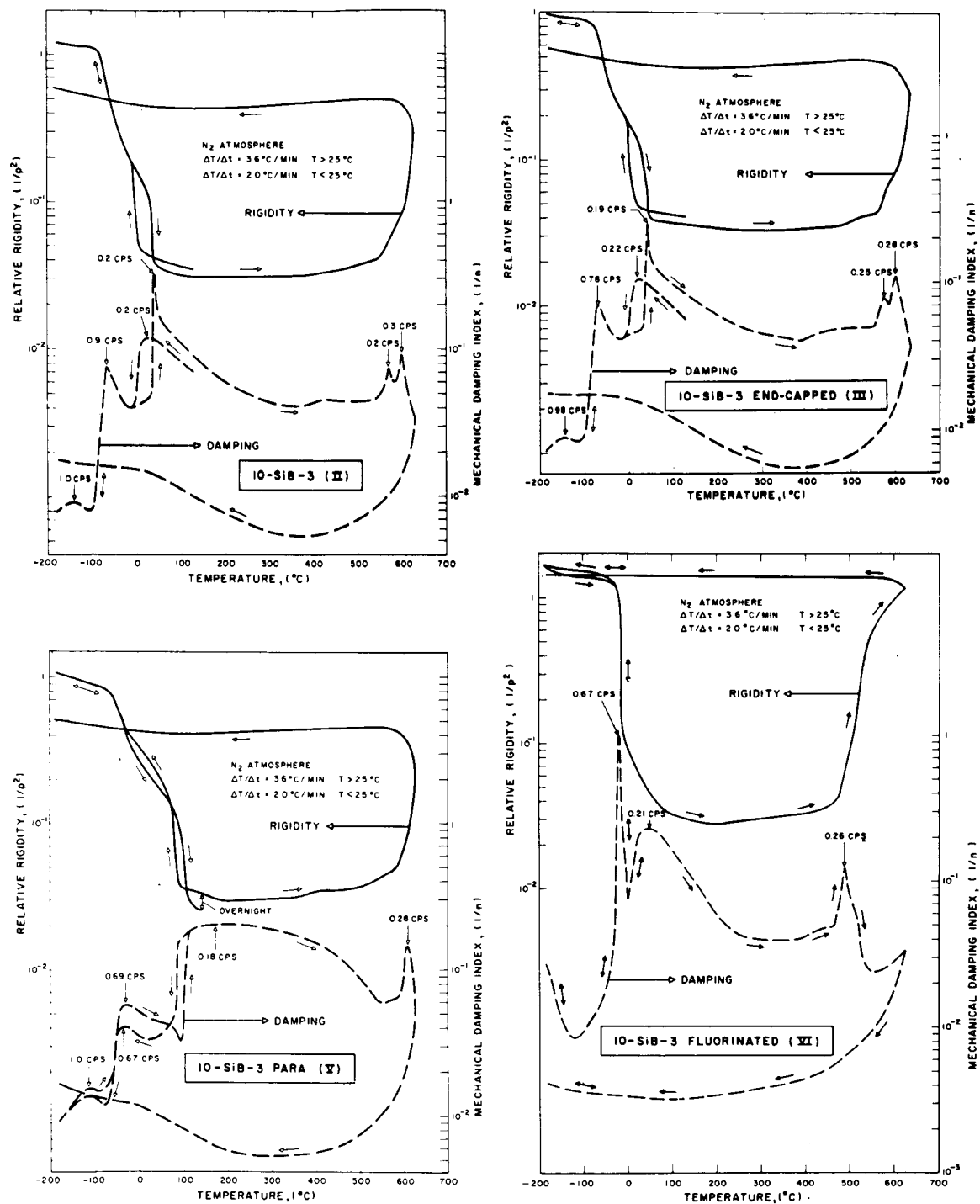FIGURE 43. 10-SiB-3 polymers. Thermomechanical behavior (–190°C ⇄ 625°C) in nitrogen. (See Figure 39 for 10-SiB-3 HIGH M.W.).
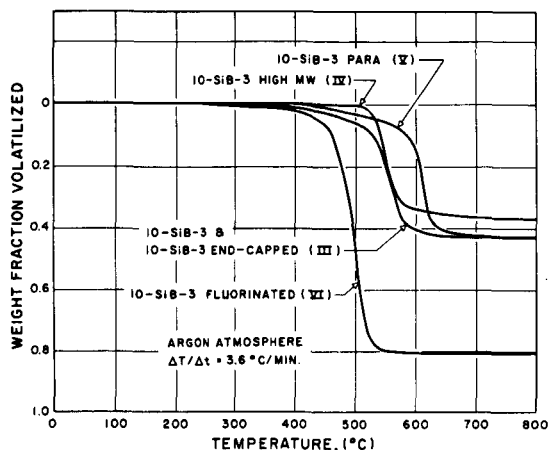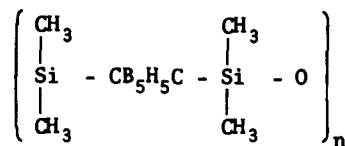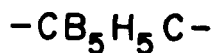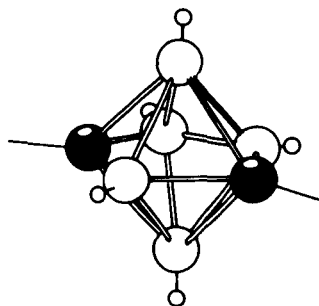
FIGURE 44. 10-SiB-3 polymers. Thermogravimetric analyses in argon.

−135°C, a glass transition temperature at about −75°C and stiffening begins at about 500°C. The phenylated polymers lost about half as much weight by 800°C as did the parent structure: this is in accord with the expectation that materials which crosslink earlier would experience lower loss of weight on pyrolysis. All the 10-SiB-4 polymers were highly crosslinked resins after pyrolysis to 625°C. The -$CB_{10}H_{10}$C- polymers all experienced a mode of stiffening which began at about 560°C (VI had already crosslinked by 550°C). This indicates that the initial stiffening of 10-SiB-3, at 550°C, is at the limit of thermomechanical stability in nitrogen for all the 10-SiB polymers characterized to date.

-CB_5H_5C-nuclei[42] — Polymers are emerging which contain carborane cages with less than 10 boron atoms per cage. One such experimental polymer is designated 5-SiB-1 and incorporates the 5-boron cage.[89,90]

$$-CB_5H_5C-$$

$$\left[\begin{array}{ccc} CH_3 & & CH_3 \\ | & & | \\ Si & - CB_5H_5C - & Si & - O \\ | & & | \\ CH_3 & & CH_3 \end{array} \right]_n$$

Modified forms of 5-SiB-1 have also been synthesized which incorporate a small fraction of larger carboranes (5 to 20%) to disrupt the crystallinity of 5-SiB-1 and render the polymer more elastomeric.[90,91]

Torsional braid analysis has been applied to the study of the thermomechanical properties in inert and in oxidative atmospheres of linear, uncompounded 5-SiB-1 and of a linear, random, uncompounded copolymer containing 20 mole percent 10-SiB-1. This copolymer was studied because of its inherent elastomeric character which was reported to be uncomplicated by crystallinity.[91] The results bear on the inherent transitions and high temperature stability of the linear polymers per se; and include mechanical spectra from −180°C to +625°C and the results of thermomechanical cycling experiments which were designed to determine the effect of high temperature history. The polymers were synthesized and provided by Dr. R. E. Kesting, Chemical Systems Incorporated, Santa Ana, California. The results of these TBA experiments on the 5-SiB-1 were helpful in assigning[91] the value of the glass transition, which (up to the galley proof stage of the later publication[91]) had been assigned incorrectly[90] on the basis of uncertain DTA evidence. Torsional Braid Analysis is probably the easiest unambiguous method for assigning transitions in the field of polymers!

5-SiB-1 homopolymer — The polymer was synthesized by a condensation procedure which would be expected to produce polymer of the correct structure.[90] The material was a hard light brown wax with molecular weight, $\overline{M}n = 12,500 \pm 10\%$.

Thermogravimetric analysis (TGA) and differential thermal analysis (DTA) data are displayed in Figure 47.

The thermomechanical behavior of 5-SiB-1 in nitrogen and in air were obtained on specimens which were prepared by heating (in situ at 2°C/min to 250°C in nitrogen) a glass braid soaked in a 10% (g polymer/ml chloroform) solution.

Figure 48 shows the thermomechanical spectra in dried nitrogen. On cooling from 130°C,
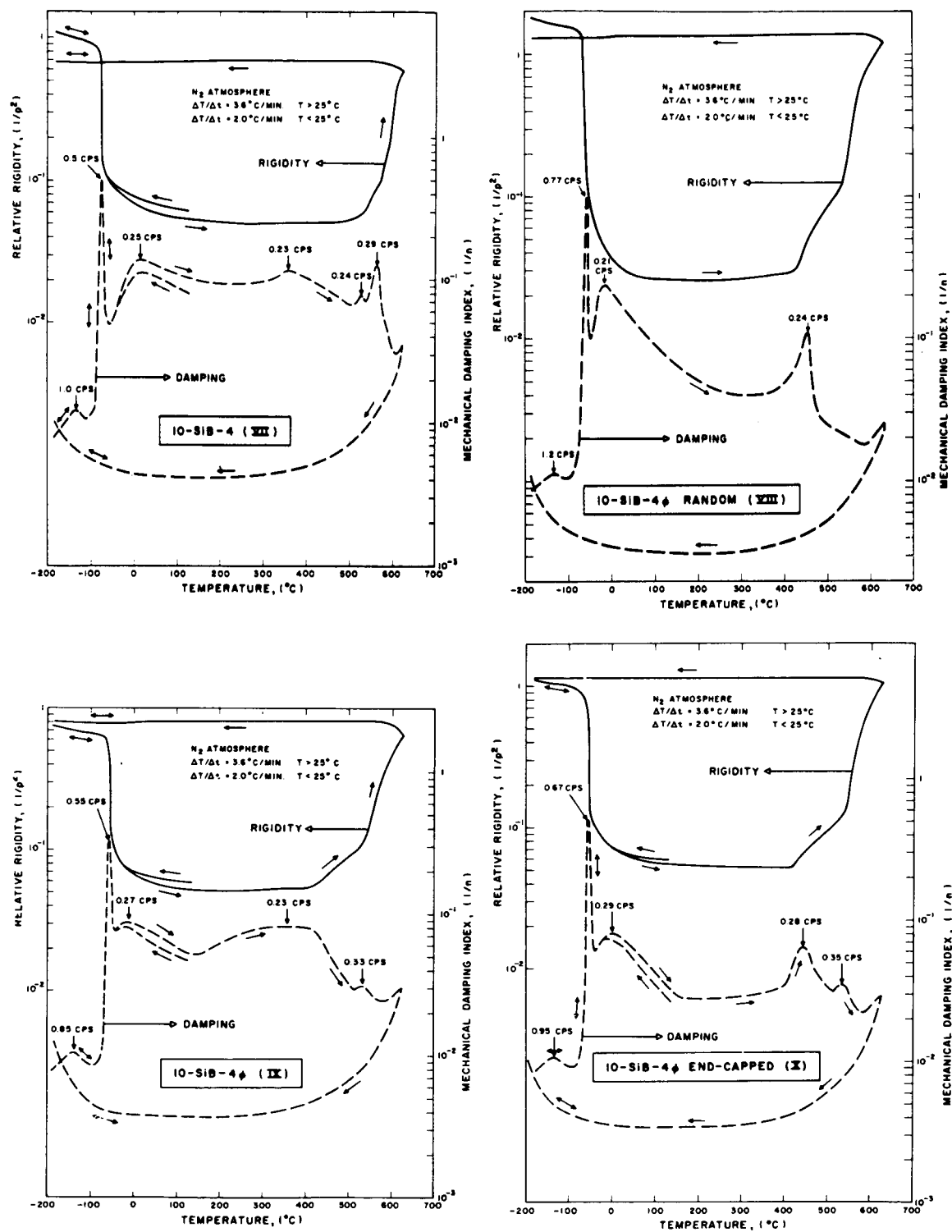
FIGURE 45.   10-SiB-4 polymers. Thermomechanical behavior (–190°C ⇄ 625°C) in nitrogen.
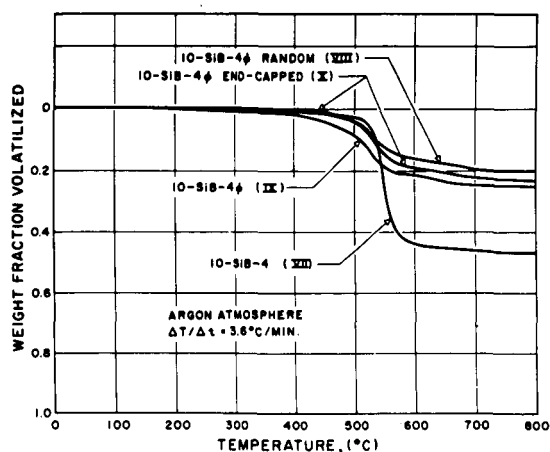
FIGURE 46. 10-SiB-4 polymers. Thermogravimetric analyses in argon.
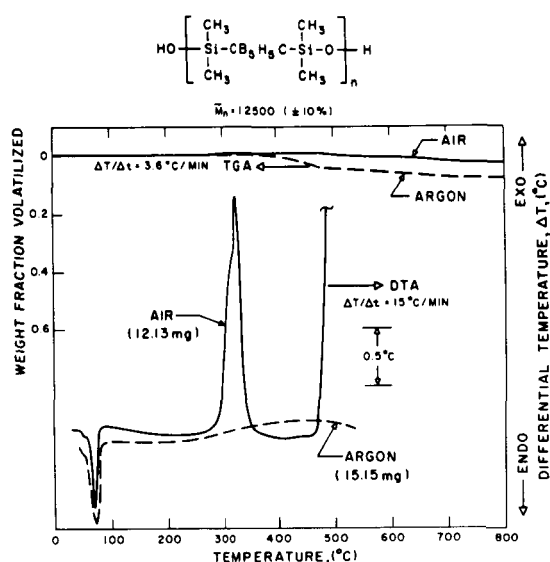
FIGURE 47. 5-SiB-1 homopolymer. Thermogravimetric and differential thermal analyses in argon and in air.

FIGURE 48. 5-SiB-1 homopolymer. Thermomechanical behavior ($-190°C \rightleftarrows 625°C$) in nitrogen.

The rigidity begins to rise at 400°C sigmoidally to 625°C, presumably due to crosslinking. The damping peaks at 560°C corresponding to the catastrophic increase in rigidity. On cooling from 625°C to -180°C, the rigidity rises to a high constant level by 500°C and the damping drops to a very low level, which are characteristic of a highly crosslinked resin. (After the pyrolysis, the behavior below 25°C was reversible.)

In air (Figure 49) the rigidity decreases slightly from 130°C to 250°C, where it rises sharply (corresponding to an increase in weight by TGA and a large exotherm by DTA) to a broad maximum in the vicinity of 380 to 400°C. There is a minimum at 460°C and then a large sigmoidal rise, corresponding to weight loss, which flattens out in the 600 to 625°C range. The damping rises slowly from 130°C to a sharp peak at 295°C corresponding to the first rise in rigidity. There is a damping minimum at 375°C leading to a broad flat peak in the 450° to 530°C range. On cooling from 625°C, the rigidity rises slowly to a constant high level below 400°C. The damping decreases just below 625°C to a minimum at 580°C, rises to a peak at 465 to 470°C, after which it drops

crystallization is accompanied by a damping maximum at 50°C (0.3 cps), the glass transition occurs at -60°C (0.7 cps), and a low temperature transition is revealed at -140°C (0.9 cps). It is noteworthy that similarly located glassy state transitions are observed on the 10-SiB-X polymers (Table 3). On the subsequent heating from -180°C some thermo-hysteresis is displayed (the consequence of the crystallinity) which, for the most part, occurs above T_g; T_m is 70°C. Above 150°C, the rigidity drops to a minimum near 200°C and then rises to a plateau at about 320°C. The damping has a corresponding peak at 220°C.

$$HO \left[\begin{array}{c} CH_3 \\ | \\ Si-CB_5H_5C-Si-O \\ | \\ CH_3 \end{array} \begin{array}{c} CH_3 \\ | \\ \\ | \\ CH_3 \end{array} \right]_n H$$

$$\bar{M}_n = 12500 \ (\pm 10\%)$$

FIGURE 49. 5-SiB-1 homopolymer. Thermomechanical behavior (120°C $\rightleftharpoons$ 625°C) in air.

sharply to a very low level near 130°C. The behavior of the rigidity and damping indicates a broad glass transition region between 400°C and 500°C for the oxidatively-cured (to 625°C) homopolymer.

5-SiB-1 copolymer — The copolymer was prepared by a procedure which would be expected to place the 5-SiB-1 and 10-SiB-1 units randomly in the chain backbone.[90,91]

The majority of the work presented used a sample with molecular weight, $\bar{M}_n$ = 3830 ± 10%. A sample with $\bar{M}_n$ = 11,400 ± 10% was received later and some work on it is discussed. The lower $\bar{M}_n$ copolymer sample was received as a glossy, black, soft, and tacky disk; the higher $\bar{M}_n$ sample was glossy and black, but less tacky and harder than the former.

Thermogravimetric (TGA) and differential thermal analyses (DTA) are shown in Figure 50. The DTA data in argon on the polymer "as received," reveals a very small but sharp endothermic peak (T_m) at about 51°C (cf. T_m = 70°C for homopolymer) and displays behavior similar to that of the homopolymer above 100°C. The sample was insoluble after the DTA run to 530°C and appeared to have retained its original shape. Another specimen remained soluble after heating to 350°C at 3.6°C/min in nitrogen, indicating that the crosslinking occurs above 350°C where the DTA plot was relatively flat. In air, the DTA data are identical to those in argon until 230°C where a steady exothermic drift begins; above 350°C a large exotherm, peaking at 373°C, is evident. (The corresponding peak temperature is 326°C for the homopolymer.) At about 470°C another large exotherm begins. DTA data for both samples of the copolymer (as received) are similar with the exception of the intensity of the 51°C endotherm which is five times as large (area/mg) for the specimen with higher $\bar{M}_n$. Another low $\bar{M}_n$ specimen of the "as received" polymer was preheated at 3°C/min in nitrogen to 250°C and cooled to room temperature before placement in the DTA sample holder several days later; it was then run in air as previously described. The only apparent difference is the disappearance of the small 51°C endotherm, which led to the conclusion that a small degree of crystallinity developed on prolonged

$$HO \left[\left(\begin{array}{c} CH_3 \\ | \\ Si - CB_5H_5C - Si - O \\ | \\ CH_3 \end{array} \begin{array}{c} CH_3 \\ | \\ \\ | \\ CH_3 \end{array} \right)_{0.8} \left(\begin{array}{c} CH_3 \\ | \\ Si - CB_{10}H_{10}C - Si - O \\ | \\ CH_3 \end{array} \begin{array}{c} CH_3 \\ | \\ \\ | \\ CH_3 \end{array} \right)_{0.2} \right]_n H$$

5-SiB-1   10-SiB-1

standing, as has been reported for similar copolymers incorporating less $C_2B_{10}H_{10}$.[91] The crystallinity appeared to be eliminated in the initial heating cycle. The 51°C m.p. compares favorably to the values 57°C, 56°C, and 52°C previously reported[91] (by differential scanning

calorimetry, DSC) for 5%, 10%, and 15% (mole %) $C_2B_{10}H_{10}$ in the copolymer. The different degrees of crystallinity for the $\bar{M}_n$ = 3830 and $\bar{M}_n$ = 11,400 samples would contribute to the different appearances and "feel" of the two "as received" samples.
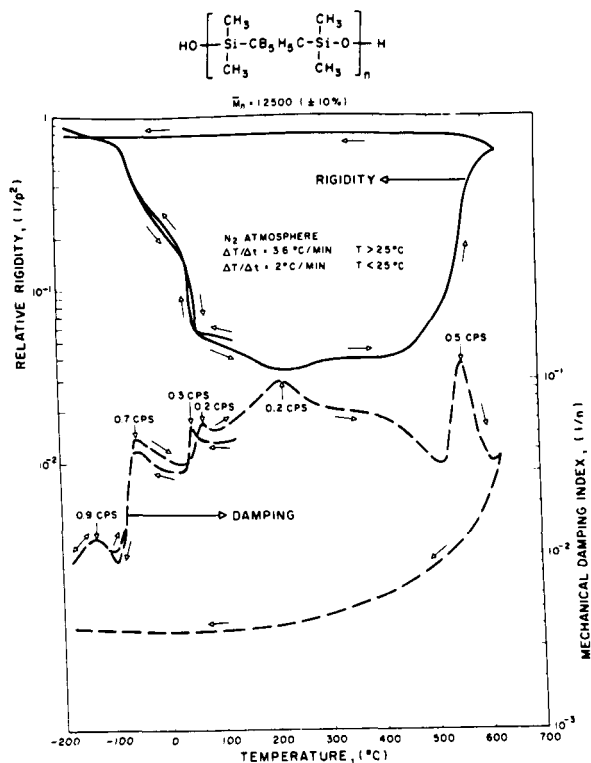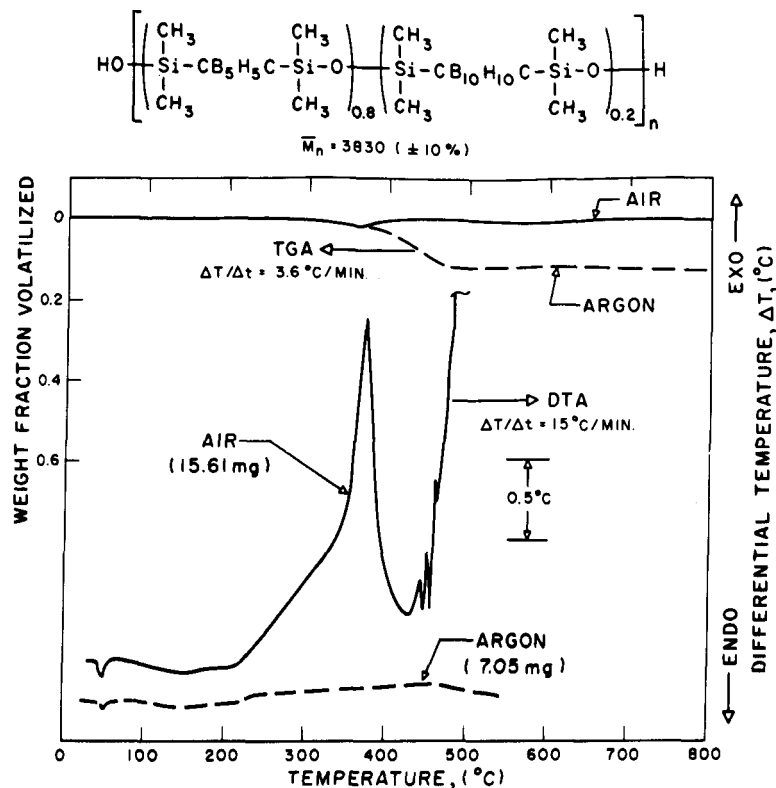
FIGURE 50. 5-SiB-1 copolymer. Thermogravimetric and differential thermal analyses in argon and in air.

The TGA and DTA data alone would suggest (to some) a rather high degree of thermal stability to 500°C and above. Oxidatively there is a high degree of stability in terms of weight loss, but the large exotherm in air (DTA) and the TGA results in argon suggest that the lower oxidative weight loss is in some way related to a reaction occurring in the neighborhood of 300 to 350°C.

Thermomechanical behavior of the copolymer in nitrogen and in air — The specimens for TBA were prepared from a 10% solution in xylene for the $\overline{Mn}$ = 3830 sample and from a 10% solution in chloroform for the $\overline{Mn}$ = 11,400 sample in the manner described above for the homopolymer.

Master curves — The master curves are continuous plots from 130°C → -180°C → 130°C (at $\sim$ 2°C/min) → 625°C → 130°C (at 3.6°C/min) → -180°C →20°C (at $\sim$2°C/min) in dried N_2 (Figure 51); and 120°C → 625°C → 120°C at 3.6°C/min in air (Figure 52).

The low temperature dynamic mechanical properties of the polymer are displayed in Figure 51. There is a damping peak at -52°C (0.65 cps) accompanied by a large decrease in rigidity. This

corresponds well to the value -54°C for Tg determined by differential scanning calorimetry (DSC).[91]

The glass transitions of -60°C and -52°C for the homopolymer and copolymer, respectively, are indicative of a high degree of flexibility in the polymer chain or of a high free volume which could result from the kinked nature of the molecule. It is interesting to compare the behavior with that of the analogous 10-SiB-X polymers for which data[44] on the transitions as a function of X are available (Table 3). It is apparent that 5-SiB-1 corresponds most closely to the 10-SiB-3 polymer which has four more silicon-oxygen flexible bonds in the repeat unit. This leads to the conclusion that the smaller carborane cage influences the transitions, and/or the carbon-silicon bond differs significantly in its nature and flexibility, depending on the type of carborane cage in which the carbon is incorporated. Application of the empirical copolymer relationship $T_g^{-1} = W_1/T_{g1} + W_2/T_{g2}$ to the above glass transition temperatures for the homopolymer and copolymer, where W_1 and W_2 are the weight fractions of each of the two
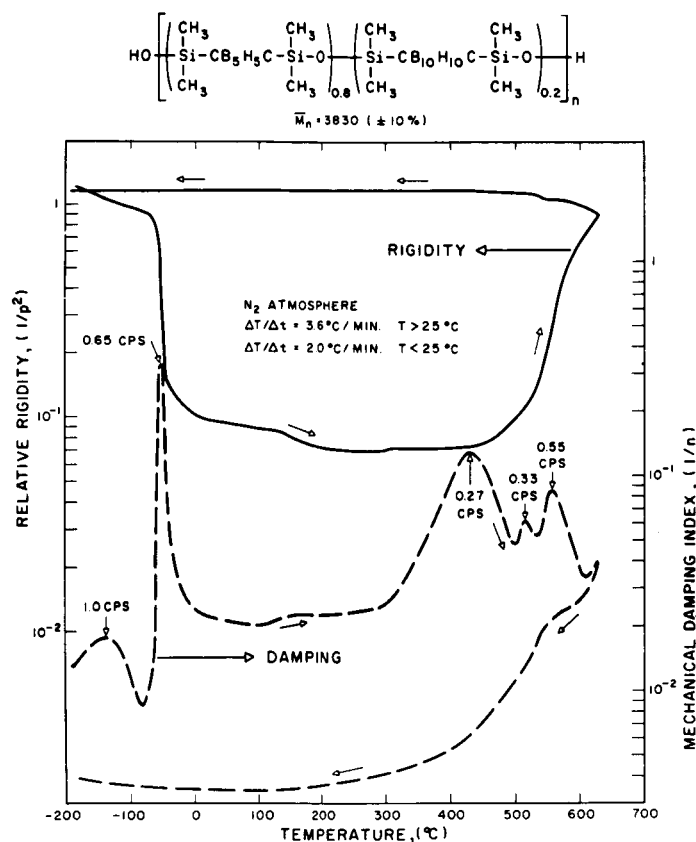
FIGURE 51. 5-SiB-1 copolymer. Thermomechanical behavior (-190°C ⇄ 625°C) in nitrogen.

components of the copolymer, predicts a T_g for 10-SiB-1 of $\sim$ -24°C. Although it does not correspond to the value of +25°C (Table 3), it does indicate a significantly higher intrinsic stiffness for 10-SiB-1 relative to 5-SiB-1. Extending this approach to the homopolymer (i.e. 5-SiB-1 as a 1:1 copolymer of 5-SiB-O and dimethylsiloxane), and assuming the equation would apply to the non-random copolymer, the equation predicts a Tg for $[-Si(CH_3)_2 - CB_5H_5C-]_n$ of $\sim$ +3°C. If valid, this would again demonstrate the unusual flexibility of the particular silicon-carbon (carborane) bond. The non-applicability of the equation to this alternating copolymer would be attributable to the effect of regular in-chain geometry on intermolecular interaction and not on inherent chain flexibility.[41]

In the glassy state there is a small well-defined damping peak at -140°C (1.0 cps) which is accompanied by an inflection in the rigidity curve. A similarly located secondary transition is revealed in the glassy state of the homopolymer (Figure

48). In the range of 130°C to 160°C there is also a small drop in modulus and increase in damping similar to that seen in the homopolymer. At about 295°C, a small step-rise in rigidity occurs which is accompanied by the onset of a large damping peak which reaches a maximum at $\sim$ 425°C (0.27 cps). The rigidity begins to rise further at 400°C. There is a very small damping peak at 515°C (0.33 cps) and another larger one at 560°C (0.55 cps). The high temperature responses (T > 400°C) in nitrogen of the homopolymer and the copolymer are virtually identical, with the rigidity rising sigmoidally from 400°C to 625°C. On cooling from 625°C the rigidity experiences a small step-rise at $\sim$ 550°C (this temperature is sensitive to the time lapsed reversing the direction of temperature programming) and is accompanied by a shoulder in the rapidly decreasing damping. The rigidity remains flat from 550°C to -180°C (and back reversibly to 20°C). The damping, below 300°C, remains at a low, almost constant level. A specimen with $\overline{M}n$ = 11,400, examined in a similar

manner, gave identical results with a few minor exceptions: a) the step-rise in rigidity at 290°C was not present; b) the 515°C damping peak was not present; and c) the 560°C damping was about the same amplitude as the 425°C peak (unlike that for the $\overline{Mn}$ = 3830 sample where it was smaller). It is interesting to note that the T_g (-52°C) and the secondary transition (-140°C) were not shifted when the number average molecular weight ($\overline{Mn}$) of the polymer increased from 3830 to 11,400. The sample of the lower Mn "as received" polymer that was preheated at 3.6°C/min in N_2 to 250°C before the oxidation DTA run (see above) showed evidence of puckering and bubble marks indicating that some low molecular weight volatiles had been driven off, whereas a specimen of the $\overline{Mn}$ = 11,400 sample did not display evidence of bubbling. (These volatiles may contribute significantly to the low $\overline{Mn}$ reported for the first sample.)

In air (Figure 52) the rigidity rises slowly above 175°C until 340°C where it rises sharply to a maximum between 420°C and 445°C. There is a small drop at 460°C and then a slow rise to about the same level as the maximum reached at 420°C
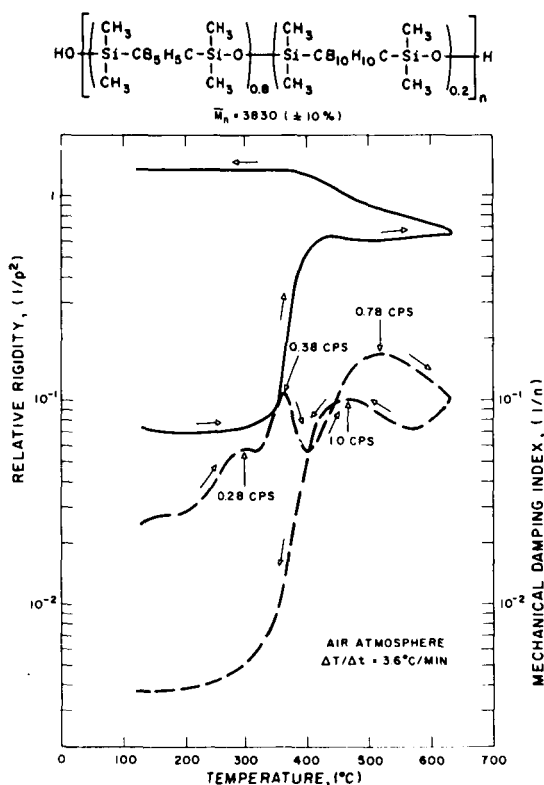

$$\text{HO}\left[\begin{matrix}CH_3 \\ | \\ Si-C_6H_5C \\ | \\ CH_3\end{matrix}\begin{matrix}CH_3 \\ | \\ -Si-O \\ | \\ CH_3\end{matrix}\right]_{0.8}\left[\begin{matrix}CH_3 \\ | \\ Si-C_8{}_{10}H{}_{10}C \\ | \\ CH_3\end{matrix}\begin{matrix}CH_3 \\ | \\ -Si-O \\ | \\ CH_3\end{matrix}\right]_{0.2}{}_n H$$

$\overline{M}_n = 3830 \ (\pm 10\%)$

FIGURE 52. 5-SiB-1 copolymer. Thermomechanical behavior (120°C ⇌ 625°C) in air.

These features are less pronounced than for the homopolymer. The damping starts with a small increase (as in nitrogen), but at 200°C it begins a large rise to a shoulder between 290°C and 320°C; there is a sharp peak at 360°C, a minimum at 400°C, and a broad peak near 520°C which falls off to 625°C. The maximum in the rigidity curve indicates that there is a reaction (scission) competing successfully near 450°C. The thermal (in argon) TGA curve displays the maximum rate of weight loss in this region for the linear copolymer in absence of oxidative crosslinking. This leads to the conclusion that the reduction in rigidity observed during oxidation, in the already highly crosslinked and immobile network, has the same thermal origin (chain scission by generation of an active species) as the weight loss and crosslinking experienced in the absence of air where the chains are still mobile. On cooling from 625°C, the rigidity climbs slowly through what appears to be a broad glass transition region between 400°C and 500°C; from 400°C to 100°C the rigidity is flat. Correspondingly the damping decreases from 625°C to 570°C; there is a broad peak at 460°C, and a large decrease between 410°C and 240°C below which the decrease continues slowly. The mechanical behavior of the copolymer oxidatively-cured to 625°C and the similarly treated homopolymer are very similar.

Comparison of the oxidative thermomechanical data for the homopolymer and the copolymer, indicates that although the homopolymer's cross-linking threshold temperature ($\Delta T/\Delta t$ = 3.6°C/min) is 50°C lower than that of the copolymer (which is about 340°C), the initial stage (i.e. to $\sim$ 400°C) of crosslinking in the homopolymer results in a less densely crosslinked structure. This is evidenced for the homopolymer first by the lower rigidity at 400°C (relative to the final crosslinked product); second by the larger subsequent decrease in rigidity by 460°C apparently due to thermal scission of a looser network; and third by a large degree of subsequent stiffening corresponding to the formation of a very tightly crosslinked system — possibly of similar origin to the catastrophic stiffening observed in nitrogen in the same temperature range (450 to 625°C).

Cycling — Thermomechanical cycling experiments were carried out on the $\overline{Mn}$ = 3830 copolymer in both nitrogen and air (Figures 53 and 54). The cycles were closed loops from 130°C
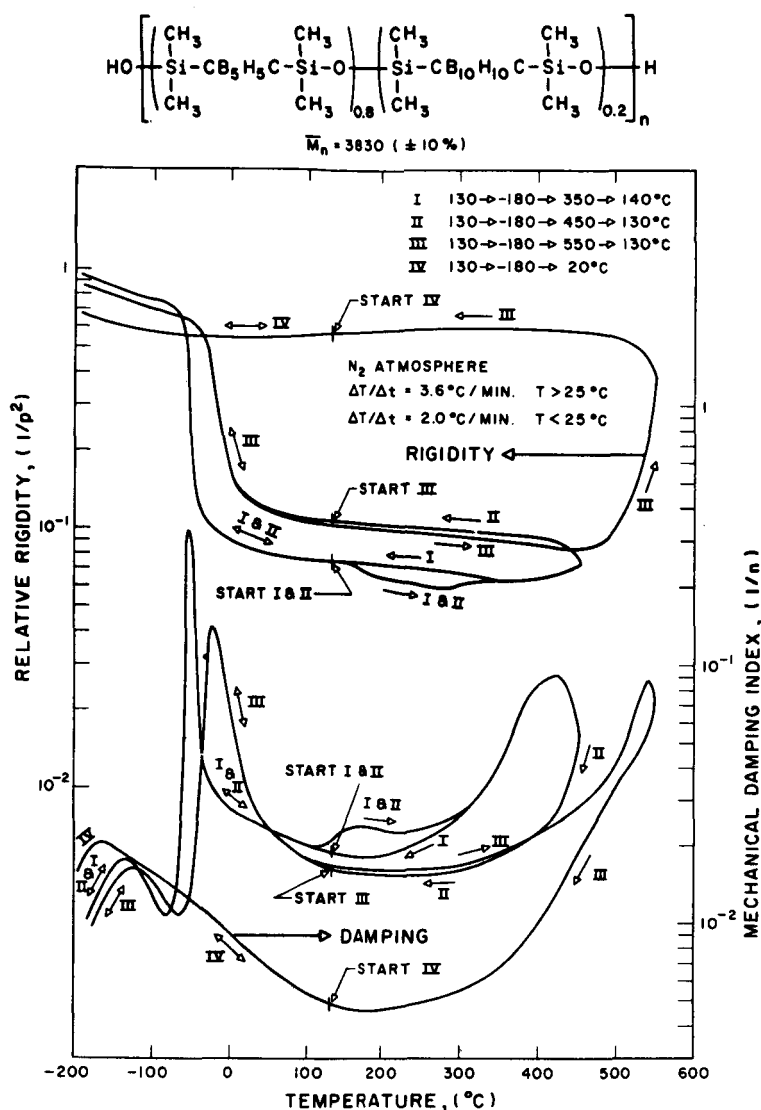
$\overline{M}_n = 3830\ (\pm 10\%)$

FIGURE 53. 5-SiB-1 copolymer. Thermomechanical behavior on cycling in nitrogen.

→ -180°C → cycle maximum → 130°C with the final segment from 130°C → -180°C → 20°C (to test for reversibility of the low temperature region after pyrolysis). In nitrogen the maximum cycle temperatures were 350°C, 450°C, and 550°C. In air they were 250°C, 350°C, and 450°C. In general, the cycling data amplify the data of the master curves.

The first new information is that the 130 to 160°C damping peak and drop in rigidity are not reversible on heating and subsequent cooling. This is observed in both nitrogen (to 350°C) and air (to 250°C) cycling. The lack of change in the pro-

perties of the inert glass substrate per se at 130°C coupled with the response of the glass/polymers composite (Figures 53 and 54), points to some change in the properties of the polymer or composite property.

The next interesting feature of the cycling experiments is that in both cases the first cycle (to 350°C in nitrogen and to 250°C in air) had no apparent effect on the secondary transition (-140°C) or on the glass transition temperature (-52°C). This is in spite of the fact that in both cases the damping had begun to rise to the peaks seen in the master curves, before the cycle
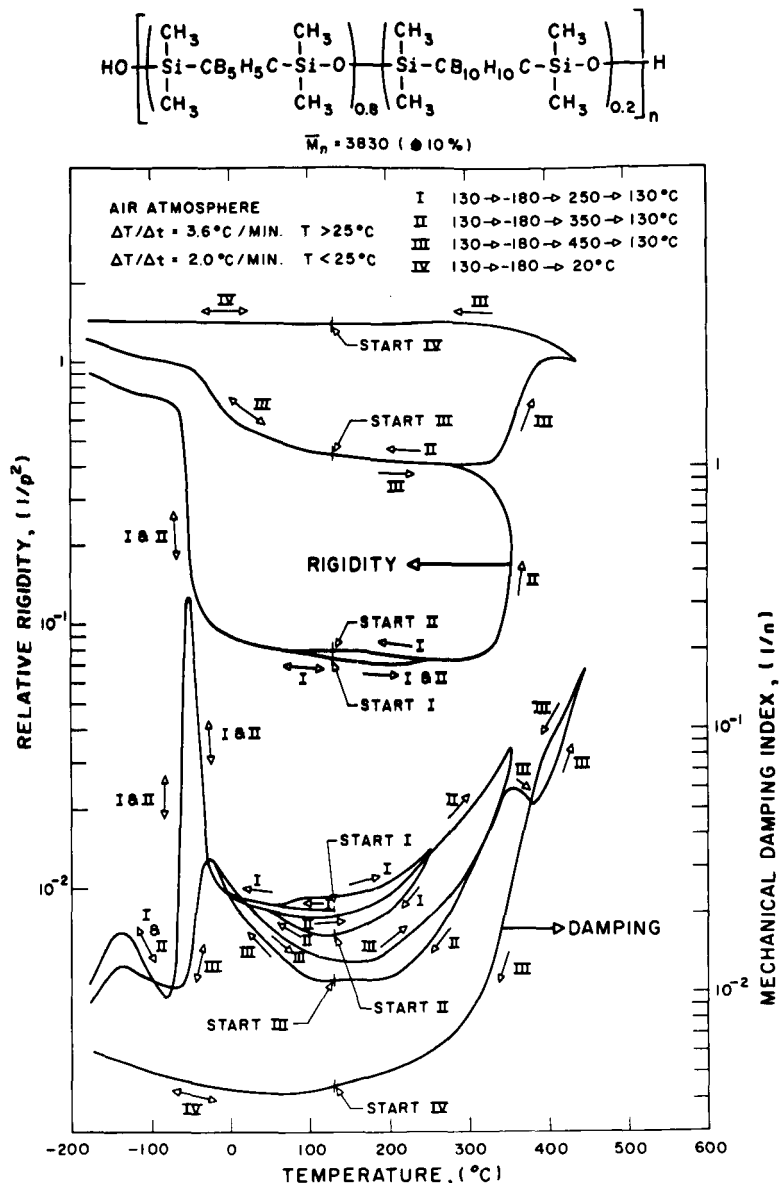
FIGURE 54.   5-SiB-1 copolymer. Thermomechanical behavior on cycling in air.

maximum was reached. In other experiments it was found that the applied heating cycle (to 350°C in N_2 and to 260°C in air) left the polymer soluble in xylene, indicating that no significant crosslinking had occurred. It is of interest to note that in the air run there is a marked increase in the degree of thermo-hysteresis in damping above the glass transition temperature (relative to cycling in nitrogen).

In the second stage of each experiment (to 450°C in nitrogen; to 350°C in air) the polymer entered a reaction region. In both cases the rigidity

is higher on cooling from the cycle maximum than from heating up to it. The rise in rigidity in the air run is significantly higher than in the nitrogen run. This is consistent with the relative shapes of master curves in the temperature region of the maximum temperature of the cycle. The damping level in both cases decreases, and the glass transition peak is broadened, decreased in amplitude, and is shifted up to about −25°C. In nitrogen, the −140°C damping peak is shifted to −130°C and its magnitude decreased slightly. In air, the −140°C peak is not shifted in temperature, but is decreased

in magnitude significantly. The different effect of each environment on the glassy state secondary transition would lead one to suspect that the crosslinking sites for the two environments are different.

In the third stage of each experiment (550°C in nitrogen; 450°C in air) the material progressively enters the mechanical state of highly crosslinked rubber and highly crosslinked resin, respectively. The nitrogen pyrolysis (to 550°C) product is a highly crosslinked rubber since it displays a small *decrease* in rigidity with *decreasing* temperature below 330°C (i.e. G' has a positive temperature coefficient) and an increase in damping at low temperature where the rigidity begins to rise again on further cooling. This is typical elastomeric behavior and has been seen with other carborane-siloxane polymers studied in this laboratory. The master curve (Figure 53) in nitrogen shows that after 625°C the polymer becomes a highly crosslinked resin.

The low temperature damping peak (-140°C in both polymers) indicates the onset of some intramolecular motion more localized than for example that associated with T_g. The absence of low temperature damping peaks after pyrolysis to 625°C and also after oxidation to 450°C indicates that the crosslinking occurred at short enough range to prevent the localized motion related to the -140°C transition of the linear polymer. Thermal and oxidative cycling data show the effect of increasing crosslink density on both T_g and the secondary transition. A difference between the nitrogen and air cycling experiments is that in nitrogen, each successive cycle decreases the rigidity in the glassy state (until the 625°C turnaround in the master curve brings the rigidity of the crosslinked resin above that of the uncrosslinked glass), while the glassy state rigidity of the oxidative curve increases with each step. Although weight loss can affect relative rigidity in the manner seen in nitrogen on account of changes in geometry, a study of the TGA data shows that the large change in weight occurs in the temperature range where the decrease in rigidity is small and vice versa.

Conclusions

Thermomechanical spectra in nitrogen of linear 5-SiB-1, and a linear copolymer of 5-SiB-1 with 20 mole % 10-SiB-1 in the backbone show that the

polymers do not begin to crosslink until about 400°C. In air the copolymer appears to be quite stable to about 300°C where crosslinking occurs. The homopolymer appears to be less stable oxidatively and crosslinking commences at about 250°C.

The mechanical data on the polymers indicate that the low level of weight loss in air revealed by TGA was due to the formation of crosslinks (cf. polydimethylsiloxane decomposition which in nitrogen gives cyclic volatiles). The DTA data in argon gave no hint of the crosslinking that occurs below 500°C, while DTA data in air do correspond well to the rapid stiffening detected by TBA. This points up a problem of trying to evaluate, *via* TGA and DTA, a material whose proposed applicability (i.e. an elastomer) is very sensitive to its structure (i.e. degree of crosslinking).

From the TBA data at 3.6°C/min the following broad categories have been established to reflect the state of the 5-SiB-1, 20% 10-SiB-1 copolymer: in nitrogen, a linear polymer to 400°C, a rubber to 500°C and a thermoset to 625°C; in air; a linear polymer to 300°C, a rubber to 350°C, and a thermoset to 625°C. The states of the homopolymer in nitrogen are similar, with the low temperature properties reflecting the material's crystallinity, different glass transition temperature and similarly located secondary transition. The homopolymer in air is a linear polymer to 250°C, a hard rubber to 450°C, and a thermoset to 625°C.

From the point of view of making an elastomer with stability at elevated temperatures, the advantage gained by adding 20% $-CB_{10}H_{10}C-$ to the 5-SiB-1 backbone is indicated by virtually identical high temperature mechanical properties of the two polymers in nitrogen and the improved properties of the copolymer relative to the homopolymer in air, while the useful low temperature limit (as an elastomer) is extended from the 70°C T_m of the homopolymer to the -52°C T_g of the copolymer.

5-SiB-X series — Results on low molecular weight random copolymers, each with overall composition 5-SiB-X where X = 1,2,3,4, and 5, have recently been obtained.[49] The designation of each polymer, its chemical structure, and data on transitions are summarized in Table 4. The 5-SiB-X series of polymers, taken as copolymers of $[-Si(CH_3)_2-O-]$ and $[-Si(CH_3)_2-CB_5H_5C-]$, fit the copolymers equation well (see Figure 40).

DESIGNATION	STRUCTURE	T_m	T_{crys}	T_g	T_{sec}	T_m/T_g
5-SiB-1	$HO-[Si(CH_3)_2-C_6H_5C-Si(CH_3)_2-O]_n-H$; $\overline{M}_n = 12{,}500 \pm 10\%$	70°C	50°C	-60°C	-140°C	1.61
5-SiB-2 RANDOM COPOLYMER	$HO-\{[Si(CH_3)_2-C_6H_5C-Si(CH_3)_2-O]_{1/2}[Si(CH_3)_2-O]_{1/2}\}_n-H$; $\overline{M}_n = 6170 \pm 10\%$	A	A	-88	-145	
5-SiB-3 RANDOM COPOLYMER	$HO-\{[Si(CH_3)_2-C_6H_5C-Si(CH_3)_2-O]_{1/3}[Si(CH_3)_2-O]_{2/3}\}_n-H$; $\overline{M}_n = 5860 \pm 10\%$	A	A	-96	-145	
5-SiB-4 RANDOM COPOLYMER	$HO-\{[Si(CH_3)_2-C_6H_5C-Si(CH_3)_2-O]_{1/4}[Si(CH_3)_2-O]_{3/4}\}_n-H$; $\overline{M}_n = 4270 \pm 10\%$	A	A	-102	-140	
5-SiB-5 RANDOM COPOLYMER	$HO-\{[Si(CH_3)_2-C_6H_5C-Si(CH_3)_2-O]_{1/5}[Si(CH_3)_2-O]_{4/5}\}-H$; $\overline{M}_n = 3920 \pm 10\%$	A	A	-108	-145	
5-SiB-∞ SE-30	$CH_3-Si(CH_3)_2-O-[Si(CH_3)_2-O]_n-Si(CH_3)_2-CH_3$; $MW > 10^6$	-40	-55	-125	A	1.58

TABLE 4. Chemical Formulae and Transitions of 5-SiB-X Polymers.

VII. Effectiveness of Polymer Additives*[21,40]

Introduction

This section by Dr. Williams of the American Cyanamid Company, Bound Brook, New Jersey, examines the application of the Torsional Braid Analysis technique for assessing the effectiveness of polymer additives in preventing or retarding reactions, such as crosslinking or chain scission, which are manifested by modulus changes in the polymer. The technique is particularly useful in studying systems such as unvulcanized elastomers or film coatings where the material itself cannot support its own weight. Regardless of the elaborateness of the apparatus, the criterion is merely that it be capable of monitoring modulus changes which result from a softening or embrittlement of the polymer under study, such changes being dependent upon the mode of degradation. In this manner the effectiveness of polymer additives can be evaluated. This is accomplished by dip-coating glass fiber braids with a polymer containing given concentrations of selected additives. A coated braid prepared without additives serves as a control. These coated braids can then be conditioned at constant elevated temperatures and/or controlled environments which could cause a degradative change in the polymer. This degradation will be more or less inhibited or retarded in accordance with the concentration and activity of the stabilizers present. The intermittent measurement of the torsional rigidity of the braids during the course of their conditioning provides a convenient and sensitive measure of the rate of change in the structure of the polymer. This change is monitored by following the change in the relative rigidity of the polymer/glass braid composite. The relative rigidity, G'_t/G'_0, is defined as the ratio of the rigidity modulus, G'_t, obtained after some environmental aging time, t, to the rigidity modulus G'_0 obtained initially. In terms of experimentally-determined quantities, the relative rigidity is given by P_0^2/P_t^2, where P is the period of oscillation of the torsional pendulum and the subscripts are as indicated previously.

Since the rigidity modulus is temperature-

*The text for this section was written by Dr. B. L. Williams.

dependent, it is essential that both P_O and P_t be measured at the same temperature. One method of obtaining these measurements is to mount a braid specimen in the TBA apparatus, thermostated at a specific heat-aging temperature or under the specific environmental conditions desired. In this case, the conditioning is accomplished directly in the TBA apparatus, and both P_O and P_t are measured under these conditions. With this method, however, the environmental aging data in the form of a G_t'/G_O' vs. aging time curve can be obtained for only one braid specimen at a time. In additive or stabilizer screening studies, where such data are required on a series of stabilized braid specimens as well as on an unstabilized control, an alternative method of measurement can be used. In this method, a fixed length of each coated braid is permanently fastened at either end to light spring loaded clamps. These clamps are readily attached through simple set screw couplings to the extension rods of the torsional braid apparatus. With this arrangement any braid can be readily and repreatedly inserted in and removed from the torsional braid apparatus without altering its dimensions or condition. It is then possible to measure P_O for a series of braids at room temperature in the torsional braid apparatus and also condition the braids in an oven or controlled environment. During the conditioned aging, intermittent measurements of P_t can be made at room temperature by transferring the braids from the oven to the torsional braid apparatus. In this manner G_t'/G_O' vs. conditioned aging time curves can be obtained on the whole series of braids at one time. A comparison of rate curves obtained in this manner on braids containing additives, with that obtained on an unprotected control, provides a convenient quantitative measure of the desired activity of the additive.

Results and Discussion

The mechanical spectra were determined on essentially three systems: carboxylated styrene-butadiene latex, cis-polybutadiene, and natural rubber.

In the systems under investigation, the effect of whatever change was taking place was found to be one of embrittlement. That is, as a function of accelerated heat aging or environmental conditioning, the relative modulus of the composite polymer/glass braid sample was found to increase. Thus, by plotting these parameters — relative modulus vs. heat aging time — on a log-log graph, a characteristic curve could be obtained, such as shown in Figure 55. The profile of this curve was found to exhibit a certain pattern very similar to that of the absolute modulus profile obtained when a polymer is cooled from a rubber to a glassy state. In the latter instance, the inflection point of the curve is used to determine the glass transition temperature (T_g) of the system. In a similar manner, the inflection
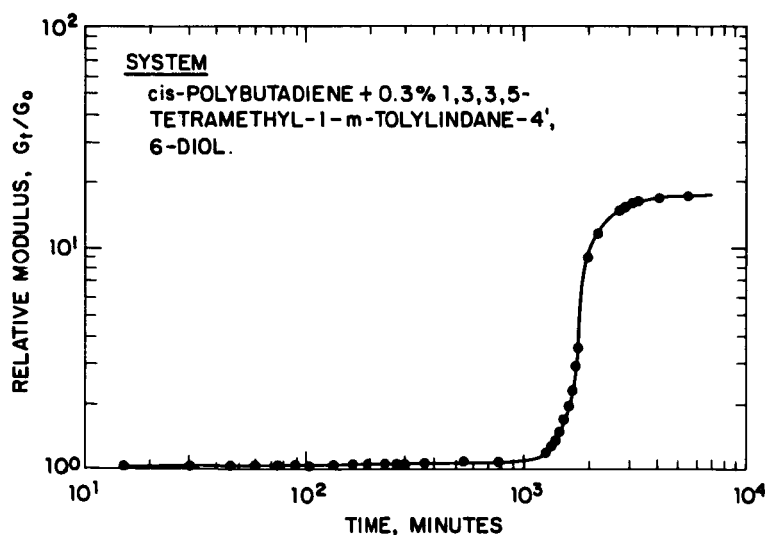

FIGURE 55. Cis-polybutadiene. Effectiveness of polymer additives. Relative modulus as a function of aging time in the Torsional Braid Apparatus at 100°C. Actual measurements performed at the aging temperature.

point of the profile obtained in this study of additive/polymer/glass composite systems is used to determine an embrittlement point. The dependence of this embrittlement point on the aging or conditioning time is in turn taken as a measure of the ability of a particular additive to inhibit the crosslinking of the system.

The reproducibility of this technique can readily be seen from the results shown in Figure 56. In this case the relative modulus as a function of aging time is plotted for three different impregnated braids prepared from the same elastomer/antioxidant system and a control containing no antioxidant. It can be seen that the systems containing the antioxidant produce a profile with an embrittlement point occurring after a longer period of aging time than that of the control. Furthermore, although the profiles are not completely superimposable, particularly in the crosslinked plateau region, the reproducibility of the embrittlement point (180 min of accelerated aging time) of each of these profiles is excellent. The aforementioned variation in the magnitude of the relative modulus in the crosslinked plateau region most likely occurs from minor variations in the deposition of the elastomer on the braid.

Effect of antioxidants in carboxylated styrene-butadiene latex system — The materials used in this study included the elastomer system, carboxylated styrene-butadiene (Goodyear Pliolite® 480 Latex), and the antioxidants, (A) crude

2,2'-methylene *bis* (6-nonylparacresol); (B) the reaction product of nonylated paraethylphenol and formaldehyde; and (C) α,α'-2,6-*bis* (2 hydroxy-3-*tert*-butyl-5-methylphenyl) xylenol. The antioxidants were first emulsified and the resulting emulsion was added to the latex.

The composite elastomer/glass-fiber specimen was prepared by dip-coating a fiber-glass braid. This braid was obtained by loosely braiding multifilament glass strands (available in the form of heat-cleaned glass cloth, 181-112 of United Merchants and Manufacturers, Inc., New York). The actual coating was accomplished by dipping into the latex. The important thing to achieve during the coating step is the formation of a continuous surface film in addition to a thorough impregnation of the braid interstices. The final coated braid should contain about 50% by weight polymer, which will produce at least a 1 mil coating of polymer on the braid. Under these conditions it was found that the precision of the visual determination of the period of oscillation of the composite system was at a maximum, thus providing optimum sensitivity. Because the solids concentration of the carboxylated styrene-butadiene latex was high, 58% by weight, only one coating dip was necessary. The length of the composite elastomer/glass-fiber specimen actually used in the measurement was 10 in.

Since Torsional Braid Analysis is to be used as a quantitative method of investigation, the repro-
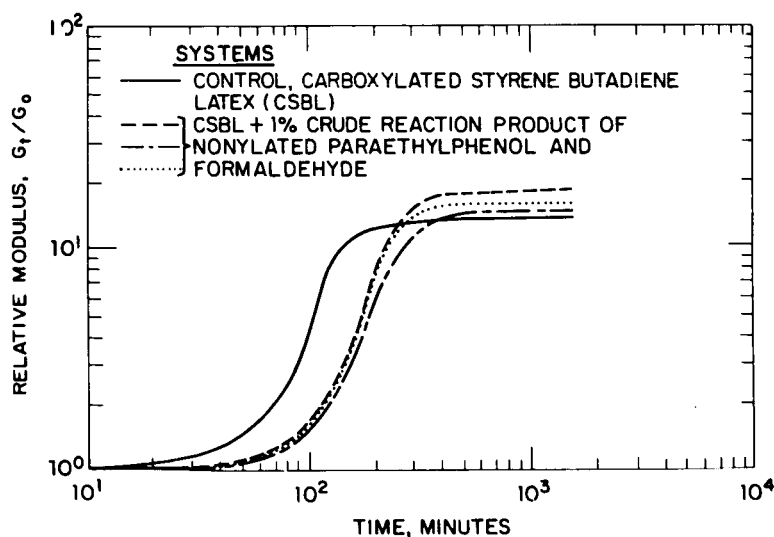

FIGURE 56. Carboxylated styrene butadiene latex. Effectiveness of polymer additives. Relative modulus as a function of aging time in a circulating air oven at 150°C. Actual measurements performed at 25°C.

ducibility of the coating technique requires special consideration. The coating procedure can be controlled to produce (on the glass support) the required elastomer deposition which varies only by 2% of the weight of the elastomer. The solvent removal from the solution or emulsion dipped systems is readily achieved by vacuum-drying; because essentially only thin films are being considered, a maximum drying time of two.hours is sufficient.

The effectiveness of antioxidants in inhibiting embrittlement of carboxylated styrene-butadiene latex systems was studied as a function of aging time at 150°C in a circulating air oven. By measuring the change in the period of oscillation of the elastomer/glass composite specimen over a period of aging time, a profile of the change in relative modulus was obtained. The use of a thin film in the study of a carboxylated styrene-butadiene latex is of particular practical use, for one of the commerical applications of this latex is that of a coating on rug backings. Thus, the embrittlement of this coating as a function of the temperature history produced by the processing variables is of primary importance. The results obtained on a control and three samples containing different potential antioxidant compounds are shown as Relative Modulus-Aging Time profiles in Figure 57. The aging time required to reach the embrittlement point, obtained from each of these curves, is tabulated in

Table 5. It can be seen from these results that each of the three additives improved the stability of the latex. Using the control sample as the standard, compound A increased the aging time stability by a factor of 2 and compounds B and C increased it by a factor of 4.

Effect of antioxidants in cis-Polybutadiene — The materials used in this study included the elastomer system, cis-polybutadiene (American Synthetic Rubber) and the antioxidants: (D) 4,4'-methylene bis (2,6-di-tert-butylphenol); (E) 1,3,3,5-tetramethyl-1-m-tolylindane-4',6-diol; (F) 2,2,'-methylene bis (6-tert-butyl-paracresol); (G) 4,4'-isopropylidene bis (2,6-di-tert-butylphenol); and (H) 4,4,'-isopropylidene bis (o-tert-butylphenol). The antioxidant was dissolved in toluene and this solution was added to the toluene solution of the elastomer.

The composite elastomer/glass-fiber specimens were prepared in the same manner as were the carboxylated styrene-butadiene specimens. However, since cis-polybutadiene was obtained at a 7% solids content in toluene solution, two coating dips were necessary to achieve the required thickness of polymer coating as previously discussed.

The effectiveness of antioxidants in inhibiting embrittlement of this cis-polybutadiene system was studied. One study investigated the comparative effectiveness of three antioxidants which differed in chemical structure. Another study was
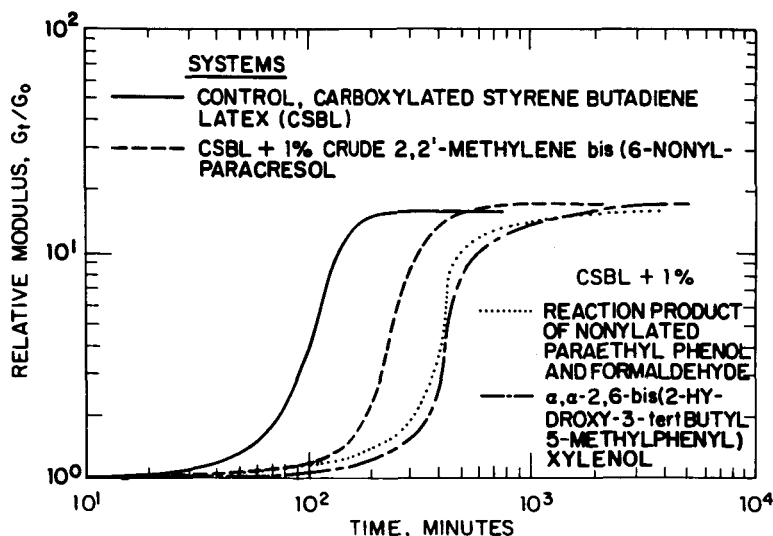

FIGURE 57. Carboxylated styrene butadiene latex. Effectiveness of polymer additives. Relative modulus as a function of aging time in a circulating air oven at 150°C. Actual measurements performed at 25°C.

TABLE 5

Effectiveness of Polymer Additives: Time Required to Reach Embrittlement Point on the Relative Modulus Profiles Obtained for Carboxylated Styrene-Butadiene Latex Aged at 150°C

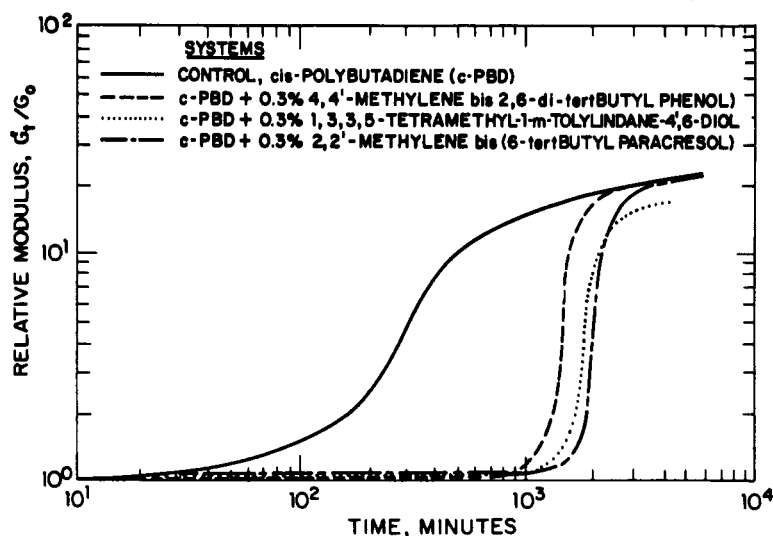| Identification	System	Time (min)
	Control	1.05×10^2
A	1% Crude 2,2'-Methylene bis (6-nonylparacresol)	2.35×10^2
B	1% reaction product of nonylated paraethylphenol and formaldehyde	4.00×10^2
C	1% a,a'-2,6-bis (2 hydroxy-3-$tert$-butyl-5-methyl phenyl) xylenol	4.20×10^2

FIGURE 58. Cis-polybutadiene. Effectiveness of polymer additives. Relative modulus as a function of aging time in the Torsional Braid Apparatus at 100°C. Actual measurements performed at the aging temperature.

undertaken to determine the effect of subtle structural changes on one basic molecular structure. A third study was also made on the effect of concentration and aging temperature on a particular antioxidant-based system.

The Relative Modulus-Aging Time profiles obtained in the comparative study are shown in Figure 58. In this series the samples were aged in situ in a thermoregulated fluidized bed torsional braid apparatus. In this manner the measurements were obtained at the aging temperature. The aging time required to reach the embrittlement point for these systems is tabulated in Table 6. These results indicate that each of the three additives improved

the stability of the cis-polybutadiene elastomer towards oxidative embrittlement. The effectiveness of compounds D, E, and F were thus found to differ essentially by a factor of 5, 6.5, and 7, respectively, from that of the unprotected control.

In order to determine the effect of specific chemical groups on a basic chemical structure, a series of three compounds was studied. The particular advantage of the torsional braid technique in such an application is clearly one of using a minimum of experimental material for a comparison purpose. The structures of the three compounds studied are listed in Table 7. Their effectiveness in preventing embrittlement is listed
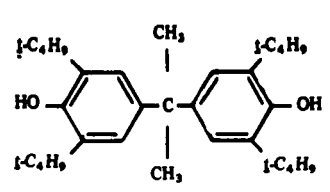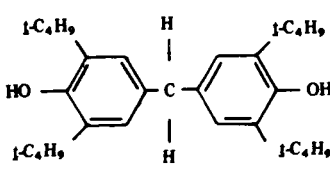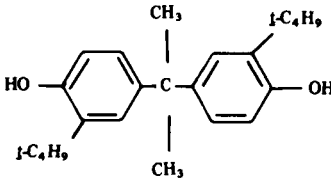
TABLE 6

Effectiveness of Polymer Additives: Time Required to Reach Embrittlement Point on the Relative Modulus Profiles Obtained for cis-Polybutadiene Aged at 100°C

Identification	System	Time(min)
	Control	2.75×10^2
D	0.3% 4,4'-Methylene bis (2,6-di-tert-butyl phenol)	1.40×10^3
E	0.3% 1,3,3,5-Tetramethyl-1-m-tolylindane-4', 6-diol	1.80×10^3
F	0.3% 2,2'-Methylene bis (6-tert-butyl paracresol)	1.95×10^3

TABLE 7

Effectiveness of Polymer Additives: Stability Improvement Factor for Three Structually Similar Antioxidant Compounds in cis-Polybutadiene aged at 100°C.

Identification	Compound	Structure	SIF
G	4,4'-isopropylidene bis (2,6-di-tert-butyl phenol)		2.6
D	4,4'-Methylene bis (2,6-di-tert-butyl phenol)		6.7
H	4,4'-isopropylidene bis (o-tert-butyl phenol)		8.9

in terms of a convenient parameter, the stability improvement factor, SIF. This parameter is defined as the ratio of the embrittlement time of the elastomer plus additive to that of the embrittlement time of the control-elastomer with no additive, that is $t_{emb}^{additive}/t_{emb}^{control}$. In this manner additives can readily be compared in the same elastomer system even if they are not studied simultaneously. It can be seen that compound G, which is the bulkiest molecule and is the most structurally hindered, has the lowest SIF. Furthermore, by comparing compounds D and H with G it

can be concluded that the bulky tert-butyl groups surrounding the hydroxy groups have more of an influence on the effectiveness of the compound than do the addition of methyl groups on the methylene bridge.

The effect of concentration as an experimental variable was also investigated. Compound F was selected for this study and the relative modulus of the formulated samples was determined at room temperature as a function of cell oven aging at 80°C. The resulting profiles are shown in Figure 59. It can be seen that there is very little
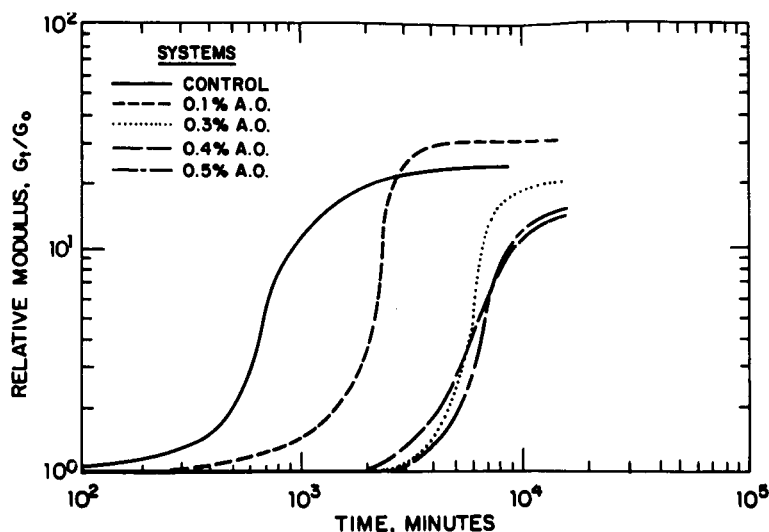
FIGURE 59. Cis-polybutadiene. Effectiveness of polymer additives. The effect of concentration of the antioxidant (designated "A.O") 2,2'-methylene bis(6-tert-butyl paracresol). Relative modulus as a function of aging time in a cell oven at 80°C. Actual measurements performed at 25°C.
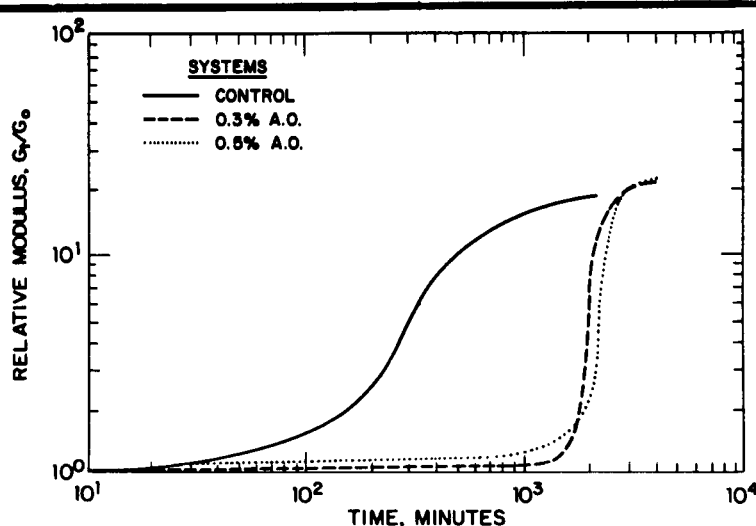

FIGURE 60. Cis-polybutadiene. Effectiveness of polymer additives. The effect of concentration of the antioxidant 2,2'-methylene bis(6-tert-butyl paracresol). Relative modulus as a function of aging time in the Torsional Braid Apparatus at 100°C. Actual measurements performed at the aging temperature.

difference in the embrittlement points obtained from these profiles after a certain concentration level has been achieved. That is, between 0.3 and 0.5% the effectiveness of these levels is essentially the same, indicating some sort of threshold level between 0.1 and 0.3%. To determine if this threshold behavior was temperature dependent, two levels of concentration, 0.3 and 0.5%, were studied at 100°C. These samples were aged and

run directly in the apparatus at this temperature. The profiles obtained are shown in Figure 60. Once again, no marked concentration effect is noted (above the 0.3% level). However, the higher aging temperature did exert an influence on all of the systems in this study. Table 8 lists the various times required to reach the embrittlement point as compiled from the profiles generated from the data obtained at 80 and 100°C. It can be seen that

TABLE 8

Effectiveness of Polymer Additives: Time Required To Reach Embrittlement Point on the Relative Modulus Profiles Obtained for cis-Polybutadiene as a Function of Aging Temperature

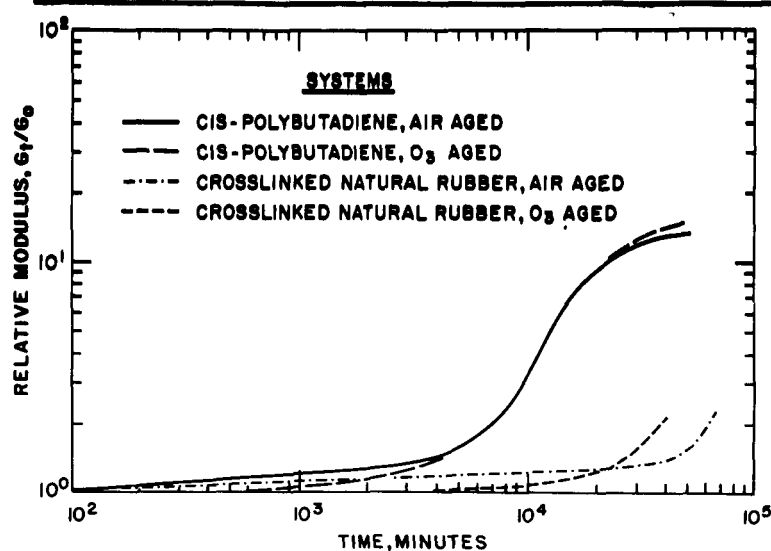|			Time (min)	
Identification	System	Conc.	at 80°C	at 100°C
	Control		6.5×10^2	2.75×10^2
F	2,2'-Methylene bis (6-tert-butyl paracresol)	0.3%	5.9×10^3	1.95×10^3
F	2,2'-Methylene bis (6-tert-butyl paracresol)	0.5%	6.0×10^3	2.2×10^3

FIGURE 61. Cis-polybutadiene and natural rubber. Effectiveness of polymer additives. Relative modulus as a function of aging under an ozone concentration of 50 pphm at 26°C. Actual measurements performed at 26°C

the unprotected control reached the embrittlement point in less than half the time in going from 80 to 100°C. The effective protection afforded to this elastomer by the addition of the antioxidant, however, provided essentially a tenfold increase in time before the embrittlement points at both temperatures were reached.

Application to ozone studies — The feasibility of studying the effectiveness of antiozoants using the same technique developed for antioxidants has also been investigated. Two particular elastomers, natural rubber and cis-polybutadiene, were examined. The latter was prepared as the elastomer/glass-braid composite in the same manner as previously discussed. The natural rubber necessitated an additional step in the specimen preparation. The pale crepe, topgrade (IX), was milled for fifteen min and then dissolved in toluene to prepare a 15 wt % solution. To this solution was added a peroxide curative (DiCup) at a level which was 3% by weight of rubber. The braid was dip-coated from this solution and then dried and cured at 150°C for 1 hr. This crosslinked natural rubber/glass-fiber composite was used in the study. Both the natural rubber and the cis-polybutadiene were conditioned in an ozone chamber (O_3 concentration at 50 pphm) for a total time of 6×10^4 min at 26°C. The samples were removed intermittently for purposes of measurement. Both systems were also aged in air at 26°C and these served as the controls. The results obtained are illustrated in Figure 61. It can

be seen that the crosslinked natural rubber which was exposed to the ozone environment began to show signs of embrittlement only after 4×10^4 min. The control on the other hand did not show any sign of embrittlement until after 6×10^4 min. Thus, the torsional braid technique could be used to determine ozone effects in natural rubber. However, the ozone exposure conditions selected for any such study would have to be of a practical time duration. The time span of the study discussed here would be impractical for screening antiozonants. This could be altered by increasing the ozone concentration and conditioning temperature.

The cis-polybutadiene elastomer was too sensitive to oxidative crosslinking to be detectably affected by the ozone exposure; that is, the embrittlement time for the control and the ozone exposed sample were the same. While discussing the cis-polybutadiene system it is of interest to note that by combining the data obtained at 26°C with data previously obtained at 80 and 100°C, it is possible to calculate an activation energy for the oxidative crosslinking reaction of cis-polybutadiene. An analysis similar to that used to obtain the activation energy for the polymerization of a carboxyl-terminated polybutadiene with an aziridinyl compound[13] was followed. The appropriate Arrhenius plot, using time to embrittlement vs. 1/T, yielded an activation energy of 10.9 kcal/mol for the oxidative crosslinking of cis-polybutadiene.

Summary

The torsional braid apparatus has been successfully adapted for use in studying the effectiveness of polymer additives, in particular antioxidant compounds in elastomer systems. This was accomplished by utilizing the concept of the embrittlement point on the generated relative modulus-accelerated time aging profiles. The reproducibility of the torsional braid technique for such a study was shown for a particular antioxidant, the crude reaction product of nonylated paraethylphenol and formaldehyde, in a carboxylated styrene-butadiene latex. In this same elastomer system and in a cis-polybutadiene system, the relative effectiveness of series of antioxidant compounds was determined in a quantitative manner. In the latex, the antioxidants, at a 1% level, were found to decrease in effectiveness as follows: α,α'-2,6-bis (2 hydroxy-3-tert-butyl-5-methylphenyl) xylenol > reaction product of nonylated paraethylphenol and formaldehyde > crude 2,2'-methylene bis (6-nonyl-paracresol). In the cis-polybutadiene the antioxidants, at a 0.3% level, were found to decrease in effectiveness as follows: 2,2'-methylene bis (6-tert-butyl paracresol) > 1,3,3,5-tetramethyl-1-m-tolylindane-4',6-diol > 4,4'-methylene bis (2,6-di-tert-butylphenol).

In the cis-polybutadiene system the effect of specific structural changes yielded the following order of effectiveness: 4,4'-isopropylidene bis (o-tert-butylphenol) > 4,4,'-methylene bis (2,6-di-tert-butyl phenol) > 4,4'-isopropylidene bis (2,6-di-tert-butyl phenol). In addition, the effectiveness of 2,2'-methylene bis (6-tert-butyl paracresol) was found to be essentially independent of concentration between 0.3 and 0.5%. Though the overall stability of this particular system was found to decrease as a function of increased aging temperature from 80 to 100°C, the approximate tenfold difference in stability of the antioxidant protected system was found to prevail over that of the control. The activation energy for the oxidative crosslinking of the cis-polybutadiene was calculated to be 10.9 kcal/mol.

VIII. Miscellaneous Applications

A. Pyrolytic Conversion of a Resin to a Semiconductor[4]

The polymerization of a phospho-nitrilic condensation-type thermosetting resin (Dynalak-HU®, General Dynamics Corporation, San Diego, California) was monitored by TBA for the conditions of time and temperature which were recommended by the manufacturer for the formation of castings. The curing behavior is presented in "finger-print" form in Figure 62-A in terms of changes in relative rigidity, as G_t/G_f. Here G_f is the rigidity modulus of the "cured" product at the temperature of the final curing isotherm, while G_t is the rigidity modulus at time t. (The dotted line connecting the two successive isotherms of Figure 62-A represents the changes which occurred in changing the temperature from the first to second isotherm). The fact that the modulus had not leveled off at the end of the cure cycle illustrates the arbitrary nature of commercial curing programs. It is well known that plastics technology lacks a reliable method for measuring cure: studies using TBA should permit the establishment of reliable curing programs and
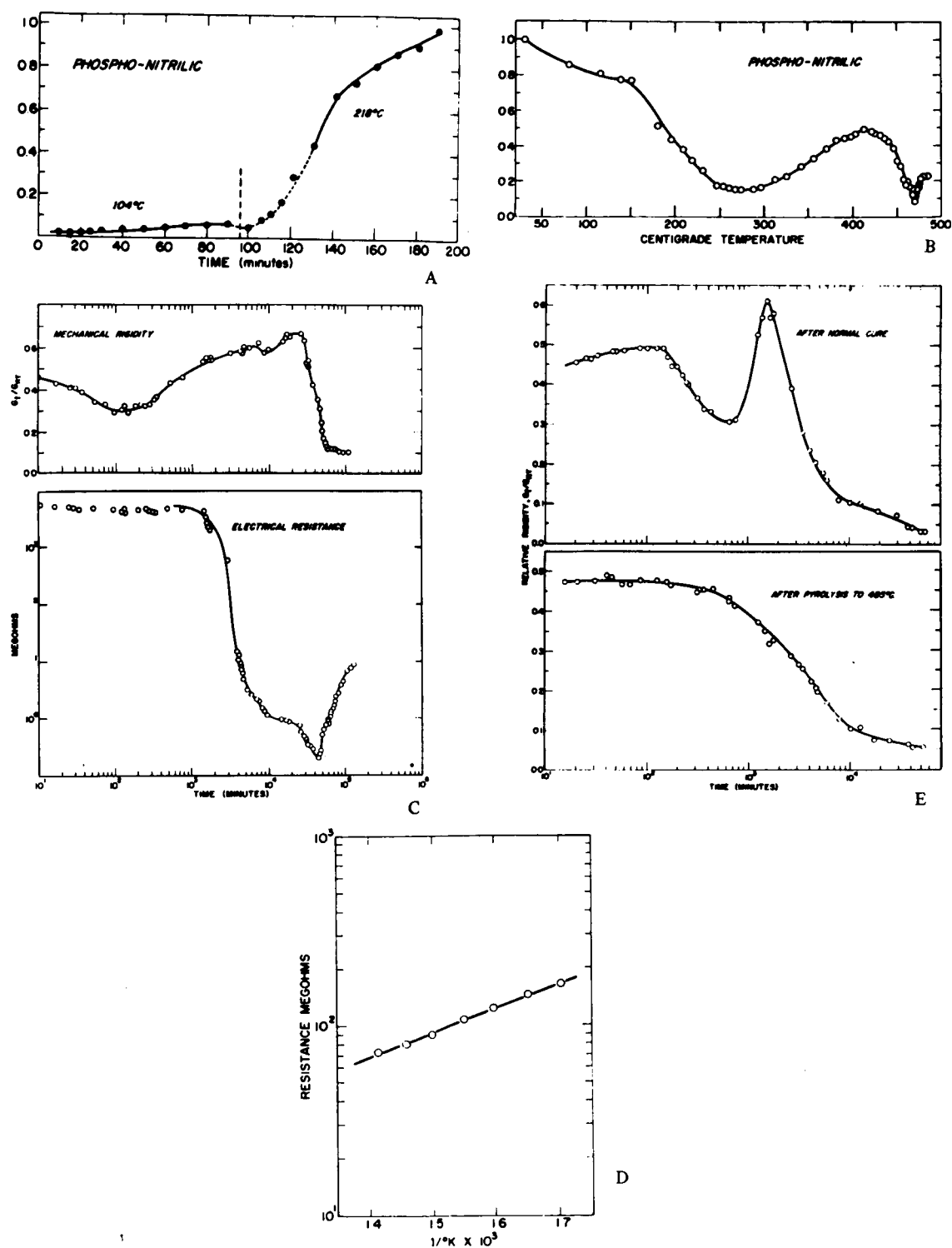
FIGURE 62.   Phospho-nitrilic resin. A. Cure in nitrogen. B. Thermomechanical behavior in nitrogen. C. Simultaneous monitoring of rigidity and electrical resistance during pyrolysis at 427°C in nitrogen. D. Dependence of electrical resistance on temperature (1/° K). E. Air oxidation (400°C) of cured and pyrolyzed resins.

curtail the use of laborious empirical methods for determining optimum curing conditions in new systems. On raising the temperature of the "cured" material (Figure 62-B; the rigidity at RT is the new reference state), the resin softened appreciably before stiffening — which probably represented a continuation of the curing process. Above 400°C the material again softened (to about 470°C) and then hardened again. The latter softening was interpreted as being the result of chemical reactions distinctly different from the curing reactions and preceded the formation of a pyrolyzed rigid new material. Striking differences in the electrical resistivity of the initial polymer, cured according to the manufacturer's recommendations ($> 10^{14}$ ohm-cm at 25°C), and the pyrolyzed (to 485°C) polymer (2.4 x 10^4 ohm-cm at 25°C) were found in the composite braid specimens.

Since the pyrolysis of the phospho-nitrilic resin resulted in a material with relatively low electrical resistivity, concurrent mechanical and electrical changes which accompanied pyrolysis were studied. The torsional braid apparatus was modified so that the impregnated braid was an integral part of an electrical circuit. This was accomplished by having the free end of the inertial mass carry a fine copper wire extension which dipped into a pool of mercury held at room temperature. The electrical circuit was completed through electrodes at the top and bottom of the apparatus, and incorporated an ohmmeter. Since the damping of the oscillations by the mercury was small, the sample could be subjected simultaneously to dynamic mechanical and electrical resistance testing.

A "cured" phospho-nitrilic resin specimen was heated to 427°C and the subsequent electrical and mechanical changes which occurred isothermally at 427°C were monitored. The results are presented in Figure 62-C.

The first minimum in the mechanical rigidity plot of Figure 62-C corresponds to the last minimum (at 470°C) of the thermal softening curve of Figure 62-B. The increase in rigidity, after this minimum, was attributed to the formation of a pyrolyzed continuum and was accompanied by a decrease in electrical resistance. After several weeks at 427°C, the pyrolyzed continuum itself breaks down and apparently loses its continuity; the decrease in rigidity parallels in a general way the increase in electrical resistance.

The limit of sensitivity of the ohmmeter was about 10^4 megohms. Therefore, the early stages of isothermal pyrolysis could not be followed with confidence. Hence, in this region, the data points of Figure 62-C were left unconnected.

Further considerations of the electrical resistivity of the pyrolyzed phospho-nitrilic resin were based on the assumption that the electrical conduction could be considered as a rate process. Hence the Arrhenius-type equation was invoked. The data of Figure 62-D show the temperature dependence of the pyrolyzed (27,700 min at 427°C) phospho-nitrilic resin between 428 and 314°C. The energy of activation for electronic conduction was calculated to be 5.9 kcal/mol (0.256 e.v.).

Pyrolysis of the phospho-nitrilic resin in an inert atmosphere produced a structure which differed from the normally cured resin not only in its electrical properties. The difference in structure is also apparent from thermomechanical studies. The thermal softening behavior of the resin after pyrolysis to 485°C was characterized by the absence of maxima and minima. This is in contrast to the thermal softening behavior of the normally cured resin (Figure 62-B). Furthermore, a comparison of the oxidative behavior at 400°C of the resin after normal cure (Figure 62-A) and after pyrolysis to 485°C (Figure 62-B), emphasizes the difference between the two structures. The relevant results are presented in Figure 62-E. The rigidity minimum at ca 600 min on oxidation of the normally cured resin at 400°C very likely corresponds to the minimum at ca 475°C in Figure 62-B and to the minimum at ca 150 min in Figure 62-C. If this is so, it means that treatment in air at 400°C of the phospho-nitrilic resin leads to a stepwise reaction, in which pyrolysis occurs prior to oxidative degradation. This, too, is apparent from the similar characteristics of the two results of Figure 62-E in the later stages of oxidation.

B. Poly(Triallyl Cyanurate) and Poly (Triallyl Isocyanurate)[8]

Isocyanurates are thermodynamically more stable than the isomeric cyanurates and so poly(triallyl isocyanurate) would be expected to be more stable than poly(triallyl cyanurate). In fact, there is infrared evidence that poly(triallyl cyanurate) isomerizes to poly(triallyl isocyanurate) on heating, which is most interesting in that the isomerization process changes a cross-

linked structure into a crosslinked isomerized structure. Interrelationships may be summarized thus:

$$TAC \rightarrow TAIC$$
$$\downarrow \qquad \qquad \downarrow$$
$$POLY(TAC) \rightarrow POLY(TAIC)$$
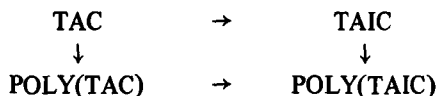
Analyses of poly(triallyl cyanurate) and poly(triallyl isocyanurate) have been conducted using various criteria as measures of stability. The results for changes in weight (TGA), heat content (DTA), and rigidity (TBA) for each polymer in being heated to 500°C in nitrogen are presented schematically in Figure 63. The crosslinked polymers were formed in nitrogen by heating each monomer with 1% benzoyl peroxide for a period of 2 days at 95°C. Poly(triallyl isocyanurate) lost little weight and rigidity below 400°C, but degraded completely after 450°C. Poly(triallyl cyan-

urate), in contrast, suffered weight loss, exothermic processes, and decreases in rigidity in the vicinity of 250°C. It appears from these results that the exothermic isomerization process occurs in regions where the crosslinked structure has its lowest rigidity and highest molecular mobility. This interesting phenomenon is receiving further attention.[92]

C. Brittle Materials

Although most of the changes in the mechanical behavior of the composite specimens used in TBA can be attributable to the polymer, changes which are the consequence of the composite nature of the specimen are to be anticipated and form the basis of current investigations. Complications can arise from fracture of the polymer, from adhesive failure, and from polymer-substrate and polymer-water interactions. Very brittle
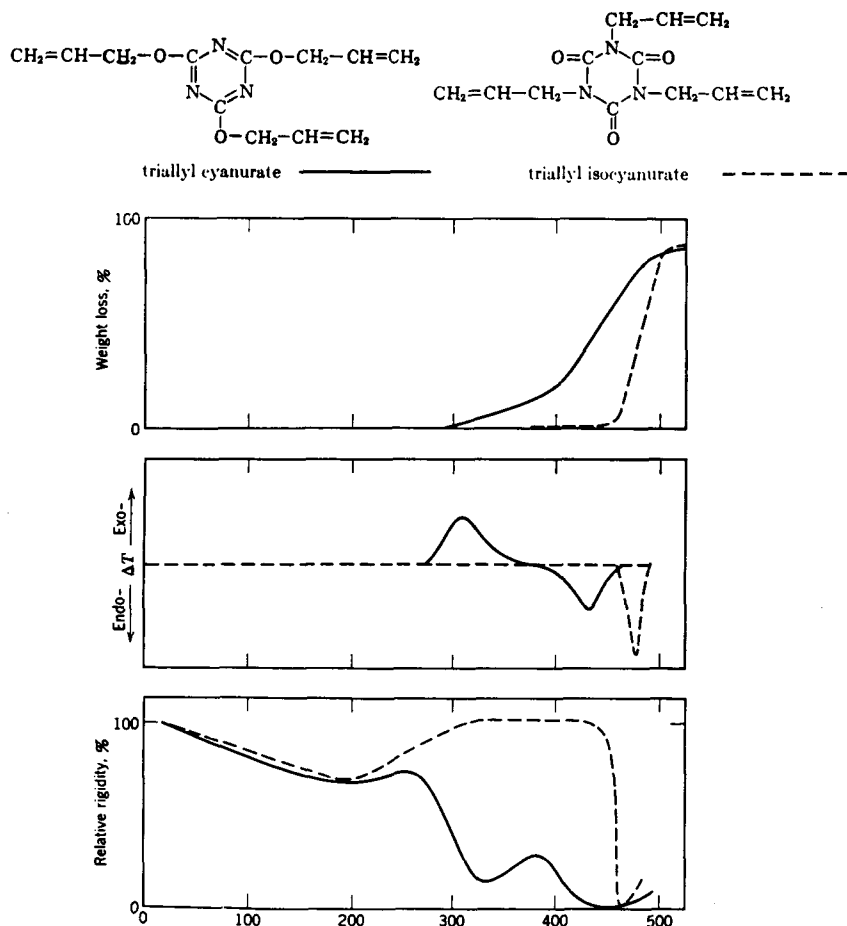

FIGURE 63. Poly(triallyl cyanurate) and poly(triallyl isocyanurate). Thermogravimetric, differential thermal, and Torsional Braid Analyses.

materials in the composite specimens of TBA do crack and give rise to thermohysteresis effects. This has been noticed in TBA experiments with very highly crosslinked organic glasses, with inorganic polymers such as cement, and with very low molecular weight organic glasses. The thermohysteresis of a poly(chromium III bisphosphinate) is a particular example which has been alluded to in the review (see Figure 38). Another example follows.

A composite specimen of glass braid and polysiloxane prepolymer, prepared from a commercially available alcoholic solution ("Glass Resin"-type 650[®], Owens-Illinois, Inc.), was heated to 500°C at 1°C min^{-1} and then immediately cooled to 25°C at the same rate. The results,[14] presented in Figure 64, show that the rigidity increased to 500°C, whereas on cooling it *decreased*. The resulting specimen was highly crazed, suggesting that the treatment of the experiment produced a highly crosslinked resin which, in the composite structure, cannot accommodate the stresses introduced thermally and by the polymerization processes. This represents an example of "overcure" in a thermosetting composite system. One might predict from the behavior of the mechanical

damping in Figure 64 that resin/glass fiber composites would not be structurally useful above 280°C.

These very brittle materials should not be dismissed, for in practice it is this very type which can produce composites which are competitive with steel! For example, the highly crosslinked polyesters used in polyester/glass fiber-reinforced laminates (as in boats) are brittle and useless as unfilled castings.

Further studies of the cracking phenomena which occur in glass fiber-reinforced brittle materials have led to some very interesting observations of spiral and helical cracks which propagate around filaments and yarns which form inclusions inside castings of highly crosslinked organic polymers.[93] A helical fracture around a multifilamented glass strand embedded in a block of brittle crosslinked polyester resin is shown in Figure 65 (top). A spiral fracture around a glass yarn embedded in poly(triallyl isocyanurate) is shown in Figure 65 (middle). The phenomenon is a general one in that spiral or helical cracks will tend to form when another crack crosses the inclusion. This tendency is demonstrated in Figure 65 (bottom) by the satellite spiral cracks which form when the growing face of a main spiral crack
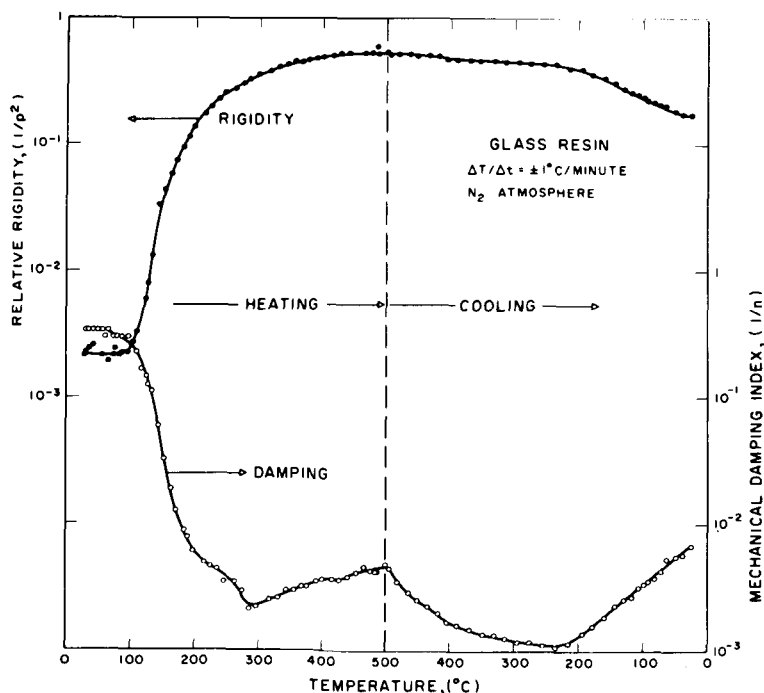

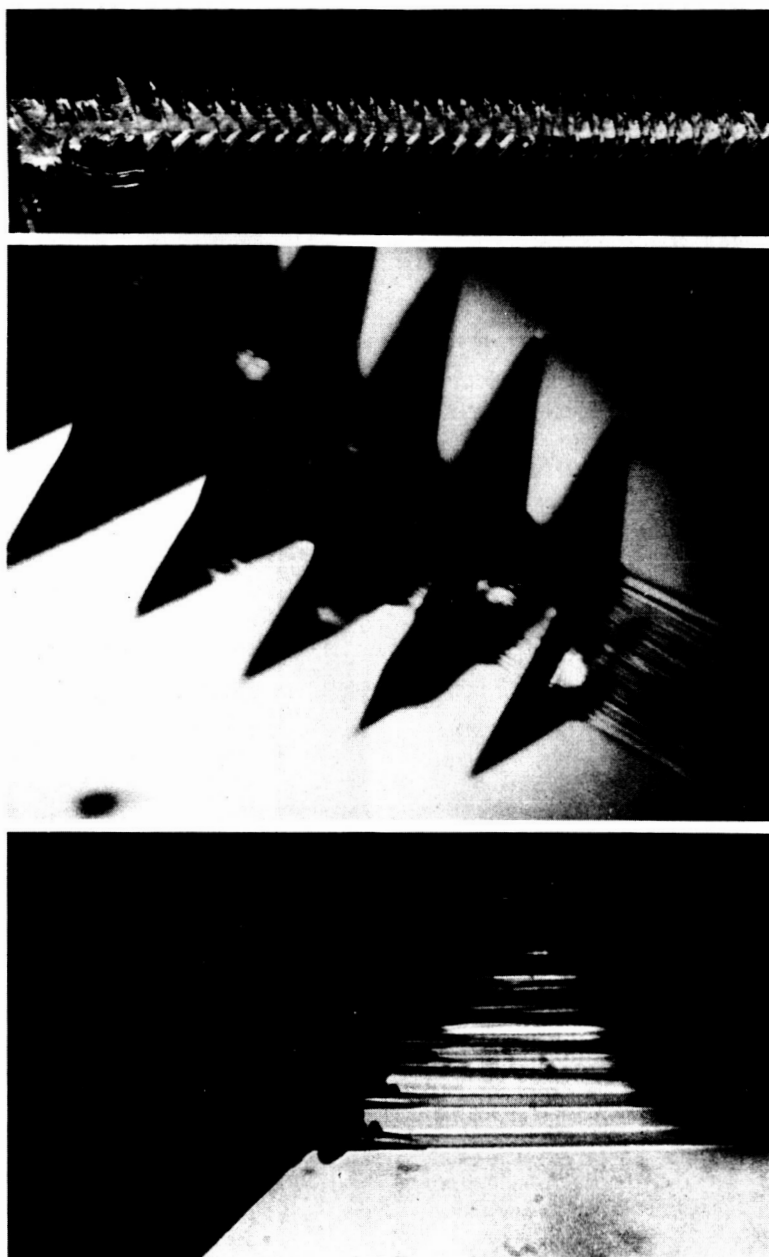FIGURE 64.   Glass resin. Cure and thermomechanical behavior.

FIGURE 65. Helical (top), spiral (middle), and spiral satellite cracks (bottom) around inclusions in brittle crosslinked polymers.

crosses a single filament (of the yarn). An implication of the geometric regularity is that the stress field is in control throughout the process of growth.

D. Small Molecules[7,17]

As a supported sample technique, torsional braid analysis permits the examination of low molecular weight materials. Glassy specimens often crack at cryogenic temperatures, in which case more scatter and discontinuities generally arise in the rigidity than in the damping parameter.

The thermomechanical spectra of some of the di-esters of phthalic acid serve as examples for glass-forming liquids.

A composite specimen of di-n-butyl phthalate

and glass braid was prepared using undiluted liquid ester. The specimen was cooled to -190°C and the thermomechanical spectra were obtained (Figure 66). Two damping maxima and concomitant changes in modulus are apparent. The main glass to liquid transition is at about -85°C; another relaxation process is made apparent by the damping maximum in the glassy state at about -170°C. Di-isobutyl phthalate gives rise to very similar spectra. On the other hand, the thermo-mechanical spectra of di-cyclohexyl phthalate display a major loss maximum (T_g) at -35°C, a sharp loss peak at -95°C, and a suggestion of a loss maximum peaking below -190°C. A more complicated molecule, the diglycidyl ether of *bis* phenol A (Epon 828®, Shell Chemical Corp.), displays (Figure 67) a glass transition temperature at -15°C and a dispersion region peaking at -150°C.

In the current attempt to develop the mechanical spectroscopy of macromolecules by correlating loss maxima with the motions of specific parts of polymer molecules, systematic studies of model and small compounds by torsional braid analysis should facilitate the interpretation of dynamic mechanical spectra of polymers.

The thermomechanical spectra of a specimen consisting of discrete crystals of diphenyl terephthalate dispersed among the glass filaments are displayed in Figure 68. Crystals were formed on the braid by evaporation of chloroform from an applied solution. Fine structure in the spectra is apparent below the melting point, and decreasing rigidity with a maximum in damping occurs as the temperature is raised through the melting point (190°C). Meaningful results may well be obtained in examining noncontinuous matrices.

As an example of a crystalline monomer which reacts on melting to form a crosslinked polymer, the trifunctional vinyl monomer, 1,3,5-trisacryl-hexahydro-s-triazine, is discussed. In the absence of an inhibitor, attempts to obtain a melting point are accompanied by the formation of an insoluble and infusible polymer. This complication presented a challenge to the technique since impregnation of the polymer onto the braid is not possible. Therefore, crystals of monomer were deposited on the braid by brushing with a solution (5%) of the monomer in chloroform, and allowing the solvent to evaporate. This monomer-
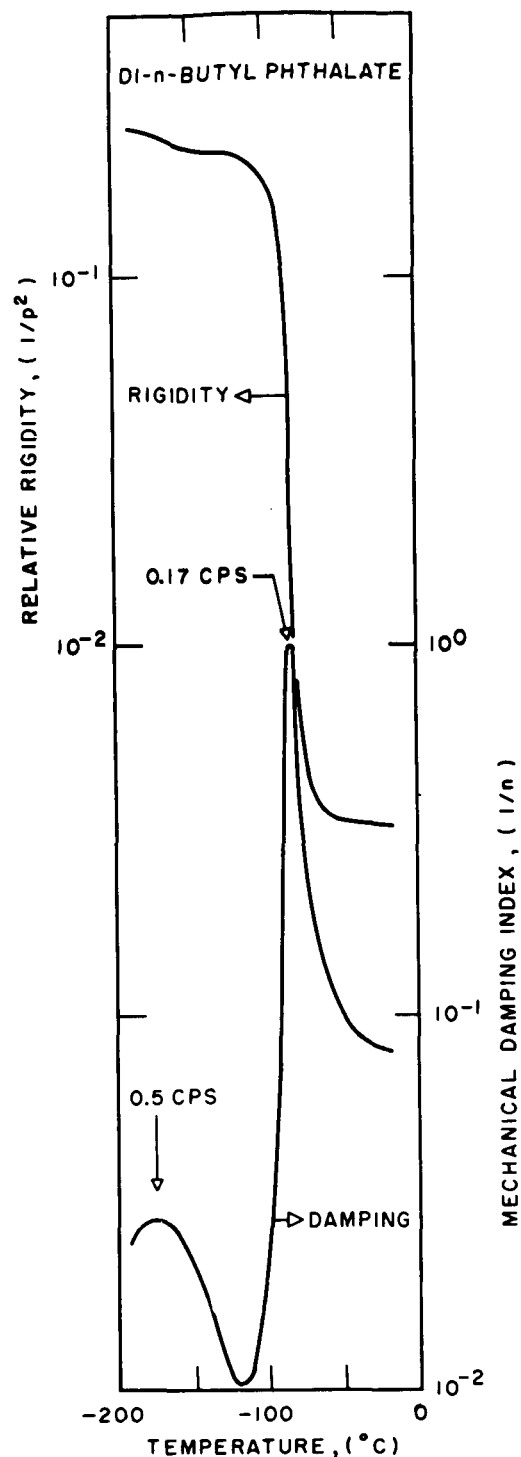

FIGURE 66.   Di-*n*-butyl phthalate.

impregnated braid formed the sample for the thermal softening experiment, the results of which are presented in Figure 69. An interpretation is
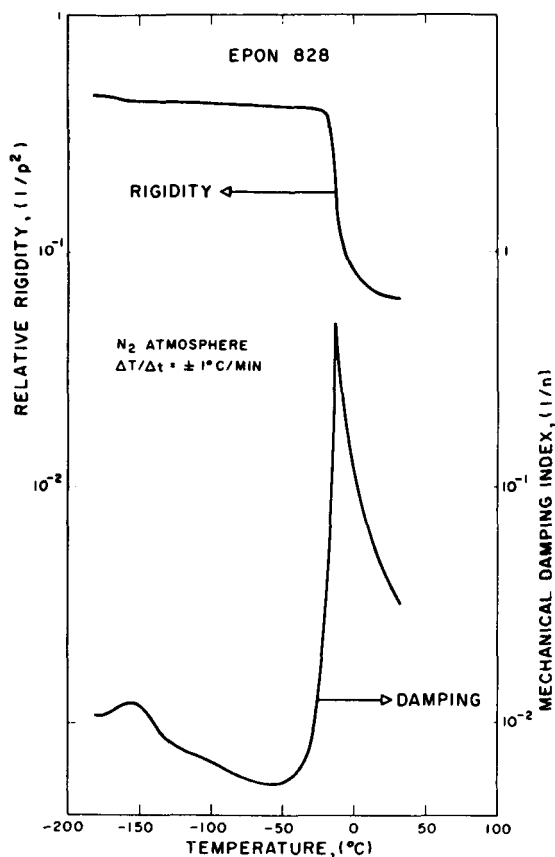
FIGURE 67. Epon 828. The diglycidyl ether of bisphenol A.

FIGURE 68.   Di-phenyl terephthalate.

aided by complementary examination of the monomer by DTA and TGA (Figure 69).

Melting (158°C) is accompanied by an endotherm, a maximum in damping, and a decrease in rigidity. Polymerization is detected immediately after melting by the increase in rigidity and the exotherm. The damping maximum in the vicinity of the melting point shows some dispersion and appears to be resolved partially into two peaks. The sharper maximum at lower temperature is attributable to the melting region itself while the subsequent shoulder is probably the maximum in damping which is associated with the curing process. The polymer appears to be thermally stable to about 350°C after which a decrease in rigidity occurs with a concurrent exotherm. A subsequent increase in rigidity is accompanied by loss of weight and an endotherm. The latter might well be accounted for by heat of volatilization. Indeed an oil condensed in the cooler part of the apparatus.

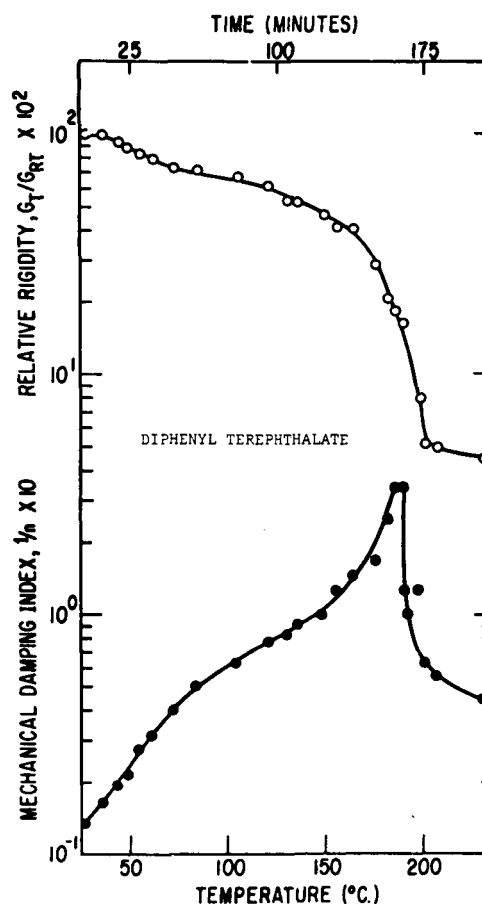Parallel analysis by infrared spectroscopy supported the interpretations. The only changes in the infrared spectrum to about 350°C were attributable to disappearance of unsaturation in the vinyl polymerization process. Subsequent changes at higher temperatures showed that the structure of the residue had lost amide-absorbing groups and had approached the structure of polyacrylonitrile pyrolyzed similarly to 400 to 500°C. This is not too surprising since the hexahydro-s-triazine monomer can be synthesized from acrylonitrile and formaldehyde. On the other hand, the condensate (about 50% yield) consisted of saturated primary amides. Further analysis of the oil by gas phase chromatography demonstrated the presence of at least a dozen constituents. Since the purposes of this research are to show how Torsional Braid Analysis fits into a scheme of polymer analysis further investigations concerning the specific chemical processes were not pursued.

E. Poly (Norbornadiene) [49]

Norbornadiene can be polymerized cationically[56] to give an amorphous linear hydrocarbon
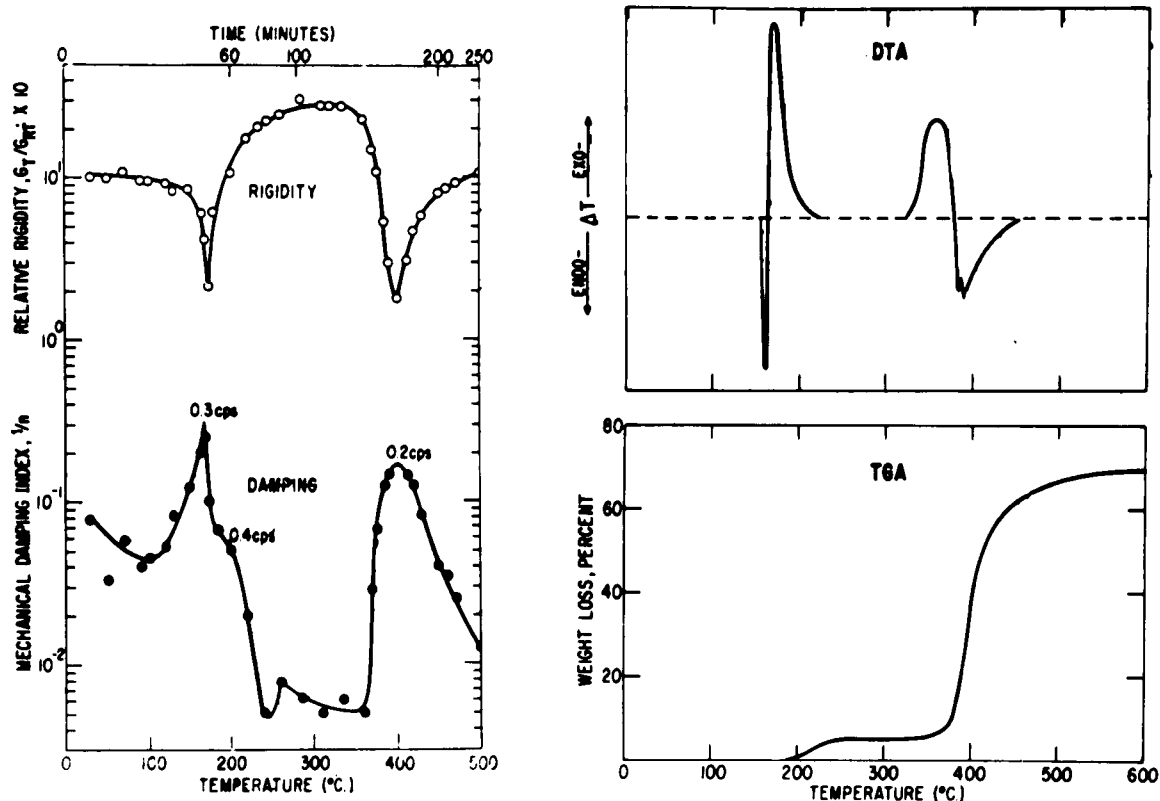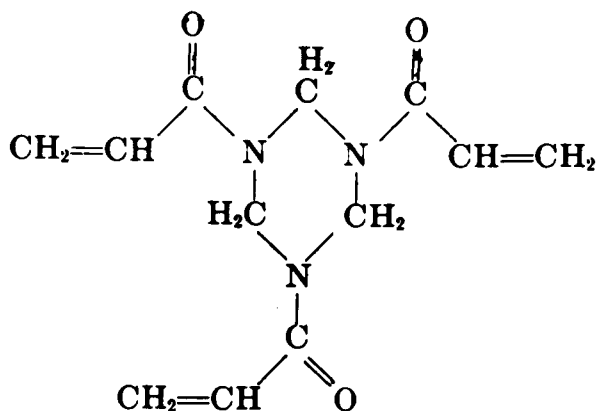
FIGURE 69. 1,3,5-trisacrylhexahydro-s-triazine.

containing units of the structure shown in Figure 70. The polymer is of interest in being constructed of rigid cages connected by single bonds. The TBA specimen was prepared by using a 10% solution in benzene, removing solvent by heating to 200°C at 2°C/min in nitrogen, and cooling slowly to liquid nitrogen temperatures. Data were obtained in the program; -180°C → 350°C → 25°C. The glass transition temperature is 320°C (0.4 cps) and is

the highest known for a linear, soluble, and fusible hydrocarbon. It is also noteworthy that this polymer is formed without formation of volatile by-products. The glass transition temperature region was made more pronounced by preheating to 350°C (Figure 70). The presence of a broad and yet pronounced damping region in the glassy state (-180° → 0°C) reveals the presence of relaxations in the glassy state.
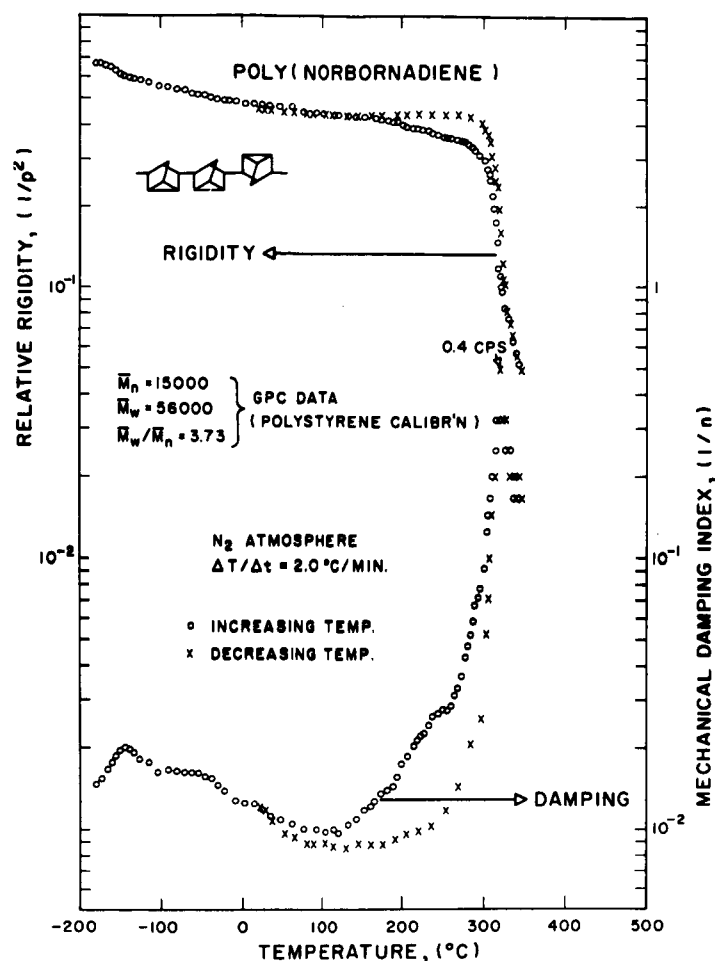
FIGURE 70. Poly(norbornadiene).

F. BBB-Polymer[32,39,48]

The synthesis of double-stranded, thermally stable linear polymers has been the main goal in the high temperature field of plastics during the past 15 years. Unfortunately, reversible thermal processibility and high temperature rigidity seem to be incompatible because of irreversible high temperature thermal reactions together with the low extent of fusibility. One of the more recently developed thermally stable polymers is synthesized from naphthalene 1,4,5,8-tetracarboxylic acid and 3,3'-diaminobenzidine to give the (idealized) repeat unit of "BBB-polymer."[94] The polymer was synthesized and provided by Dr. R. L. Van Deusen of the Air Force Materials Laboratory, Dayton, Ohio. Specimens for the thermomechanical experiments were prepared from 5% solutions of polymer in methane sulfonic acid (b.p. <200°C) by heating to 300°C ($\Delta T/\Delta t$ = ±

3°C/min). A specimen was then examined through the temperature cycle: -190°C → 650°C →-190°C (Figure 71).

Of particular interest is the increase of rigidity above 450°C which is indicative of irreversible crosslinking reactions in the inert atmosphere. The prior softening is the consequence of retained solvent which plasticizes the linear polymer and lowers the temperature of the glass transition region. At finite heating rates the T_g is inaccessible for the unsolvated polymer because of the thermal reactions. The low temperature (< -100°C) damping peak diagnoses a relaxation in the glassy state which, together with the fact of solubility and plasticization, shows that the molecule has some flexibility.

The particular solvent, methane sulfonic acid, is difficult to remove from the polymer film and reacts with it in the attempt to remove it
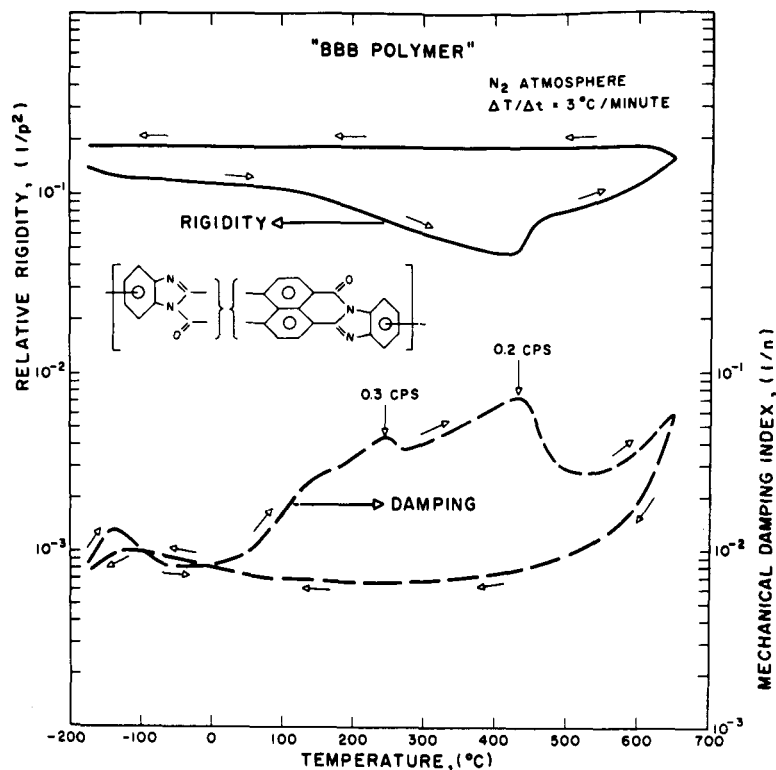
FIGURE 71. BBB-polymer.

thermally. Polymer cast from methane sulfonic acid was much more susceptible to air oxidation (by thermogravimetric analysis) than polymer formed by precipitation from the medium (polyphosphoric acid) used in synthesis. In fact the polymer reacts with the solvent at 25°C! This was diagnosed, using thermogravimetric analyses in air, by the drastic changes in oxidative stability of the solvent-cast polymer which occurred with the time of aging of solutions held at 25°C under nitrogen.

G. Biomaterials

This review has been concerned for the most part with synthetic polymeric materials. An emphasis was placed early on investigating systematic series of polymers and on amorphous polymers since molecular interpretation is simplified with, for example, noncrystalline materials. In developing the technique of application, any complications caused by "spurious" interactions (e.g. effect of water and brittle materials) could be more readily isolated and understood by studying simpler systems. It seems apparent to the author now that complications can

be understood in simple terms and for the most part are minimal or controllable. The technique of Torsional Braid Analysis has been developed to the point where the most complicated polymers can be studied uniquely and profitably. A program to study biomaterials and their synthetic analogues has therefore been initiated. Two relevant examples follow.

1. Polypeptides[49]

Poly-γ-benzyl-L-glutamate — TBA specimens were prepared by using a solution (5% in $CHCl_3$) of poly-γ-benzyl-L-glutamate and drying to 120°C in nitrogen at 2°C/min. Thermal cycling experiments (Figure 72. I → VII) were performed by heating the specimen to successively higher temperatures. No change in the thermomechanical behavior was detected after heating to 120°C and to 200°C. A major transition, with a damping peak and drastic drop in rigidity, occurred at 20°C. After heating to 250°C the shallow damping peak at 140°C had intensified. and the rigidity had increased between 25°C and 150°C. Concurrently the intensity of the damping peak at 20°C was reduced. These changes were intensified after

heating to 270°C. After heating to 300°C the thermomechanical behavior displayed only one damping peak (at 215°C) corresponding to a large decrease in rigidity before the rigidity increased above 290°C. After thermal treatment to 330°C, the mechanical damping increased monotonically from 0°C to 330°C (and peaked at 355°C). Treatment to 400°C resulted in a shift of the damping peak to a temperature above 400°C and the rigidity was rendered insensitive to temperature.

In the absence of experiments with other techniques, which need to be performed, a preliminary summation is:

1. The glass transition temperature of the unreacted polymer is at 20°C.[95]

2. The damping peak at 115 to 145°C could be associated with an ordered region. (The intensity of this peak increases while that of the glass transition decreases.)

3. The rigidity-temperature curve, after heating to 270°C, has the form of a typical semi-crystalline polymer.

4. Chemical reactions crosslink the material severely in the fluid region (T > 275°C) and eliminate the relaxations previously centered at ∿140°C and at ∿20°C. A material results with a glass transition above 300°C which can in turn be increased to above 400°C (by heating to 400°C).

Equimolar mixture of poly-γ-benzyl-L-glutamate and poly-γ-benzyl-D-glutamate — TBA specimens prepared from an equimolar solution (5% in CHCl₃) were subjected to the same thermal history as the pure poly-γ-benzyl-L-glutamate. The results were much the same for the mixture of polymers (Figure 73) and the pure polymer (Figure 72). The thermomechanical behavior of the mixture would be expected to be different from that of the pure polymer if the materials crystallize. It follows that the higher temperature peak (∿140°C) is probably due to a "paracrystalline" phase rather than to a highly ordered crystalline phase.

Poly-γ-methyl-L-glutamate — TBA specimens were prepared from a solution (5% in CHCl₃) as before and the thermal history of the thermomechanical experiments was the same as before except that the lower temperature limit was -100°C for each cycle (Figure 74). Prominent damping peaks were present at -30°C and at

150°C after heating the specimen to 200°C. Thermal treatment to 250°C and to 270°C increased the area of the 150°C damping peak and decreased that under the -30°C damping peak. After heating to 300°C, the mechanical damping was level from -100°C to +100°C and then increased to a maximum above 300°C. The corresponding rigidity was level from -100°C to 200°C and after decreasing to a minimum at 315°C, it increased. The damping peak was shifted to higher temperatures, 365°C and >400°C, after heating to 330°C and 400°C, respectively, and the plateau in the rigidity was extended correspondingly.

The pattern for the thermomechanical behavior of poly-γ-methyl-L-glutamate and poly-γ-benzyl-L-glutamate was similar. The thermomechanical spectra of both exhibited a damping peak which was intensified by thermal treatment (<270°C) at the expense of the damping region at lower temperatures. Treatment to 300°C eliminated the lower damping region and that at higher temperatures was shifted to higher temperatures.

The ratio of the temperatures (in °K) of the higher damping peak to the lower is 1.74 for poly-γ-methyl-L-glutamate and 1.41 for poly-γ-benzyl-L-glutamate for specimens not heated above 270°C. (It might be noted that for many semicrystalline polymers, T_m/T_g = 1.5-2 and for amorphous polymers T_g/T_β = ∿1.4.)

2. Hemicellulose (Xylan)[49]

The three most abundant organic macromolecules occur naturally and are cellulose, xylans, and lignin. The molecular chains of the xylans (hemicellulose) have xylose residues linked β-1,4. The particular xylan discussed here was extracted from White Birch, was designated O-Acetyl-4-O-Methyl Glucurono-Xylan, and was provided by Professor T. E. Timell of the School of Forestry at Syracuse University, Syracuse, New York.

A specimen for torsional braid analysis was prepared from an aqueous solution (10%) by impregnating the braid and heating to 140°C and cooling to room temperature. "Hi-Pure" nitrogen gas was used as the environment throughout drying and collecting data. The thermomechanical data (Figure 75) are for the temperature program RT → -190°C → 400°C. The data for decreasing temperature have been displaced vertically for the sake of clarity.

Differences in behavior between cooling and

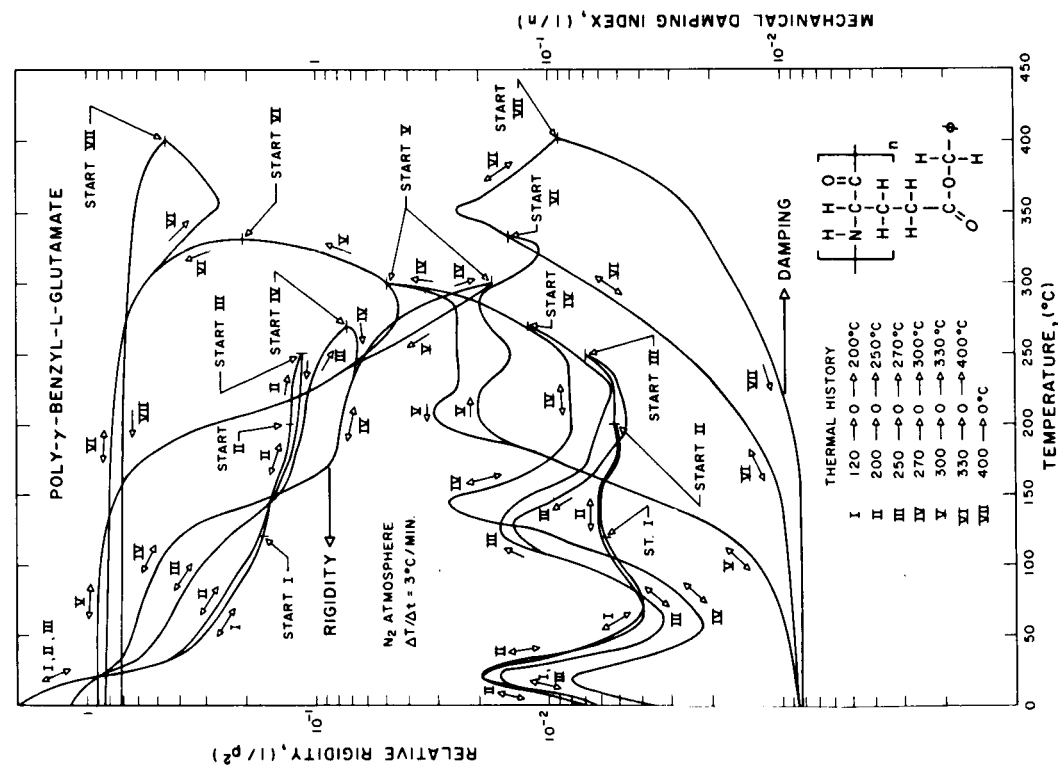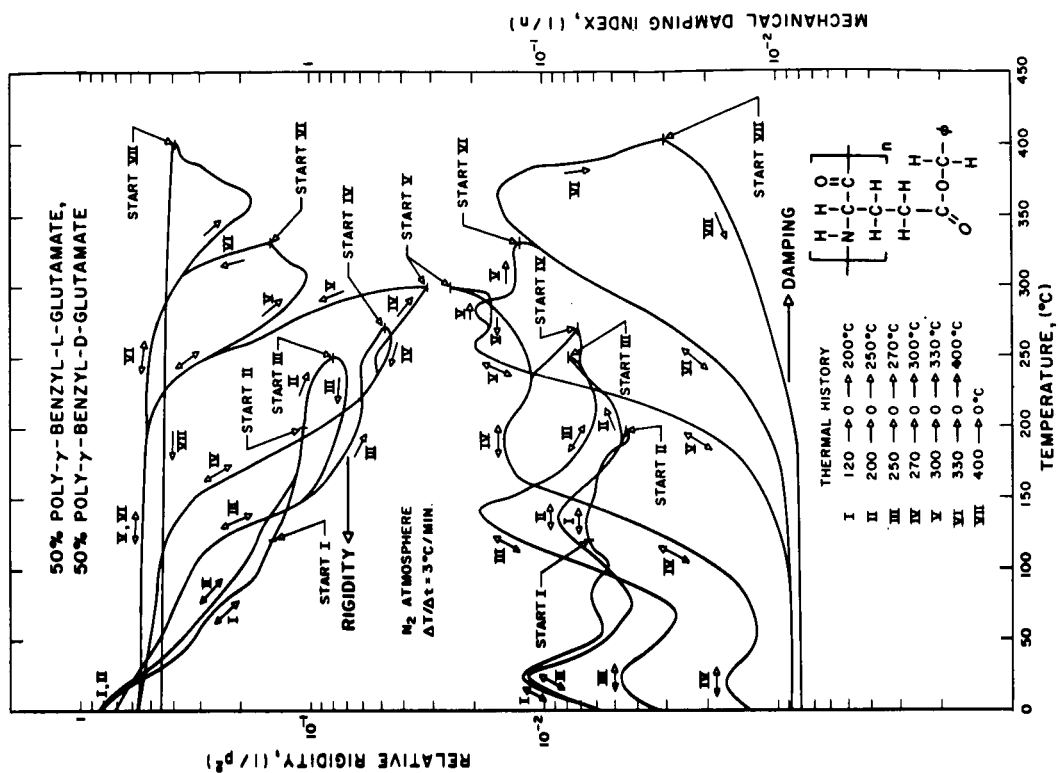FIGURE 73. Equimolar mixture of poly-γ-benzyl-L-glutamate and poly-γ-benzyl-D-glutamate.

FIGURE 72. Poly-γ-benzyl-L-glutamate.

FIGURE 75. Hemicellulose (xylan).

FIGURE 74. Poly-γ-methyl-L-glutamate.

subsequent heating are the consequence of very small amounts of water present in the nitrogen. It appears that on cooling, water vapor freezes out especially on the cooler walls of the specimen chamber, and so the thermomechanical spectra reflect the behavior of the drier material. On warming, the specimen is colder than the walls of the chamber and so water transfers to the polymer, especially towards the melting point of ice. This water plasticizes the polymer and produces the drastic changes in rigidity and damping just below $0°C$. The cooling behavior represents more the behavior of the dry polymer, for when the nitrogen gas was further dried before being used, the thermomechanical response on cooling and subsequent heating was the same (see also Figure 26; Polyimides: effect of trace moisture).

APPENDIX

I. Light Transmission through Polarizer and Analyzer[35]

Malus' Law states the relationship between the light intensity transmitted by an ideal polarizer-analyzer (P-A) pair and the angle of crossing:

$$I'(\theta) = I_o H_o \cos^2\theta = I'(0) \cos^2\theta \qquad (1)$$

where I_o = intensity of incident light, H_o = transmission factor of the parallel pair ($\theta = 0$), θ = angle of crossing of the pair from the parallel position in degrees, and $I'(\theta)$ = intensity of transmitted light. In the above law, the specification of ideal P-A pair refers to the case where $I'(90)$, the intensity of light transmitted by a perpendicular pair, is zero.

The law can be modified for a "real" pair by a translation of axes:

$$I(\theta) = I(90) + [I(0) - I(90)] \cos^2\theta \qquad (2)$$

where $I(\theta)$ = intensity of light transmitted by a real P-A pair at angle of crossing θ (in degrees). The following straight line: $Y = 1.263 - 0.0169\,\theta$ can be shown to approximate the function: $Y = \cos^2\theta$ to less than 1.0% error (relative to the 45 degree value) for $30 < \theta < 60$ (Figure 7). Similarly, it can be shown that Equation 2 can be represented to < 1% error (relative to the 45 degree value) by a straight line in this "linear" region.

In the system used by the authors, it is easy to determine either $V(0)$ [or $V(90)$] and $V(45)$

[where V is the voltage analogue of I]. Using the measurable quantity, $\Delta V = |V(45) - V(90)| = [V(0) - V(45)]$, it follows (see below) that the linear range of the transducer (as displayed on the strip-chart recorder) is $V(45) \pm \Delta V/2$.

$$V(45) = V(90) + [V(0) - V(90)] \cos^2 45°$$

$$= V(90) + 1/2\,[V(0) - V(90)]$$

$$V(45) - V(90) = 1/2\,[V(0) - V(90)] = \Delta V$$

$$V(0) - V(45) = \Delta V \quad \text{since} \quad V(45) - V(90)$$

$$= V(0) - V(45)$$

Therefore

$$V(\theta) = V(90) + 2\Delta V \cos^2\theta$$

$$V(30) = V(90) + 2\Delta V \cos^2 30°$$

$$V(60) = V(90) + 2\Delta V \cos^2 60°$$

$$V(30) - V(60) = 2\Delta V\,(\cos^2 30° - \cos^2 60°)$$

$$V(30) - V(60) = 2\Delta V\,[(\sqrt{3}/2)^2 - (1/2)^2]$$

$$\text{"Linear region"} = V(30) - V(60) = \Delta V$$

II. Maximum Torsional Strain in a TBA Specimen[35]

If it is assumed that a TBA specimen (polymer/braid composite) has a cylindrical geometry, then $\epsilon_{Max} = r\theta/L$ where θ = maximum (Max) angle (radians) of twist relative to the neutral position, r = radius of specimen, and L = length of specimen.

When using the polarizer transducer, θ_{Max} for the linear range is $\pm 15°$ but, in order to compensate for inaccuracies in finding the center of the linear range (Appendix I and Figure 8) and for practical reasons involved with drift of the baseline (see text), the peak to peak swing is usually limited to $\pm 7° = \pm 0.122$ rad. $\epsilon_{Max} = 0.122r/8 = 0.0153r$ for an 8 in. long specimen. Four measurements at different lengths along a typical specimen yielded 0.045, 0.045, 0.046, 0.046 in diameter. Allowing for variations with different polymer-solvent braid systems, a conservative estimate is r = 0.05 (not diameter = 0.05), in which case $\epsilon_{Max} = 0.0153\,(.05) = 0.00077 = 0.077\%$ while for the typical composite sample (as above) $\epsilon_{Max} = (0.0153)\,(.023) = 0.000355 = 0.0355\%$.

III. Effect of Lateral Vibrations on the Transmission of Light by a Polarizer-Analyzer Pair[3 5]

In Figure 76 are shown schematic representations of two polaroid discs oriented at an arbitrary angle to each other, as represented by the direction of the inscribed lines. Note that any motion of one disc relative to the other which can be resolved only into X and Y translational components (no angular rotation) does not change the relative angle between them and therefore does not affect the intensity of light transmitted by the pair.

In order that (spurious) flexural modes not affect the recording of required torsional modes, the translational displacement need not be restricted to a particular radius as with the previously-used linear optical wedge (Figure 2).

IV. Relationships Between Stress and Strain in Vibration[4 7]

Forced Vibration for a Linear System (see Figure 77)

A nondecaying cyclic stress $\sigma(t)$ given by the expression

$$\sigma(t) = \sigma_0 \sin\omega t$$
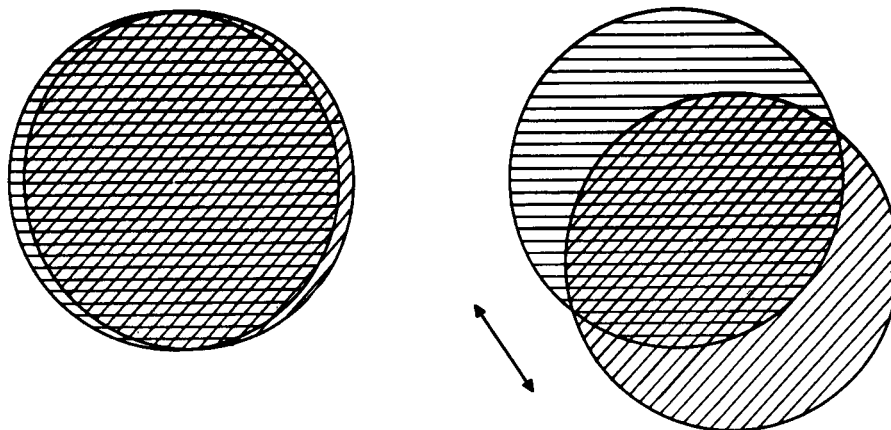
can be represented by the projection on an

FIGURE 76. Effect of lateral vibrations on the light transmission through a polarizer-analyzer pair.
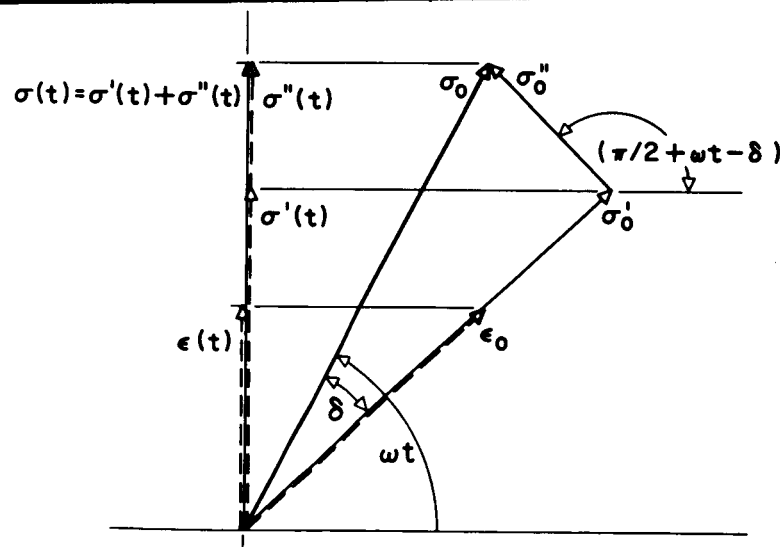

FIGURE 77. Rotating vector representation of a forced sinusoidal stress and corresponding strain of frequency ω acting on viscoelastic material.

arbitrary line of a vector of fixed length, σ_0, rotating at frequency ω about a point 0. The peak stress is σ_0 and ω is the frequency in rad/sec. The corresponding cyclic strain, $\epsilon(t)$, is given by the expression

$$\epsilon(t) = \epsilon_0 \sin(\omega t - \delta)$$

and can be represented by the projection on the same arbitrary line of a vector of fixed length, ϵ_0, rotating at frequency ω with a constant phase angle δ between the rotating stress and strain vectors. The peak strain is ϵ_0.

The rotating stress vector can be resolved into two rotating vectors of fixed magnitude, σ_0' in-phase and σ_0'' out-of-phase with the rotating strain vector.

$$\sigma_0' = \sigma_0 \cos\delta \quad \text{and} \quad \sigma_0'' = \sigma_0 \sin\delta$$

$$G' = \frac{\sigma_0'}{\epsilon_0} = \frac{\sigma_0 \cos\delta}{\epsilon_0} \qquad G' \equiv \text{in-phase modulus}$$

$$G'' = \frac{\sigma_0''}{\epsilon_0} = \frac{\sigma_0 \sin\delta}{\epsilon_0} \qquad G'' \equiv \text{out-of-phase modulus}$$

$$G''/G' = \tan\delta . \tag{1}$$
(Note. G' & G'' are constants)

ΔW = Energy dissipated per cycle.

Since $\sigma(t) = \sigma_0 \sin\omega t = \sigma'(t) + \sigma''(t)$,

(see Fig. 77)

$$\Delta W = \oint \sigma(t)d\epsilon(t) = \oint \sigma'(t)d\epsilon(t) + \oint \sigma''(t)d\epsilon(t) .$$

Further since,

$$\sigma_0'(t) = \sigma_0' \sin(\omega t - \delta) \quad \text{and} \quad \epsilon(t) = \epsilon_0 \sin(\omega t - \delta)$$

$$\text{and} \quad \frac{\sigma'(t)}{\epsilon(t)} = \frac{\sigma_0' \sin(\omega t - \delta)}{\epsilon_0 \sin(\omega t - \delta)} = G' ,$$

$$\oint \sigma'(t)d\epsilon(t) = G' \oint \epsilon(t)d\epsilon(t)$$

$$= G'\epsilon_0^2\omega \int_0^{2\pi/\omega} \sin(\omega t-\delta) \cos(\omega t-\delta)dt$$

since $\epsilon(t) = \epsilon_0 \sin(\omega t-\delta)$

and $d\epsilon(t) = \epsilon_0\omega \cos(\omega t-\delta)dt$

Also, since $\int \sin X \cos X \, dX = 1/2 \sin^2 X$,

$$\oint \sigma'(t)d\epsilon(t) = G'\epsilon_0^2\omega \frac{1}{2}\left[\sin^2(\omega t-\delta)\right]_0^{2\pi/\omega}$$

$$= \frac{G'\epsilon_0^2}{2} [\sin^2(2\pi-\delta) - \sin^2(-\delta)] = 0$$

i.e. no energy is dissipated per cycle by the in-phase component of the stress. All the dissipated energy therefore arises from the out-of-phase component of stress, and

$$\Delta W = \oint \sigma''(t)d\epsilon(t)$$
Further, since
$$\sigma''(t) = \sigma_0'' \sin(\tfrac{\pi}{2} + \omega t - \delta) = \sigma_0'' \cos(\omega t - \delta)$$
and

$$\frac{\sigma''(t)}{\epsilon(t)} = \frac{\sigma_0'' \cos(\omega t - \delta)}{\epsilon_0 \sin(\omega t - \delta)}$$

$$= \frac{\sigma_0''}{\epsilon_0} \frac{1}{\tan(\omega t - \delta)} = \frac{G''}{\tan(\omega t - \delta)}$$

and

$$\sigma''(t) = \frac{G''\epsilon_0 \sin(\omega t - \delta)}{\tan(\omega t - \delta)} ,$$

$$\Delta W = G''\epsilon_0 \oint \frac{\sin(\omega t - \delta)}{\tan(\omega t - \delta)} d\epsilon(t) .$$
Also, since
$$d\epsilon(t) = \epsilon_0\omega \cos(\omega t - \delta) dt ,$$

$$\Delta W = G''\epsilon_0^2\omega \int_0^{2\pi/\omega} \frac{\sin(\omega t - \delta) \cos(\omega t - \delta)}{\sin(\omega t - \delta)/\cos(\omega t - \delta)} dt$$

$$= G''\epsilon_0^2\omega \int_0^{2\pi/\omega} \cos^2(\omega t - \delta) dt .$$

From integral tables,

$$\int \cos^2 X dX = \frac{1}{2} \sin X \cos X + \frac{1}{2} X$$

and

$$\Delta W = G''\epsilon_0^2\omega\left[\frac{1}{2\omega} \left(\sin(\omega t - \delta) \cos(\omega t - \delta) + \omega t-\delta\right)\right]_0^{2\pi/\omega}$$

$$= \frac{G''\epsilon_0^2}{2} [\sin(2\pi - \delta) \cos(2\pi - \delta)$$

$$+ 2\pi - \delta - \sin(-\delta) \cos(-\delta) - 0 + \delta] ,$$
and since
$$\sin(2\pi - \delta) = \sin(-\delta) \quad \text{and} \quad \cos(2\pi - \delta) = \cos(-\delta),$$

$$\Delta W = \pi G''\epsilon_0^2 .$$

This expression is obtained more simply by considering the energy dissipated per cycle as being the area of the stress versus strain hysteresis loop [$\Delta W = \oint \sigma(t) \, d\epsilon(t) = \oint \sigma''(t)d\epsilon(t)$]. The out-of-phase stress versus strain curve for a cycle is an ellipse with half-axes defined by the peak strain (ϵ_0) and the peak out-of-phase stress ($G''\epsilon_0$, see Figure 78).
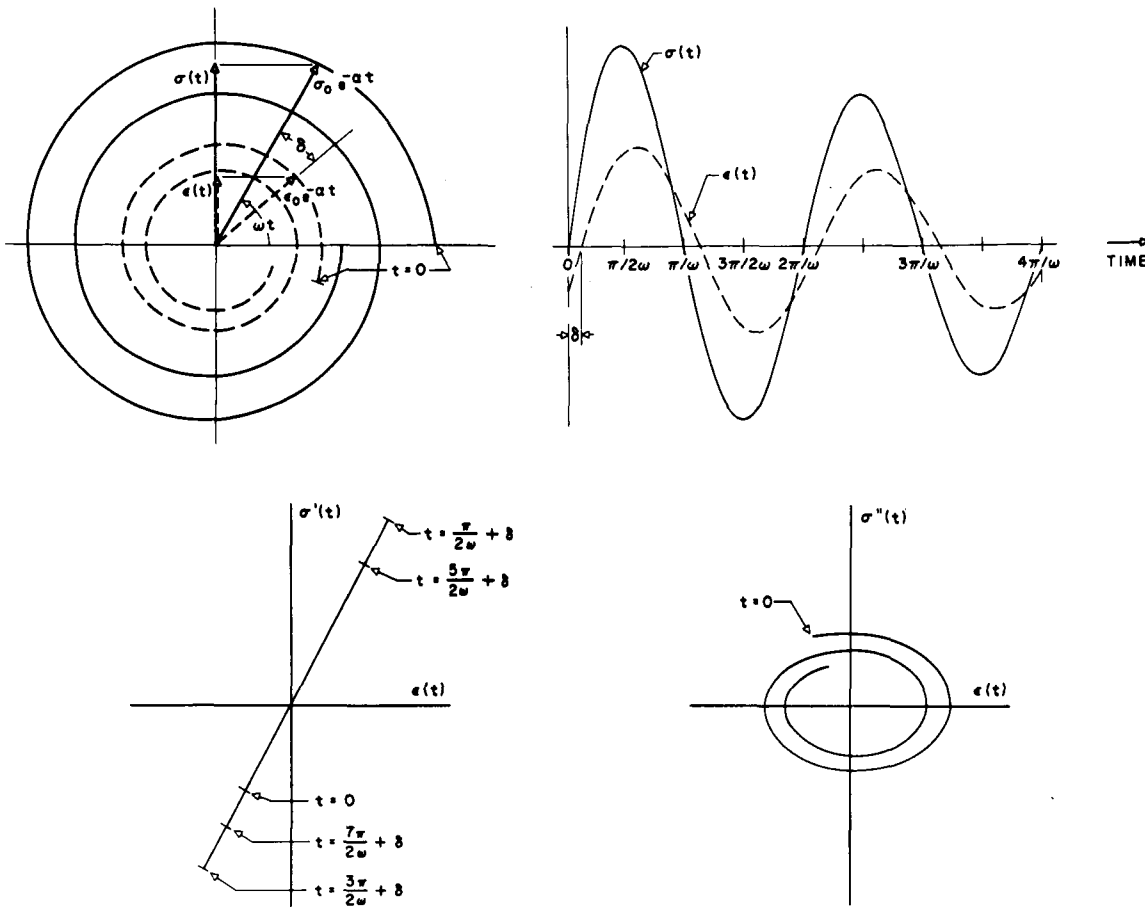
FIGURE 78. Representations of the stress and strain functions of a freely oscillating linear viscoelastic material. The figures are drawn over two cycles for the defining parameter Ai/Ai+1 = 4/3; this would define a phase angle δ = 5.25 degrees. For purposes of presentation, δ is represented as 20 degrees. The top left figure shows the rotating vector representation of the exponentially decaying sinusoidal stress and strain with the spirals being the loci swept out by the magnitude of the vectors. The top right figure is a plot of the projections, $\sigma(t)$ and $\epsilon(t)$, of $\sigma_0 e^{-\alpha t}$ and $\epsilon_0 e^{-\alpha t}$ vs. time; these are damped sine waves. The lower left figure is a plot of $\sigma'(t)$, the projection of that portion (σ_0') of σ_0 in phase with ϵ_0, vs. $\epsilon(t)$; note that this is a straight line and that there is no enclosed area on completing each cycle. The lower right hand figure is analogous to the previous one with $\sigma''(t)$ plotted vs. $\epsilon(t)$; note that the elliptical spiral traced out encloses an area which is directly related to the energy dissipated per cycle.

$\Delta W \equiv$ area of ellipse $\equiv \pi G'' \epsilon_0^2$.   (2)

Note that G'' is the material parameter which determines the dissipation of energy on cyclic mechanical deformation.

W = Maximum energy stored per cycle

$$= \int_0^{\epsilon_0} \sigma'(t) d\epsilon(t) = G' \int_0^{\epsilon_0} \epsilon(t) d\epsilon(t)$$

$\therefore$ $W = \frac{1}{2} G' \epsilon_0^2$ (3)

Note that G' is the material parameter which determines the storage of energy on cyclic mechanical deformation.

Free Vibration for a Linear System (Figure 78)

A damped sinusoidal stress can be represented (as above) by the projection of a rotating stress vector which decays according to the factor $e^{-\alpha t}$, where α is the damping constant. The damped cyclic stress is given by

$\sigma(t) = \sigma_0 e^{-\alpha t} \sin \omega t$.

The damped cyclic strain is represented by the projection on the same reference axis of a rotating vector of magnitude $\epsilon_0 e^{-\alpha t}$ rotating at the same frequency (ω) with a constant phase angle between the rotating stress and strain vectors. The damped cyclic strain is given by

$\epsilon(t) = \epsilon_o e^{-\alpha t} \sin(\omega t - \delta)$.

In these expressions σ_o and ϵ_o are the numerical constants evaluated by taking the magnitude of the rotating stress vector and rotating strain vector at $t = 0$, respectively.

In the same manner as for forced vibrations (above)

$G' = \sigma_o e^{-\alpha t} \cos\delta / \epsilon_o e^{-\alpha t}$

$G'' = \sigma_o e^{-\alpha t} \sin\delta / \epsilon_o e^{-\alpha t}$

$\dfrac{G''}{G'} = \tan\delta$

W = Maximum energy stored per cycle

$= \int_0^{\text{peak strain}} \sigma'(t)\,d\epsilon(t) = G' \int \epsilon(t)\,d\epsilon(t)$

$= \dfrac{1}{2} G'\ (\text{peak strain})^2$ (3)

ΔW = energy dissipated per cycle

= difference in potential energy for two consecutive peak amplitudes

$= \dfrac{1}{2} \times G'\ (A_i^2 - A_{i+1}^2)$

$\therefore\ \dfrac{\Delta W}{W} = 1 - \left(\dfrac{A_{i+1}}{A_i}\right)^2 = 1 - \dfrac{1}{e^{2\Delta}}$, since

$W = \dfrac{1}{2} G'\ A_i^2$

and $\log_e A_i/A_{i+1} = \Delta$,

and, if Δ is small (i.e. low loss)

$\dfrac{\Delta W}{W} = 2\Delta$.   (4)

Also, if loss is low, then

$\Delta W \simeq \pi G'' A_i^2$ (see forced vibration section)   (2)

and

$\dfrac{\Delta W}{W} = 2\pi \dfrac{G''}{G'}$ (5)

$= 2\pi \tan\delta$ (6)

$= 2\Delta$ (see above)   (4)

$= 2\dfrac{\pi}{\omega} \alpha$ (see below)   (7)

If the angular amplitude of an oscillation observed by the experimenter is

$A = A_o e^{-\alpha t} \cos 2\pi f t = A_o e^{-\alpha t} \cos\omega t$,

$\Delta \equiv$ logarithmic decrement $\equiv \log_e A_i/A_{i+1}$ where

A_i is the amplitude of the ith peak

$= \log_e \dfrac{A_o e^{-\alpha t_i} \cos\omega t_i}{A_o e^{-\alpha(t_i + \frac{2\pi}{\omega})} \cos(\omega t_i + \frac{2\pi}{\omega})}$

$= \log_e e^{(2\pi/\omega)\alpha}$ See Figure 12 where f = frequency in cycles per second ($\omega = 2\pi f$).

or, using the strain function $\epsilon(t)$, which is directly proportional to the angular amplitude

$\Delta = \log_e \dfrac{\epsilon_o e^{-\alpha t_i} \sin(\omega t_i - \delta)}{\epsilon_o e^{-\alpha(t_i + \frac{2\pi}{\omega})} \sin[(\omega t_i + \frac{2\pi}{\omega}) - \delta]}$

$= \log_e e^{(2\pi/\omega)\alpha}$

$\therefore\ \Delta = (2\pi/\omega) \times \alpha$ (7)

$\Delta = (1/f) \times \alpha$

Further,

$\Delta = \log_e A_i/A_{i+1} = \log_e A_{i+1}/A_{i+2}$

$= \log_e A_{i+2}/A_{i+3} = \cdots = \log_e A_n/A_{n+1}$

$\therefore\ \Delta = \log_e A_i/A_{i+1} + \log_e A_{i+1}/A_{i+2} + \cdots$

$+ \log_e A_n/A_{n+1}$

$\therefore\ \Delta = \left(\dfrac{1}{n}\right) \log_e A_i/A_{i+n}$ (8)

where n is the number of cycles between amplitude peaks A_i and A_{i+n}. Note that if A_i/A_{i+n} is held constant for a series of waves, then $(1/n)$ is a direct measure of the logarithmic decrement and provides a convenient hand-reduction method for determining a direct measure of the logarithmic decrement.[5,7]

DISCUSSION

The TBA approach to the characterization of polymeric materials has evolved during the past decade from what many would consider to be a rash proposition — i.e., that the behavior of a polymer could be gleaned from the behavior of a crude composite specimen ("*chemistry on a string*"). Only experience with a wide range of viscoelastic materials could show the usefulness of the approach. This task could only be undertaken

by first refining the concept itself, by developing appropriate instrumentation, and by gaining a technique of application. The basic proposition was refined early and made more tenable by introduction of an "inert" substrate: however, interactions between the matrix and substrate could be expected. The conclusion of the author is that the results on a composite specimen can be usefully interpreted directly in terms of the polymer for a surprisingly wide range of viscoelasticity without invoking spurious behavior.

Although the relative rigidity curves are not quantitatively relative and are squashed non-linearly when compared with more quantitative results obtained by using unsupported homogeneous specimens (e.g. as in more conventional studies using a Torsional Pendulum), the damping curves are not altered as significantly. However, the shapes of the mechanical rigidity and loss curves are immediately recognizable and interpretable by those working with polymers. At the present stage in the employment of polymeric materials, it is the shape and direction of changes of the mechanical storage and loss spectra which are of use, and in fact little use is made of quantitative values for the mechanical parameters which are so sensitive to chemical composition and processing history. (For the latter reasons the reproducibility of quantitative Torsional Pendulum data between different laboratories is not good.) Assignment of the temperature of transitions, and the temperature or time of nondiffusion controlled chemical transformations is accurately and easily accomplished. In fact, there probably is not a more direct and facile general method for unambiguously determining transitions and monitoring transformations in organic materials in the bulk phase. This follows in part from the great sensitivity of mechanical properties to changes in temperature (and frequency) and to chemical reactions. For example, the subtle but distinct changes in the rigidity, together with the accompanying damping peaks, pick out important relaxations to which thermal techniques such as differential thermal analysis are insensitive. As prime methods in characterizing materials, mechanical techniques relate transitions and chemical transformations directly to mechanical performance. In contrast, the response of other techniques (dilatometric, thermal, etc.) are interpreted indirectly in mechanical terms by those interested in material behavior. A useful sequence

for the initial characterization of the thermomechanical behavior of polymers would be to complement torsional braid analyses by Torsional Pendulum studies using films for the latter and using the same apparatus for both. Studies with the Torsional Pendulum would add quantitative data and an assessment of the effect of orientation to the studies of thermal and environmental influences which are so easily assessed by torsional braid analysis.

As far as the viscoelasticity of organic materials is concerned, it appears that the noncompliant glasses of very highly crosslinked and of very low molecular weight materials can give rise to complications, the interpretation of which needs to invoke specifically the composite nature of the specimen (e.g. as a source of microcracking). Since inherently brittle, high molecular weight crosslinked glasses are only useful reinforced, the fact that fracture occurs and is revealed by the behavior of the composite specimen is not to be considered an artifact. Polymeric materials which compete with steel for structural applications are of this type and pose difficult problems for laboratory analysis, not only because of their inherent brittleness (unreinforced), but because of the intractability of the final product and the necessity to process with reactive tractable intermediates. This area is a natural one for the application of TBA in which the effect of thermal history (e.g. cure) on the thermomechanical behavior is monitored so easily in situ.

The ability to perform experiments in situ permits a change in the approach to characterizing mechanical behavior, from one where series of specimens are fabricated and conditioned outside the mechanical testing equipment and then tested in it up to the limits of their thermal dimensional stabilities. This change is facilitated by using a supported specimen so that samples can be taken into temperature regions where the sample may not be able to support its own weight and where molecular mobility and diffusive processes lead to chemical reactions which alter the mechanical properties of the specimen in situ. The effect of these chemical reactions on the thermomechanical properties brings the areas of chemical and physical processes into juxtaposition. In the past, the usual approach to mechanical testing has been primarily physical. The ability to monitor changes in mechanical properties of nonself-supporting polymers permits the investigation of low

molecular weight species (e.g. from preliminary polymer synthesis) and the investigations of the curing and drying of liquid resins, varnishes, paints, adhesives, and the environmental embrittlement of elastomers, etc. TBA is especially useful for reactive systems.

There are many advantages of working with small specimens with an essentially nondestructive technique. Among these is the relatively rapid approach to thermal equilibrium of the sample with the environment. This permits thermomechanical experiments to be performed at a relatively rapid rate. A more subtle advantage in using small samples is the ability to remove difficult-to-remove foreign materials such as water, the presence of which alters the mechanical spectra. Thermohysteresis has been used in the author's laboratory as a test for reversibility. However, thermohysteresis can arise in polymers from physical time-dependent phenomena such as crystallization $\rightleftarrows$ fusion, dry atmosphere $\rightleftarrows$ water vapor, annealing $\rightleftarrows$ cracking, and from chemical reactions, not to mention incorrect assignments of temperature. The ability to take data with both increasing and decreasing temperature reveals features which might be ignored by a unidirectional experiment. It is surprising to realize that most mechanical apparatus operate in one direction of temperature change. However, the problem of maintaining a minimal variation in temperature along an 8 in. specimen as its temperature is changed at 1°C/min throughout the temperature range –190°C to 625°C in both directions is not an easy one to solve without using a fluidized bed as the heat-transfer medium. Working with small samples also presents problems. Development of instrumentation required the innovation of a no-drag transducer for converting the mechanical oscillations into an electrical analog while the use of nitrogen as an inert atmosphere must be accompanied by careful drying since water can condense at low temperatures and affect the data. TBA is a thoroughly experimental technique which depends for its successful application on care with experimental details. It is for this reason that the present manuscript has included experimental procedures which would not normally be incorporated into a discussion of the current status of an area.

A main goal of polymer science is to understand bulk behavior in terms of molecular architecture. The latter affects the submolecular motions and so the bulk properties. In locating the onset of localized motions, low frequency dynamic mechanical techniques are particularly suited to this type of investigation which is most fruitful when systematic series of polymers are examined. On this theoretical level TBA is attempting to make such a contribution.

A unique facility for investigating structure-property relationships using small quantities of polymer has been established in the author's laboratories. After an induction period, which was associated with the development of this new area, the facility is proving to be most productive. The author wishes to encourage this by forming cooperative liaisons. An invitation is extended to those who would be interested in knowing more about their own materials. To those who would consider constructing or purchasing instruments and components, the author would recommend their contacting him for information on the requisites and difficulties of this area.

To the writer, the most important contribution of the type of approach that is represented by TBA is the juxtapositioning of the chemistry, characterization, processing, and properties of polymeric materials. This places the technique in a position of great utility for both pragmatic and theoretical polymer science and engineering.

REFERENCES

(Bibliography on Torsional Braid Analysis 1 to 49)

1. Lewis, A. F. and Gillham, J. K., Novel technique for following the rigidity changes accompanying the curing of polymers, *J. Appl. Polym. Sci.*, 6, 422, 1962.

2. Gillham, J. K. and Lewis, A. F., Thermal isomerization of poly(triallylcyanurate) using a dynamic mechanical method, *Nature*, 195, 1199, 1962.

3. Lewis, A. F. and Gillham, J. K., Dynamic mechanical properties of supported polymers. I. Application of the torsional braid technique to the study of glass transition temperatures, *J. Appl. Polym. Sci.*, 7, 685, 1963.

4. Gillham, J. K. and Lewis, A. F., Dynamic mechanical properties of supported polymers. II. Application of the torsional braid technique to the study of the curing and stability of resins, *J. Appl. Polym. Sci.*, 7, 2293, 1963.

5. Gillham, J. K., Polymer Structure: Crosslinking of a polybenzimidazole, *Science*, 139, 494, 1963.

6. Saxon, R. and Lestienne, F. C., Curing relations of hexakis (methoxymethyl)melamine and its combinations with acrylic polymers, *J. Appl. Polym. Sci.*, 8, 475, 1964.

7. Gillham, J. K. and Lewis, A. F., Studies of the thermal behavior of polymers by torsional braid analysis, *J. Polym. Sci.*, C, 6, 125, 1964.

8. Gillham, J. K., Allyl s-triazine polymers, *Encyl. Polym. Sci. Tech.*, 1, 760, 1964.

9. Gillham, J. K. and Petropoulos, J. C., Polyhexaallylmelamine and related polymers, *J. Appl. Polym. Sci.*, 9, 2189, 1965.

10. Senior, A., Dynamic mechanical studies on a phenolic resole during the thermosetting curing process, Preprints, *Div. Org. Coat. Plast. Chem.*, Amer. Chem. Soc., 25, (1), 8, 1965.

11. Holden, H. W., Potentialities of torsion braid analysis in the study of protective coatings systems, *Chem. Canad.*, 17, 42, 1965.

12. Saloman, G., Adhesion and cohesion, in *Adhesion and Adhesives*, 2nd ed., Vol. I, *Adhesives*, Houwink, R. and Saloman, G., Eds., Elsevier, New York, 1965, Ch. 1.

13. Adicoff, A. and Yukelson, A. A., Torsional braid as a kinetic tool for the study of the polymerization of viscous materials. I. Initial studies, *J. Appl. Polym. Sci.*, 10, 159, 1966.

14. Gillham, J. K., Thermomechanical properties of polymers by torsional braid analysis, *J. Appl. Polym. Sci.*, Applied Polymer Symposia, 2, 45, 1966.

15. Gillham, J. K. and Schwenker, R. F., Jr., Thermomechanical and thermal analysis of fiber-forming polymers, *J. Appl. Polym. Sci.*, Applied Polymer Symposia, 2, 59, 1966.

16. Derby, M. J., (Gillham, J. K., advisor), Dynamic mechanical properties of thermoplastic polymers by torsional braid analysis, M.S.E. Thesis, Polymer Materials Program, Department of Chemical Engineering, Princeton University, Princeton, N. J., May, 1966.

17. Gillham, J. K., Torsional braid analysis. A semimicro mechanical approach to polymer analysis, *Polym. Eng. Sci.*, 7, (4), 225, 1967.

18. Nakamura, S., Torsional braid analysis, *High Polymers*, Japan, 16, 833, 1967.

19. Adicoff, A. and Yukelson, A. A., Torsional braid as a kinetic tool for the study of the polymerization of viscous materials. II. Catalytic effects in the polymerization of carboxylic acid-terminated polybutadiene prepolymers with tris[1-(2-methyl)aziridinyl] phosphine oxide, *J. Appl. Polym. Sci.*, 12, 1959, 1968.

20. Nakamura, S., Gillham, J. K., and Tobolsky, A. V., Torsional braid analysis of amylose and amylopectin, *Rep. Prog. Polym. Phys. Jap.*, 11, 523, 1968.

21. Williams, B. L. and Weissbein, L., Torsional braid analysis of antioxidant activity in elastomeric systems. I. Initial studies, *J. Appl. Polym. Sci.*, 12, 1439, 1968.

22. Hakozaki, J., Higashimura, E., and Toyoda, S., Kinetic study of the crosslinking reaction of reactive acrylic polymer by torsional braid analysis, *Kogyo Kagaku Zasshi*, 71, 887, 1968.

23. Barber, P. A., Jr., (Gillham, J. K., advisor), A study of the thermomechanical behavior of the di-alkyl phthalates, B.S.E. Thesis, Polymer Materials Program, Department of Chemical Engineering, Princeton University, Princeton, N. J., May, 1968.

24. Gillham, J. K., Pezdirtz, G. F., and Epps, L., Thermomechanical behavior of an aromatic polysulfone, *J. Macromol. Sci. Chem.*, A3(6), 1183, 1969.

25. Lewis, A. F. and Elder, G. B., Selecting adhesives for vibration damping metal laminate applications, *Adhesives Age*, 12, (10), 31, 1969.

26. Goodstein, S., (Gillham, J. K., advisor), Torsional braid analysis of poly(isophthalic hydrazide) and poly(isophthalic-terephthalic hydrazide), M.S.E. Thesis, Polymer Materials Program, Department of Chemical Engineering, Princeton University, Princeton, N. J., May, 1969.

27. Gillham, J. K., Torsional braid analysis: a semimicro thermomechanical approach to polymer characterization, in *Techniques and Methods of Polymer Evaluation*, Vol. II, *Thermal Characterization Techniques*, Slade, P.E. Jr. and Jenkins, L.T., Eds., Dekker, New York, 1970, Ch. 4.

28. Nakamura, S., Gillham, J. K., and Tobolsky, A. V., Torsional braid analysis of cellulose, *Rep. Prog. Polym. Phys. Jap.*, 13, 89, 1970.

29. Hallock, K. D., (Gillham, J. K., advisor), Thermomechanical spectra of high temperature polyimides by the torsional braid analysis technique, B.S.E. Thesis, Polymer Materials Program, Department of Chemical Engineering, Princeton University, Princeton, N. J., May, 1970.

30. Wrasidlo, W., Dielectric and mechanical relaxations in polyphenylquinoxalines, Preprints, *Div. Polym. Chem.*, Amer. Chem. Soc., 11, (2), 1159, 1970.

31. Gillham, J. K. and Roller, M. B., Investigation of structure-property relations in systematic series of novel polymers, ONR Contract N00014-67-A-0151-0024, Task No. NR 356-504, Tech. Report No. 1, 1970.

32. Glazier, K. C., (Gillham, J. K., advisor), Thermomechanical and thermogravimetric analyses of BBB polymer, B.S.E. Thesis, Polymer Materials Program, Department of Chemical Engineering, Princeton University, Princeton, N. J., May, 1971.

33. Morgan, R. J., (Kostin, M.D., advisor), Digital signal analysis of experimental data, B.S.E. Thesis, Department of Chemical Engineering, Princeton University, Princeton, N. J., May, 1971.

34. Gillham, J. K., Torsional braid analysis, *Encyl. Polym. Sci. Tech.*, 14, 76, 1971.

35. Gillham, J. K. and Roller, M. B., Advances in instrumentation and technique of torsional pendulum and torsional braid analyses, *Polym. Eng. Sci.*, 11, No. 4, 295, 1971. See also: First Symposium on Torsional Braid Analysis, Society of Plastics Engineers Annual Technical Meeting, Washington, D.C., Preprints, 17, 78, May 10, 1971.

36. Coulehan, R. E., Automatic data reduction for the TBA, in First Symposium on Torsional Braid Analysis, Society of Plastics Engineers Annual Technical Meeting, Washington, D.C., *Preprints*, 17, 86, May 10, 1971.

37. Krug, R. and Gillham, J. K., Electronic data reduction for torsional pendulum and torsional braid analyses using a digital computer, in First Symposium on Torsional Braid Analysis, Society of Plastics Engineers Annual Technical Meeting, Washington, D.C., May 10, 1971.

38. Lewis, A. F. and Pietsch, G. J., Studies of the curing behavior of polyurethane elastoplastics using torsional braid analysis, in First Symposium on Torsional Braid Analysis, Society of Plastics Engineers Annual Technical Meeting, Wasington D.C., *Preprints*, 17, 87, May 10, 1971.

39. Gillham, J. K., Applications of torsional braid analysis, in First Symposium on Torsional Braid Analysis, Society of Plastics Engineers Annual Technical Meeting, Washington, D.C., *Preprints*, 17, 89, May 10, 1971.
    Gillham, J. K., Optimization of the thermomechanical behavior of a poly(chromium II trisphosphinate), *J. Appl. Polym. Sci.*, in press.

40. Williams, B. L., Torsional braid analysis of the effectivenss of polymer additives, in First Symposium on Torsional Braid Analysis, Society of Plastics Engineers Annual Technical Meeting, Washington, D. C., *Preprints*, 17, 155, May 10, 1971.

41. Martin, J. R. and Gillham, J. K., Amorphous polyolefins: the relationship between molecular structure, molecular motion and mechanical behavior, Preprints, *Div. Polym. Chem.*, Amer. Chem. Soc., 12, (2), 554, 1971. See also: First Symposium on Torsional Braid Analysis, Society of Plastics Engineers Annual Technical Meeting, Washington, D.C., Preprints, 17, 160, May 10, 1971.

42. Roller, M. B. and Gillham, J. K., Thermomechanical behavior of poly(carborane-siloxane)s containing $-CB_8H_8C-$ cages, Preprints, *Div. Polym. Chem.*, Amer. Chem. Soc., 12, (2), 699, 1971.

43. Hiltner, A., Baer, E., Martin, J. R., and Gillham, J. K., Cryogenic relaxations in amorphous polyolefins by torsional braid analysis, unpublished results, 1971.

44. Gillham, J. K. and Roller, M. B., Investigation of structure-property relations in systematic series of poly(B_{10} carborane-siloxane)s, ONR Contract N00014-67-A-0151-0024, Task No. NR 356-504, Tech. Report No. 7, 1972. Roller, M. B. and Gillham, J. K., Thermomechanical behavior in nitrogen of a systematic series of linear poly(carborane siloxane)s containing $-CB_{10}H_{10}C-$ cages, Preprints, *Div. Polym. Chem.*, Amer. Chem. Soc., 13, (1), 1972. See also: First Symposium on Torsional Braid Analysis, Society of Plastics Engineers Annual Technical Meeting, Washington, D.C., Preprints, 17, 95, May 10, 1971.

45. Gipstein, E., Kiran, E., and Gillham, J. K., unpublished results 1970, in press.

46. Kiran, E., (Gillham, J. K., advisor), Ph.D. Thesis, Polymer Materials Program, Department of Chemical Engineering, Princeton Univeristy, Princeton, N. J., 1973.

47. Roller, M. B., (Gillham, J. K., advisor), Ph.D. Thesis, Polymer Materials Program, Department of Chemical Engineering, Princeton University, Princeton, N. J., 1972.

48. Gillham, J. K., Hallock, K. D., and Stadnicki, S. J., Thermomechanical behavior in nitrogen of systematic series of polvimides, Preprints, *Div. Polym. Chem.*, Amer. Chem. Soc., 13, (1), 1972.
    Gillham, J. K., Thermomechanical behavior of polymers by torsional braid analyses, Preprints, *Div. Organ. Coat. Plast. Chem.* Amer. Chem. Soc., 32, (1), 1972.

49. Unpublished results: Gillham, J. K., Hemicellulose, 1965. Gillham, J. K., Roller, M. B., and Kennedy, J. P., Polynorbornadiene, 1968. Gipstein, E., Kiran, E., and Gillham, J. K., Tactic polymethylmethacrylates and tactic polytert butyl methacrylates. 1970. Gillham, J. K. and Stadnicki, S. J., Polypeptides, 1971. Roller, M. B. and Gillham, J. K., 5-SiB-X polymers, 1971.

50. American Society for Testing Materials, Standard D2236-70, Dynamic mechanical properties of plastics by means of a torsional pendulum, in ASTM standards, Pt. 27, *Plastics – General Methods of Testing*, 638, American Society for Testing Materials, Philadelphia, 1971.

51. Nielsen, L. E., Dynamic mechanical testing, in *Mechanical Properties on Polymers*, Reinhold, New York, 1962, Ch. 7.

52. Thomas, A. and Bell, C. M., private communication.

53. Boyer, R. F., Ed., Transitions and relaxations in polymers, *J. Polym. Sci.*, C 14, 1966.

54. Boyer, R. F., Dependence of mechanical properties on molecular motion in polymers, *Polym. Eng. Sci.*, 8, (3), 16, 1968.

55. McCrum, N. G., Read, B. E., and Williams, G., *Anelastic and Dielectric Effects in Polymeric Solids*, John Wiley & Sons, New York, 1967.

56. Kennedy, J. P., Isomerization polymerization, *Encyl. Polym. Sci. Tech.*, 7, 754, 1967.

57. Wanless, G. G. and Kennedy, J. P., Intramolecular hydride shift polymerization by cationic mechanism. III - Structure analyses of deuterated and non-deuterated poly-4-methyl-*1*-pentene, *Polymer*, 6, 111, 1965.

58. Martin, J. R., Gillham, J. K., and Kennedy, J. P., unpublished results. See also: Martin, J. R., (J. K. Gillham, advisor), Amorphous polyolefins, Ph.D. Thesis, Polymer Materials Program, Department of Chemical Engineering, Princeton University, Princeton, N. J., 1972.

59. Johnson, G. E., (J. K. Gillham, advisor), Dielectric behavior of amorphous polyolefins, M.S.E. Thesis, Polymer Materials Program, Department of Chemical Engineering, Princeton University, Princeton, N. J., 1972.

60. Turner, A. and Bailey, F. E., Jr., An apparent anomaly in the glass transition of polyisobutylene, *J. Polym. Sci.*, *B*, 1, 601, 1963.
    Van Lohuizen, O. E. and De Vries, K. S., Cationic polymerization of some 1,1-dialkylethenes and methylenecyclo-alkanes, *J. Polym. Sci.*, *C*, 16, 3943, 1968.

61. Farrow, G., McIntosh, J., and Ward, I. M., The interpretation of transition phenomena in polymethylene terephthalate polymers, *Makromol. Chem.*, 38, 147, 1960.
    Richards, R. E., Farrow, G., and Ward, I. M., Molecular motion in polyethylene terephthalate and other glycol terephthalate polymers, *Polymer*, 1, 63, 1960.

62. Faucher, J. A. and Koleske, J. V., Estimation of the glass transition of polyethylene by extrapolation of a series of polyethers, *Polymer*, 9, 44, 1968.

63. Morawetz, H., *Macromolecules in Solution*, Interscience, New York, 1965, Ch. 3.

64. Tobolsky, A. V., *Properties and Structure of Polymers*, John Wiley & Sons, New York, 1962, Ch. 1 and 2; Flory, P. J., *Principles of Polymer Chemistry*, Cornell University Press, Ithaca, New York, 1953, Ch. 11.

65. Flory, P. J., *Statistical Mechanics of Chain Molecules*, Interscience, New York, 1969, Ch. 5.

66. Boyd, R. H. and Breitling, S. M., The conformational properties of polyisobutylene, Preprints, *Div. Polym. Chem.*, Amer. Chem. Soc., 12 (2), 611, 1971.

67. Edwards, W. M. and Chamberlain, N. F., Carbonium ion rearrangement in the cationic polymerization of branched alpha olefins, *J. Polym. Sci. A*, 1, 2299, 1963.

68. Szymanski, H. A. and Yelin, R. E., *NMR Band Handbook*, Plenum Press, New York, 1965.

69. Stehling, F. C. and Mandelkern, L., The glass temperature of linear polyethylene, *Macromolecules* 3, 242, 1970.

70. Beevers, R. B. and White, E. F. T., A note on the glass-transition temperatures of acrylonitrile + styrene copolymers, *J. Polym. Sci. B*, 1, 171, 1963.

71. Illers, K. H., Die Glastemperatur von Copolymeren, *Kolloid Z.*, 190, 16, 1963.

72. Boyer R. F., The relation of transition temperatures to chemical structure in high polymers, *Rubber Chem. Tech.*, 36 (5), 1303, 1963.

73. Shen, M. C. and Eisenberg, A., Glass transition in polymers, *Prog. Solid State Chem.*, 3, 407, 1966.

74. Fox, T. G., Garrett, B. S., Goode, W. E., Gratch, S., Kincaid, J. F., Spell, A., and Stroupe, J. D., Crystalline polymers of methylmethacrylate, *J. Amer. Chem. Soc.*, 80, 1768, 1958.

Stroupe, J. D. and Hughes, R. E., The structure of crystalline poly-(methylmethacrylate), *J. Amer. Chem. Soc.*, 80, 2341, 1958.

Brandrup, J. and Immergut, E. H., *Polymer Handbook*, III-9, Interscience, New York, 1966.

McCrum, N. G., Read, B. E., and Williams, G., Anelastic and Dielectric Effects in Polymeric Solids, John Wiley & Sons, New York, 1967.

75. Willbourne, A. H., The glass transition in polymers with the $(CH_2)_n$ group, *Trans. Faraday Soc.*, 54, 717, 1958.

76. Schatzki, T. F., Molecular interpretation of the γ-transition in polyethylene and related compounds, Preprints, *Div. Polym. Chem.*, Amer. Chem. Soc. 6 (2), 646, 1965.

77. Saito, N. K., Okano, S., and Hideshima, T., Molecular motion in solid state polymers, in *Solid State Physics*, Seitz, F. and Turnbull, D., Eds., Academic Press, New York, 1963, Vol. 14, 343.

78. Andrews, R. D. and Hammack, T. J., The molecular mechanism of the γ mechanical loss peak in ethylenic polymers, *J. Polym. Sci. B*, 3, 659, 1965.

79. Tanabe, Y., Hirose, J., Okano, K., and Wada, Y., Methyl group relaxations in the glassy state of polymers, *Polym. J.*, 1(1), 107, 1970.

80. Levine, H. H., Polybenzimidazoles and other aromatic heterocyclic polymers for high temperature resistant structural laminates and adhesives, in Air Force Materials Lab. Tech. Report 64-365, Part 1, Vol. 1, November, 1964.

81. Saraceno, A. J., King, J. P., and Block, B. P., Novel tris (phosphinates) of chromium III, *J. Polym. Sci., B*, 6, 15, 1968.

82. Block, B. P. and Nanelli, P., personal communication, December, 1970.

83. Knollmueller, K. O., Scott, R. N., Kwasnik, H., and Sieckhaus, J. F., Icosahedral Carboranes. XVI. Preparation of linear poly-m-carboranylenesiloxanes, *J. Polym. Sci. A-1*, 9, 1071, 1971.

84. Scott, R. N., Knollmueller, K. O., Hooks, H., Jr., and Sieckhaus, J. F., Icosahedral Carboranes. XIX. The preparation of linear trifluoropropyl-substituted polycarboranylenesiloxanes, Technical Report No. 49, Office of Naval Research, Contract No. N00014-7-C-0003, 1971.

85. Sieckhaus, J. F., private communication.

86. Fox, T. G., Influence of diluent and of copolymer composition on the glass temperature of a polymer system, *Bull. Amer. Phys. Soc.*, 1, 123, 1950.

87. Sperling, L. H., Cooper, S. L., and Tobolsky, A. V., Elastomeric and mechanical properties of poly-m-carboranylene-siloxanes, *J. Appl. Polym. Sci.*, 10, 1725, 1966.

88. Dietrich, H. J., Alexander, R. P., Heying, T. L., Kwasnik, H., Obenland, C. O., and Schroeder, H. A., Icosahedral carboranes. XVI. Polymerization and crosslinking mechanism of poly-m-carboranylenesiloxanes, Technical Report No. 45, Office of Naval Research, Contract No. 3395(00), 1970.

89. Ditter, J., Oakes, J., Klusman, E. B., and Williams, R., Direct synthesis of *closo*-carboranes, *Inorg. Chem.*, 9, 889, 1970.

90. Kesting, R. E., Jackson, K. F., Klusman, E. B., and Gerhart, F. J., The introduction of elastomeric behavior in polycarboranylenesiloxane SiB-1 polymers from the *closo*-carborane $C_2B_5H_5$, *J. Appl. Polym. Sci.*, 14, 2525, 1970.

91. Kesting, R. E., Jackson, K. F., and Newman, J. M., Heat-resistant polymers containing the low molecular weight *closo*-carboranes. II. Thermal behavior of polycarboranesiloxane SiB-1 elastomers from $C_2B_5H_7$, *J. Appl. Polym. Sci.*, 15, 1527, 1971. (Originally appeared as: ONR Contract N00014-70-C-0109, Tech. Report No. 3, 1971.)

92. Mentzer, C. C., Jr., (J. K. Gillham, advisor), Ph.D. Thesis, Polymer Materials Program, Department of Chemical Engineering, Princeton University, Princeton, N. J., 1972.

Mentzer, C. C., Jr. and Gillham, J. K., Thermo-setting Reactions: Thermo-chemical reactions of triallyl cyanurate and triallyl isocyanurate, Society of Plastics Engineers Annual Technical Meeting, Chicago, Illinois, Preprints, 18, 1972.

93. Gillham, J. K. and Adee, B. H., Spiral fracture characteristics in some reinforced polymers, *Nature*, 212, (5060), 391, 1966.

Gillham, J. K., Reitz, P. N., and Doyle, M. J., Spiral and helical fractures, *Polym. Eng. Sci.*, 8 (8), 227, 1968.

Slivinski, R. H., (Gillham, J. K., advisor), The observance of spiral fractures in cross-linked polymer systems, B.S.E. Thesis, Department of Chemical Engineering, Princeton University, Princeton, N.J., 1969.

94. Van Deusen, R. L., Goins, O. K., and Sicree, A. J., Thermally stable polymers from 1,4,5,8-napthalene tetra-carboxylic acid and aromatic tetraamines, *J. Polym. Sci. A1*, 6, 1777, 1968.

95. Koleske, J. V. and Lundberg, R. D., Secondary transitions in poly(γ-benzyl-L-glutamate) and in poly(γ-benzyl-DL-glutamate), *Macromolecules*, 2 (4), 439, 1969.